



NORTH-WEST UNIVERSITY
YUNIBESITI YA BOKONE-BOPHIRIMA
NOORDWES-UNIVERSITEIT
POTCHEFSTROOM CAMPUS

**The engineering and optimization of expression of
rotavirus-like particles in insect cells using a South
African G9P[6] rotavirus strain**

By

Maria J. van der Westhuizen, B.Sc. (Hons.)

Dissertation submitted for the degree Magister Scientiae (M.Sc.) in
Biochemistry at the Potchefstroom Campus of the North-West University

Supervisor: Prof. A. A. Van Dijk

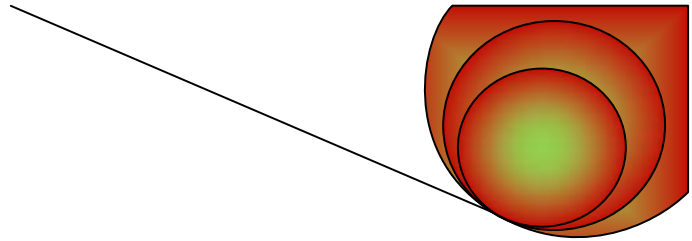
School for Physical and Chemical Sciences, North-West University
(Potchefstroom Campus), South Africa.

Co-supervisor: Dr. H.G. O'Neill

School for Physical and Chemical Sciences, North-West University
(Potchefstroom Campus), South Africa.

November 2012

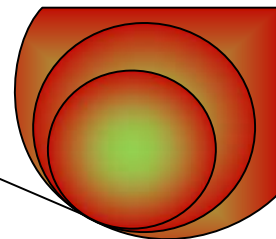
Potchefstroom



"Mystery creates wonder and wonder is the basis of man's desire to understand."
~**Neil Armstrong**

"All men dream but not equally. Those who dream by night in the dusty recesses of their minds wake in the day to find that it was vanity; but the dreamers of the day are dangerous men, for they may act their dream with open eyes to make it possible."
~**T.E. Lawrence**

ACKNOWLEDGEMENTS



I would like to show my appreciation and express gratitude to the following people and institutions, for their contributions to the project as without them this project would not have been possible:

Prof Albie van Dijk (North-West University) – thank you so much for all the time, guidance and motivation you gave me. Thank you for inspiring the same passion for biochemistry that lives within you.

Dr. Trudi O'Neill (The University of the Free State) - thank you so much for all of your patience, time, energy, encouragement and helpful scientific ideas. Thank you for teaching me what it means to be a true scientist and how to think and analyse like a scientist would.

North-West University, National Research Foundation and Department of Science and Technology (DST) of the Republic of South Africa - for financial support.

Many thanks to Mrs. W. Pretorius (North-West University), Mr J. Putterill [Onderstepoort Veterinary Institute (OVI)] and Mrs. E. van Wilpe (University of Pretoria) - for preparing the electron micrographs.

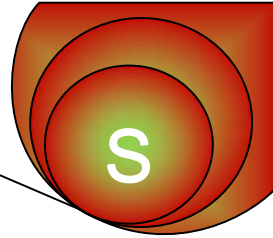
Dr. A. Christiaan Potgieter (Deltamune, Centurion) - for providing the pFASTBACquad plasmid as well as the G9P[6] consensus sequences.

Mrs. Rencia van der Sluis (North-West University) – for all her technical support, help and advice in the cell culturing laboratory.

Thank you to all the postgraduate students (Department of Biochemistry, North-West University) for all the technical support and motivation.

Lastly, I would like to thank my family and friends at home - for all their love, patience and encouragement; and especially for believing in me and never losing faith.

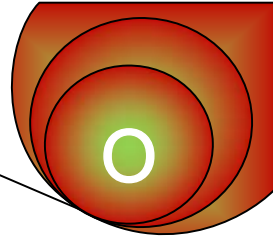
SUMMARY



Rotavirus infection causes gastroenteritis, specifically severe gastroenteritis, affecting children younger than five globally, regardless of hygiene and water quality. Current licensed, live, attenuated vaccines do not contain the G9 genotype, which is a prevalent rotavirus strain circulating in sub-Saharan Africa, a region that carries a high rotavirus disease burden. Rotavirus-like particles (RV-VLPs) is an attractive non-live vaccine candidate, which has shown promising results in animal studies. Previously, dsRNA was extracted from a stool sample containing a South African human G9P[6] neonatal strain, and amplified cDNA using a sequence-independent procedure. The consensus sequence was obtained for the genome segments using 454® pyrosequencing. The insect-cell-codon-optimized genome segments 2 (VP2), 4 (VP4), 6 (VP6) and 9 (VP7) were cloned into a modified pFASTBACquad vector (pFBq). Several combinations of the genome segments were cloned to produce double-layered particles (DLP; pFBqVP2VP6) or triple-layered particles (TLP; pFBqVP2VP6VP7). In the current study, a Δ TLP (pFBqdVP2-VP8*VP6VP7) construct was generated. The first 92 amino acids of VP2 are not necessary for the conformation of recombinant RV-VLPs. The ORF of VP8*, which contains immune important epitopes, was fused to the 5' end of the dVP2 coding region resulting in a dVP2-VP8* fused protein which was expressed in the presence of VP6 and VP7 to produce Δ TLPs. The Bac-to-Bac® Baculovirus Expression System and *Spodoptera frugiperda* (Sf) 9 insect cells were used for expression. All the proteins were successfully expressed. VP2, VP6, VP4 and the dVP2-VP8* fused protein were visible on Coomassie stained SDS-PAGE. Expression of VP7 could only be confirmed with western blot analysis. Particle formation, as assessed by transmission electron microscopy (TEM), was observed for DLPs. No TLPs of dVP2-8*/6/7 or VP2/6/7 were visualized due to the lower expression level of VP7 and the lack of calcium supplements during the assembly process. In conclusion, it was possible to produce RV-DLPs derived from the consensus sequence determined for a G9P[6] rotavirus directly from stool without prior propagation in cell culture or virus isolation. This strain contains both the G9 and P[6] genotypes that are currently prevalent in sub-Saharan Africa.

Keywords: Rotavirus, Gastroenteritis, sub-Saharan Africa, G9P[6], Rotavirus-like particles, Non-live vaccine, Baculovirus Expression System, *Spodoptera frugiperda*, Transmission electron microscopy, Double-layered particles, Triple-layered particles.

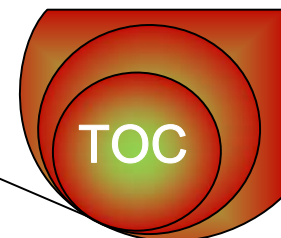
OPSOMMING



Rotavirus infeksie veroorsaak ernstige gastro-enteritis wat kinders jonger as vyf jaar, ongeag hulle higiëne en watergehalte, wêreldwyd affekteer. Huidige gelisenseerde, lewende, verswakte entstowwe bevat nie die G9 genotipe van die rotavirus stam wat wydverspreid oor die algemeen in sub-Sahara Afrika voorkom nie. Hierdie streek gaan huidiglik gebuk onder 'n groot las ten opsigte van rotavirus siekte. Rotavirus, virusagtige partikels (RV-VAPs) is 'n aantrekklike nie-lewendige entstof kandidaat, wat belowende resultate in diere studies getoon het. Voor die aanvang van die huidige studie, is dubbel-string RNS (dsRNS) van die G9P[6] stam uit 'n Suid-Afrikaanse neonatale stoel monster geïsoleer en as komplementêre DNS (kDNS) vermeerder met behulp van 'n volgorde-onafhanklike vermeerderingsprosedure. Die konsensus volgordes vir die genoomsegmente is verkry met behulp van 454 pirobasispaarvolgordebepaling. Die konsensus nukleotiedvolgorde van die genoomsegmente wat kodeer vir VP2, VP4, VP6 en VP7 is geoptimeer vir inkseluitdrukking. Hierdie genoomsegmente is gekloneer in die aangepaste pFASTBACquad vektor (pFBq). Verskeie kombinasies van die genoomsegmente is gekloneer om dubbellaag RV-VAPs (DL-RV-VAPs; pFBqVP2VP6) en trippellaag RV-VAPs (TLP-RV-VAPs; pFBqVP2VP6VP7) te produseer. Gedurende die huidige studie is 'n Δ TLP (pFBqdVP2-VP8*VP6VP7) konstrueer. Die eerste 92 aminosure van VP2 word nie gebruik vir die konformasie van rekombinante RV-VAPs nie. Die ooplesraam van VP8*, wat belangrike epitope bevat in terme van die gasheer se immuun-reaksie, is verbind aan die 5'punt van die koderingstreek van dVP2. Die verbintenis vorm die dVP2-VP8* proteïene, wat saam met VP6 en VP7 uitgedruk is om Δ TLPs te produseer. Die Bac-to-Bac Baculovirus uitdrukkingstelsel en *Spodoptera frugiperda* (SF) 9 inkselle is gebruik tydens die uitdrukkingproses. Al die rotavirus rekombinante proteïene is uitgedruk. Die uitdrukking van VP2, VP6, VP4 en die dVP2-VP8* gekoppelde proteïene was sigbaar op Coomassie gekleurde SDS-PAGE. Die uitdrukking van VP7 kon slegs bevestig word met behulp van westelike kladanalises. Partikelvorming, gebaseer op morfologie, is met TEM waargeneem vir DL-RV-VAPs. Geen TLP-RV-VAPs van dVP2-8*/6/7 of VP2/6/7 was waargeneem nie waarskynlik vanweë die laer uitdrukkingvlakke van VP7 en die gebrek aan kalsiumaanvullings tydens die partikelproduksie versamelproses. Dit was dus moontlik om DL-RV-VAPs te produseer vanaf die konsensus genomiese basisvolgorde genoomsvolgordes van die G9P[6] stam, sonder dat hierdie stam voorheen in selkulture gekweek is of dat virus geïsoleer is. Hierdie stam bevat beide die G9 en P[6] genotipes wat tans wydverspreid voorkom in sub-Sahara Afrika.

Sleutelwoorde: Rotavirus, Gastro-enteritis, sub-Sahara Afrika, G9P[6], Rotavirus virusagtige partikels, Nie-lewendige entstof, Baculovirus Uitdrukings Stelsel, Spodoptera frugiperda, Transmissie elektron mikroskopie, Dubbellaag partikels, Trippellaag partikels.

TABLE OF CONTENTS



Chapter 1: Literature review	pg.
1.1. Introduction to study	1
1.2. Classification of rotavirus	3
1.2.1. <i>Reoviridae</i>	3
1.2.2. Genus: Rotavirus	3
1.2.3. Rotavirus serogroup and serotypes	3
1.3. Rotavirus evolution	4
1.4. Virion structure	4
1.4.1. Viral proteins	5
1.4.2. Genome structure and organisation	9
1.4.3. Interactions between viral proteins (VP4, VP6, VP7 and VP2)	10
1.5. Rotavirus disease burden	10
1.6. Rotavirus pathogenesis	12
1.7. Rotavirus life cycle	12
1.8. Host response upon natural rotavirus infection and correlates of protection	14
1.8.1. Innate response	14
1.8.2. Humoral responses	14
1.8.3. Cellular immune responses	15
1.9. Rotavirus vaccination	15
1.9.1. Vaccine history	15
1.9.2. Current vaccines	16
1.9.3. Experimental vaccines	19
1.10. Motivation of the study	26
1.11. Aims of the study	26
Chapter 2: Construction and expression of dVP2-8*/VP6/VP7 particles of a South African G9P[6] rotavirus strain	pg.
2.1. Introduction	27
2.2. Materials and Methods	28
2.2.1. Virus strain, bacterial strains and cell lines	28
2.2.2. Cloning vector	29

2.2.3.	Oligonucleotides	31
2.2.4.	Recombinant DNA techniques	31
2.2.4.1.	Polymerase chain reaction (PCR) amplification of the coding regions of interest	31
2.2.4.2	Agarose gel electrophoresis	31
2.2.4.3	Purification of PCR products	32
2.2.4.4.	Spectrophotometric analysis of DNA	32
2.2.4.5.	Restriction enzyme digestion	32
2.2.4.6.	DNA ligation reaction	33
2.2.4.7	Electroporation of dsDNA vector and inserts (pFBqdVP2-8*/6/7) into competent E.coloni cells	33
2.2.4.8	Mini plasmid extraction	33
2.2.4.9	Long-term storage of the bacteria containing plasmids of interest in glycerol	34
2.2.4.10.	Preparation of plasmids for sequencing	34
2.2.4.11	DNA sequencing	35
2.2.5.	Baculovirus expression system (BVES)	35
2.2.5.1	Bacmid DNA construction	35
2.2.5.2.	Bacmid DNA isolation	36
2.2.5.3.	Screening for appropriate recombinant bacmids	36
2.2.5.4.	Transfection of Sf9 cells with bacmid DNA	37
2.2.5.5.	Preparation of P1 viral stocks	37
2.2.5.6.	Infection of Sf9 cells with recombinant baculovirus, expressing the genes of interest	37
2.2.5.7.	Harvesting of the recombinant baculovirus and cells	38
2.2.5.8.	SDS-PAGE	38
2.3.	Results and Discussion	39
2.3.1.	Design of primers used during the amplification of genome segments encoding dVP2 and VP8*	40
2.3.2.	Polymerase chain reaction (PCR) amplification of the regions of genome segments 2 and 4 encoding dVP2 and VP8*, respectively	45
2.3.3.	Cloning of the truncated regions of genome segments 2 and 4 encoding dVP2 and VP8*, respectively, into pFBq containing the coding regions of VP6 and VP7	47

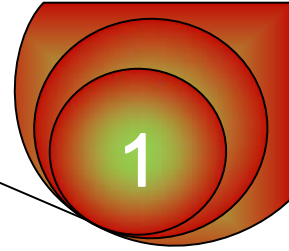
2.3.4.	Molecular characterisation of the pFBqdVP2-8*/6/7	51
2.3.5.	Expression of dVP2-8*/6/7 in insect cells	56
2.3.6.	Investigation of protein solubility of recombinant dVP2-8*/6/7	61
2.4.	Summary	62

Chapter 3: Analysis of various recombinants of rotavirus VP2, VP6, VP4, VP7 and dVP2-8* of G9P[6] baculovirus expression and particle formation pg.

3.1.	Introduction	64
3.2.	Materials and methods	64
3.2.1.	Extraction of baculovirus DNA (gDNA) from insect cells	64
3.2.2.	Western blot assay	65
3.2.3.	Amplification of virus-stock	66
3.2.4.	Viral plaque assay	66
3.2.5.	Infection of Sf9 cells with recombinant baculovirus	67
3.2.6.	Sucrose gradient purification of rotavirus-like particles	67
3.2.7.	Bicinchoninic (BCA) assay for protein quantification	68
3.2.8.	Transmission electron microscope (TEM) visualisation of rotavirus particles	68
3.3.	Results and Discussion	69
3.3.1.	Generation of a pFBq-based recombinant baculovirus control	69
3.3.2.	Description of baculoviruses used for expression of various combinations of rotavirus proteins VP2, VP4, VP6, VP7 and dVP2-8*	74
3.3.3.	Analysis of protein expression with SDS-PAGE	75
3.3.4.	The verification of the presence of coding region of genome segments 9(VP7) and 6(VP6) in DNA isolated from baculoviruses expressing combinations of VP2/6, VP2/6/7, VP2/6/4/7 and dVP2-8*/6/7, respectively	76
3.3.5.	Verification of VP7 expression in recombinant baculoviruses expressing combinations of VP2/6/7, VP2/6/4/7 and dVP2-8*/6/7, respectively	78
3.3.6.	Evaluation of recombinant rotavirus protein expression VP2, VP6, VP7, VP4 and dVP2-8* in Sf9 Mimic cells	84
3.3.7.	Rotavirus-like particle production, purification and visualisation	85
3.3.8.	Analysis of the production of double-layered (VP2/6) rotavirus-like particles	86

3.3.9.	Analysis of the production of triple-layered (VP2/6/7 and dVP2-8*/6/7) rotavirus-like particles	87
3.4.	Summary	91
Chapter 4:	Concluding Remarks	93
Appendix 1	List of materials utilised during study	97
Appendix 2	Preparation of buffers utilised in study	101
Appendix 3	Oligonucleotides utilised during study	104
Appendix 4	List of Figures	105
Appendix 5	List of Tables	108
Appendix 6	List of Abbreviations	109
Appendix 7	References	113

CHAPTER 1: LITERATURE REVIEW



1.1. Introduction to study

Rotavirus infection causes gastroenteritis, which leads to approximately 453 000 deaths globally (Tate *et al.*, 2012) in children younger than five every year. These infections affect all children, regardless to aspects such as hygiene, behaviour, or food and water quality (Parez, 2008). Rotavirus infections affect populations in both developed and developing countries. The majority of deaths, however, occur in developing countries, due to the lack of adequate and fast medical attention (Glass *et al.*, 2006).

Two vaccines have been developed and licensed to decrease the rotavirus burden of disease, RotaTeq and Rotarix. These vaccines contain live attenuated viruses, which are associated with a number of potential risks (section 1.9.2). In addition, vaccine trials performed in South Africa and Malawi, only showed an estimated combined efficacy of 61.2% (Madhi *et al.*, 2010). These efficacy results are much lower than the results obtained in developed countries. The latter is speculated to be a result of the strain diversity found in these countries, as prevalent circulating strains are not present in current vaccines. Furthermore, there are still other unresolved issues concerning the safety, efficiency and production costs of these oral, live attenuated virus vaccines.

Non-replicating rotavirus vaccines are being considered as an alternate approach for vaccine development (Vieira *et al.*, 2005). These alternative vaccines include the development of rotavirus-like particle (rota-VLP) vaccines and inactivated vaccines. The rota-VLP system exhibits the equivalent antigen presentation of rotavirus (Parez, 2008), but is not associated with any of the side effects of the replication of the virus, since it does not contain the double-stranded RNA (dsRNA) genome of the virus. VLPs might be able to provide a broader range of protection, since these particles can be engineered to contain structural proteins corresponding to different rotavirus strain serotypes, specifically occurring in developing countries. Furthermore, because of a non-oral administration route, setbacks concerning effective delivery of antigens to the site of infection are eliminated. The assembly of the rotavirus-VLP requires the expression of the four major capsid proteins (Crawford *et al.*, 1994) in insect cells, where three of the proteins contain antigenic properties. The approach of developing new generation VLP-vaccines might provide a safer, more effective alternative to current rotavirus vaccines.

The project of the M.Sc. presented here, formed part of a consortium effort aimed at the production of rotavirus-like particles (rota-VLPs) in different expression systems. Our group at the North-West University focused on virus-like particle production in insect cells using the Bacto-Bac baculovirus expression system (Invitrogen). Before the start of this project, dsRNA of a South African human G9P[6] neonatal strain was extracted from stool, prepared and amplified as cDNA using a sequence-independent procedure (Potgieter *et al.*, 2009). The consensus sequence for the genome segments was obtained using 454® pyrosequencing (Potgieter *et al.*, 2009). Synthetic genes encoding the four major structural proteins, which comprise the rotavirus capsid, were optimized for expression in insect cells and synthesised by from Geneart. Dr. H.G. O'Neill cloned insect cell codon-optimized genome segments 2 (VP2), 4 (VP4), 6 (VP6) and 9 (VP7) into a modified pFASTBACquad vector (pFBq), which was used during subsequent expression in insect cells. The pFBq vector was previously modified by Dr. A.C. Potgieter to contain the multiple cloning site of pBascGus 4x1 from Novagen.

The work presented in this dissertation aimed to engineer and optimize the production and expression of rotavirus-VLPs in insect cells, through the use of the South African rotavirus field strain, G9P[6].

The dissertation is divided into the following 4 chapters:

Chapter 1: Literature review

Chapter 2: Construction and expression of dVP2-8*/VP6/VP7 particles of a South African G9P[6] rotavirus strain

Chapter 3: Analysis of various recombinants of rotavirus VP2, VP6, VP4, VP7 and dVP2-8* of G9P[6] baculovirus expression and particle formation

Chapter 4: Concluding remarks

Appendix 1-7

1.2. Classification of rotavirus

1.2.1. *Reoviridae*

The *Reoviridae* family consists of twelve genera: *Orthoreovirus*, *Orbivirus*, *Coltivirus*, *Rotavirus*, *Aquareovirus*, *Cypovirus*, *Phytoreovirus*, *Fijivirus*, *Seadornavirus*, *Idnoreovirus*, *Mycoreovirus* and *Oryzavirus*. These viruses infect mammals, birds, amphibians, reptiles, fish, plants and invertebrates. The “reo” in *Reoviridae* refers to “respiratory enteric orphan”, since the enteric and respiratory tracts (of both animals and humans) were the locations of first isolated reovirus. These viruses have a double-stranded RNA (dsRNA) genome (Estes and Kapikian, *Fields Virology*, 2007).

1.2.2. *Genus: Rotavirus*

Rotaviruses belong to the *Reoviridae* virus family. The dsRNA genome of rotavirus consists of 11 genome segments (Figure 1.1), which is surrounded by a triple-layered capsid. Each of the genome segments encodes a viral protein, except for genome segment 11, which encodes two proteins and has two open reading frames (ORFs) (Pesavento *et al.*, 2006). The genome segments encode six structural viral proteins (VP1-4, 6, 7) and six non-structural proteins (NSP1-6). RNA-dependant RNA polymerase and other enzymes are found inside the virus particles. These enzymes exhibit the capacity of producing capped RNA transcripts (Estes and Kapikian, *Fields Virology*, 2007).

1.2.3. *Rotavirus serogroup and serotypes*

Rotaviruses are classified into seven or eight groups (A – E, tentatively F and G, and possibly N-ADRV). The antigenic properties of viral protein 6 (VP6) determine the serogroup of a rotavirus (Matthijnssens *et al.*, 2012). Serogroup A can be further divided into different serotypes. These serotypes are determined by VP7 (G-type) and VP4 (P-type) (Estes and Kapikian, *Fields Virology*, 2007). Different serotypes can be further classified into subgroups, distinguished by the non-neutralizing epitopes located on the intermediate capsid protein, VP6. There are four subgroups that can be distinguished under group A rotaviruses. They may contain one; many or no forms of the subgroup epitopes, which are produced during the trimerisation process of VP6 (Ito *et al.*, 1996). The detailed properties of the VP6, VP7 and VP4 proteins will be discussed in section 1.4.1.

1.3. Rotavirus evolution

Rotaviruses evolve via three mechanisms: Point mutations, genetic reassortment and genome recombination (Desselberger *et al.*, 2001). Point mutations occur frequently within rotaviruses as the RNA-dependent RNA polymerase used for replication purposes, lacks proof-reading activity. Genetic reassortment is a consequence of rotavirus segmented genomes, where two rotaviruses create new progeny viruses by mixing of their genome segments (Gouvea and Brantly, 1995). The progeny viruses contain genome segments from both of the parental strains. This can occur either *in vitro* or *in vivo* between animals and human rotavirus strains – more specifically known as zoonotic transmission (Martella *et al.*, 2010). Genetic reassortment between viruses is restricted to viruses belonging to the same serogroup (Franco *et al.*, 2006). When rotaviruses from heterotypic strains infect a host cell simultaneously, intragenic genome recombination can occur and further expand the diversity of circulating rotavirus strains. The occurrence of this phenomenon in rotaviruses was first reported by Susuki and co-workers (1998). Recombination can either occur inter-sub-lineage (Phan *et al.*, 2007) or intra-lineage (Parra *et al.*, 2004). The mechanism behind intragenic genome recombination is still unclear.

1.4. Virion structure

The complete rotavirus virion is known as a triple-layered particle (TLP), as represented in Figure 1.1. The TLP possesses an icosahedral surface lattice of T=13 (Settembre *et al.*, 2010).

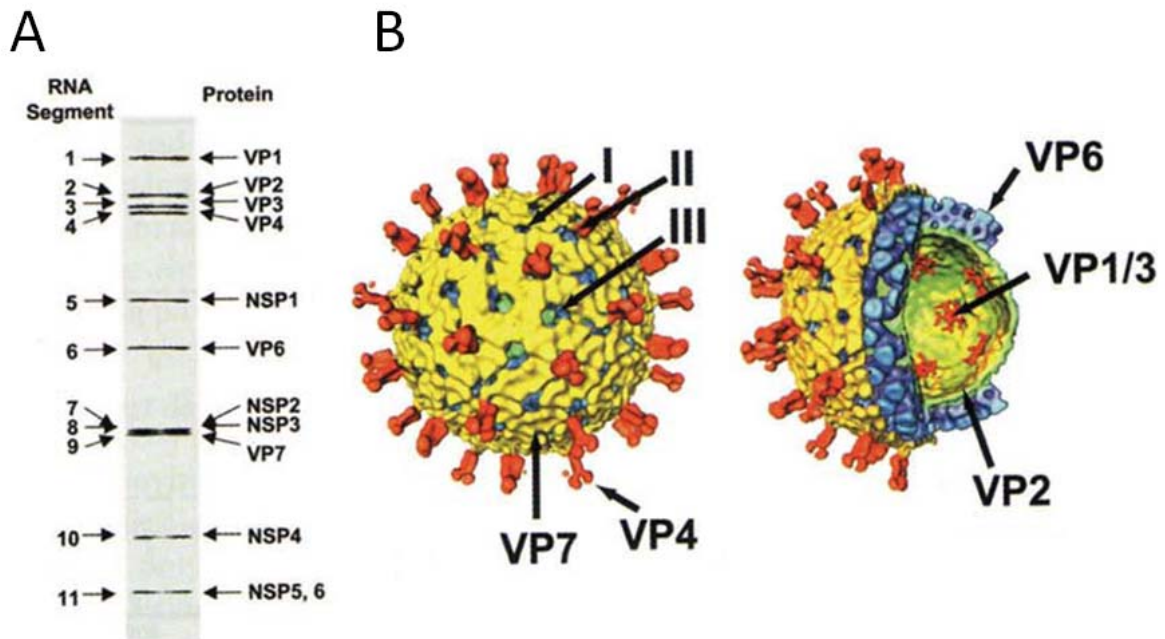


Figure 1.1. The structural organization of rotavirus: A) Illustration depicting the 11 dsRNA genome segments and their corresponding coding assignments. B) Illustration depicting the composition of the three concentric layers, along with the structural viral proteins found in each corresponding layer. The different classes of channels (I, II and III) are also indicated. Illustration taken from Desselberger *et al.*, (2009).

1.4.1. Viral proteins

The rotavirus genome, consisting of 11 segments of dsRNA, encodes for six structural and non-structural proteins. These proteins are named, based on their molecular weights, where VP1 (125 kDa) is the biggest of them all (Pesavento *et al.*, 2006). The six structural proteins are known as VP1, VP2 (102.7 kDa), VP3 (88 kDa), VP4 (88 kDa), VP6 (44.9 kDa) and VP7 (37.2 kDa). The indicated molecular weights of the viral proteins are based on that of rotavirus strain SA11. Each of these viral proteins, contain different functions and locations. The structural proteins form the concentric layers of the triple-layered virion particle. The three concentric layers can be integrated into an internal, intermediate and external layer (Estes and Kapikian, *Fields Virology*, 2007).

1.4.1.1. Internal layer

The internal layer contains the three structural proteins namely, VP1, VP2 and VP3. These proteins (along with VP6) form the necessary enzymatic machinery which is used during the synthesis of capped mRNA transcripts from the genomic segments of dsRNA (Pesavento *et al.*,

2006; Jayaram *et al.*, 2004). VP1 and VP3 are respectively known as RNA-dependent RNA polymerase and guanylyl and methyl transferase (Valenzuela *et al.*, 1991; Chen *et al.*, 1999; Liu *et al.*, 1992). Rotavirus particles that only exhibit the internal layer are referred to as single-layered particles (SLPs).

VP2 surrounds the segmented, viral genome of the rotavirus virion (Prasad *et al.*, 1996). Research performed by Prasad and co-workers (1996) and Zeng and co-workers (1998), respectively, suggested that VP2 is extremely important in the organisation of the genomic core dsRNA and endogenous core transcription apparatus. The inner core protein possesses the binding activity of both dsRNA and single stranded RNA (ssRNA). According to Jayaram *et al.* (2004) only VP2 exhibits the ability of assembling independently in order to form the SLP. This suggests that the essential assembly determinants, of the other structural proteins, are found in VP2.

1.4.1.2. Intermediate layer

The intermediate layer consists of 260 trimers (Prasad *et al.*, 1988) of VP6. These trimers are sandwiched between the external ($T=13$) and internal ($T=1$) capsid layers, formed by VP7 and VP4, and VP2, respectively.

VP6 plays an important role in maintaining the structural integrity of the virus particle. It maintains the appropriate organization of the transcriptional complex, which is compiled with core proteins (Estes and Cohen 1989). Studies by Zeng *et al.* (1994) showed that VLPs formed in the presence of the VP6 layer (surrounding the VP2 layer) exhibit an increased morphologic homogeneity and continuing stability. The amino acid points of interaction of VP6 with the other proteins (VP2, VP4 and VP7) are thought to be the most conserved. Biochemical studies indicated that although VP6 lacks the enzymatic machinery necessary to transcribe dsRNA, it is still required during the endogenous transcription process. VP6 might function in translocating the budding transcripts during the endogenous transcription process (Lawton *et al.*, 2000).

The intermediate layer structural protein is highly immunogenic and antigenic. VP6 contains cross reactive epitopes that are typed as common- and subgroup epitopes. VP6 subgroup epitopes have been explored extensively for serotyping (Hoshino *et al.*, 1987). It is still unclear whether VP6 may play a role in the induction of protective immunity.

1.4.1.3. **External layer**

The external layer, or the TLP, is composed of 780 monomers (Prasad *et al.*, 1988) of VP7 (a glycoprotein) and 180 hemagglutinin VP4 spike proteins (Pesavento *et al.*, 2006). As mentioned earlier, these two surface proteins (VP7 and VP4) contain G- (glycosylated structure) and P-type (protease sensitivity) determinants, respectively. Both of the two external capsid proteins are the targets of both neutralizing and monoclonal antibodies (MAbs) (Matsui *et al.*, 1989).

➤ **Glycoprotein, VP7**

The VP7 glycoprotein is encoded by genome segment 9 and mainly contains N-linked high-mannose oligosaccharide residues. It is in all likelihood a trimer which is stabilised by calcium ions (Shaw *et al.*, 1993).

VP7 may modulate certain functions of VP4, such as cell attachment and cell entry (Beisner *et al.*, 1998; Méndez *et al.*, 1996). Furthermore, VP7 serves as an integral membrane protein (Kabcenell and Atkinson, 1985). Dormitzer and co-workers (2000) showed that the presence of calcium is required when producing VP7 trimers, since calcium may assist in maintaining the structural integrity of VP7. Alternatively, low calcium concentrations (achieved with calcium chelators such as EDTA) lead to the dissociation of the VP7 layer from the virion particle. This is an important event during the rotavirus replication cycle, as transcriptionally competent DLPs can be delivered to the cytoplasm of the host cell (Jayaram *et al.*, 2004). To summarize, VP7 is involved in the rotavirus entry and assembly steps, which respectively concerns membrane-displacement and membrane-disruption (Aoki *et al.*, 2009).

This capsid protein is the second most abundant and is highly immunogenic, since it induces neutralizing antibodies. Sabara and co-workers (1985) discovered a highly conserved fragment of VP7, which had the immune-dominant function of inducing neutralizing antibodies. Certain antibodies directed at VP7, inhibit the dissociation of the TLP into transcriptionally competent DLPs. This neutralises the virus, since these DLPs cannot reach the cytoplasm of the host cell for replication (Ludert *et al.*, 2002).

➤ **Spike protein, VP4**

Each rotavirus particle contains 180 unglycosylated (Shaw *et al.*, 1996) VP4 copies. The spike protein consists of a central body, two distal domains and an internal globular domain (“tucked” inside the VP7 layer) (Li *et al.*, 2009).

The VP4 protein is mainly involved in the attachment to sialic-acid containing cellular receptors, cell penetration, neutralization, virulence, hemagglutination (Shaw *et al.*, 1996) and host range specificity. The spikes contain VP4-specific monoclonal antibodies, as confirmed by cryo EM studies (Prasad *et al.*, 1990; Tihova *et al.*, 2001).

❖ **VP5* and VP8***

In order for rotavirus to infect a cell, VP4 has to be converted to VP5* and VP8* (Shaw *et al.*, 1996; Pesavento *et al.*, 2006). The properties of these cleaved proteins are given in Table 1.1. The modification of VP4 into VP5* and VP8* is achieved by cleaving the VP4 protein with intestinal lumen protease, trypsin (Angel *et al.*, 2007; Jayaram *et al.*, 2004; Lopez *et al.*, 1985). This fact is particularly important because rotavirus replication takes place in the protease rich environment of the small intestines’ enterocytes. The cleavage of VP4 functions to increase viral infectivity, although the molecular mechanism is not fully understood. The distal globular domain of the spike protein, VP4, is composed of VP8* and the internal globular domain of VP5* (Pesavento *et al.*, 2006) as depicted in Figure 1.2. Estes and Cohen (1989) illustrated two possible cleavage products of VP4 at either amino acid 241 or 247.

Table 1.1 - Characteristics of the VP4 trypsin cleavage products

Viral protein	Size (kDa)	Region on VP4	Amino acid range
VP8*	28	C- terminal region	1- 247
VP5*	60	N- terminal region	248-776

The multistep process of cell entry by rotavirus requires receptors containing sialic-acid along with integrins for primary- and post-attachment, respectively. Both VP5* and VP8* play important roles in the latter process. VP8* contains a hemagglutination

domain which interacts with the sialic acid receptors. VP5* permeabilizes membranes by interacting with the integral proteins (Mackow *et al.*, 1989). Whilst interacting with cellular receptors, the trypsin cleavage products (of VP4) remain in association with the virion (Fiore *et al.*, 1991; Ruggeri and Greenberg, 1991; Dowling *et al.*, 2000).

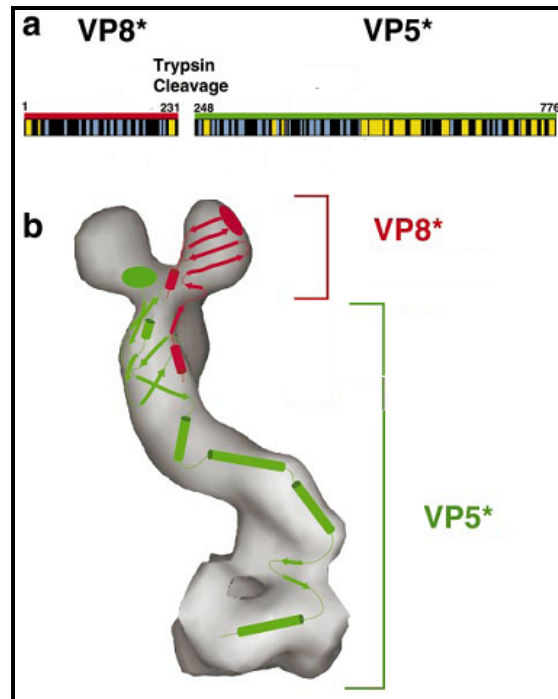


Figure 1.2 - The structural organization of VP4: A, the schematic representation of VP4 polypeptide showing the trypsin cleavage site as well as the coding regions of VP8* and VP5*. The following features are represented by these respective colours: VP8* in red, VP5* in green; and B, the schematic representation of the cleavage products, VP8* and VP5*. Although VP8* is located at the top of the monomer and VP5* located at the base, epitopes from both coding regions are situated in the head of the monomer. These epitopes are indicated with ovals. Although Figure 1.2 only indicates 231 amino acids for VP8*, the remainder of amino acids (232 – 247) form part of the trypsin cleavage site located on VP8*. Illustration taken: Tihova *et al.*, 2001.

1.4.2. Genome structure and organisation

As described in section 1.2.2 rotaviruses contain a genome of dsRNA with 11 segments. Prasad and co-workers (1996) showed the first structural visualization of the rotavirus genome through cryo-electron microscopy. The authors indicated that the transcription complexes (which are situated at the icosahedral vertices) are surrounded by RNA double helices. In turn, these

packed complexes are surrounded by viral dsRNA, in order to form a dodecahedral structure. Rotavirus virions contain their own necessary transcription machinery or RNA-dependent RNA polymerase in order to transcribe active mRNA from the segmented dsRNA genome. Evidence supporting this phenomenon states that deproteinized dsRNA of rotaviruses are not infectious (Cohen, J, 1977).

1.4.3. Interactions between viral proteins (VP4, VP6, VP7 and VP2)

A number of 132 channels are located inside the TLP and function as a connection between the different capsid layers. Three different types of channels have been distinguished. These channels are classified according to size and position in the virion. There are 12 type I channels, 60 type II channels and 60 type III channels (Estes and Kapikian, Fields Virology, 2007). These channels serve as a means of interaction between the various viral proteins. The interactions play an important role in the assembly and stability of infectious TLPs as well as the efficiency of disassembly of the virion when entering the host cell.

1.5. Rotavirus disease burden

Rotavirus infection causes gastroenteritis (fever, vomiting and diarrhoea), which leads to approximately 453 000 global deaths (Tate *et al.*, 2012) in children younger than five, annually. These deaths mainly occur in developing countries (such as sub-Saharan Africa and south Asia), and constitute approximately 5% of all child deaths (Glass *et al.*, 2006). Specifically, sub-Saharan Africa contains 6 of the 7 countries with the highest mortality due to rotavirus infection, estimated as 230 000 deaths per annum (Madhi *et al.*, 2010). Figure 2.3 illustrates the estimated rotavirus diarrhoea mortality globally. Adults can also suffer from rotavirus infections, especially those who travel can come in contact with young children. Both the elderly and hospitalized patients are also at risk (Pickering *et al.*, 1981; Vollet *et al.*, 1979; Marshall *et al.*, 2003). The most frequent cause of hospitalisations among young children is rotavirus diarrheal-associated disease. These gastroenteritis cases also lead to increased clinical visits and home care (Angel *et al.*, 2007). Although current vaccines do exist, there is an increasing need for the development of a safe and efficient non-replicating rotavirus vaccine, to reduce the disease burden; especially in sub-Saharan Africa.

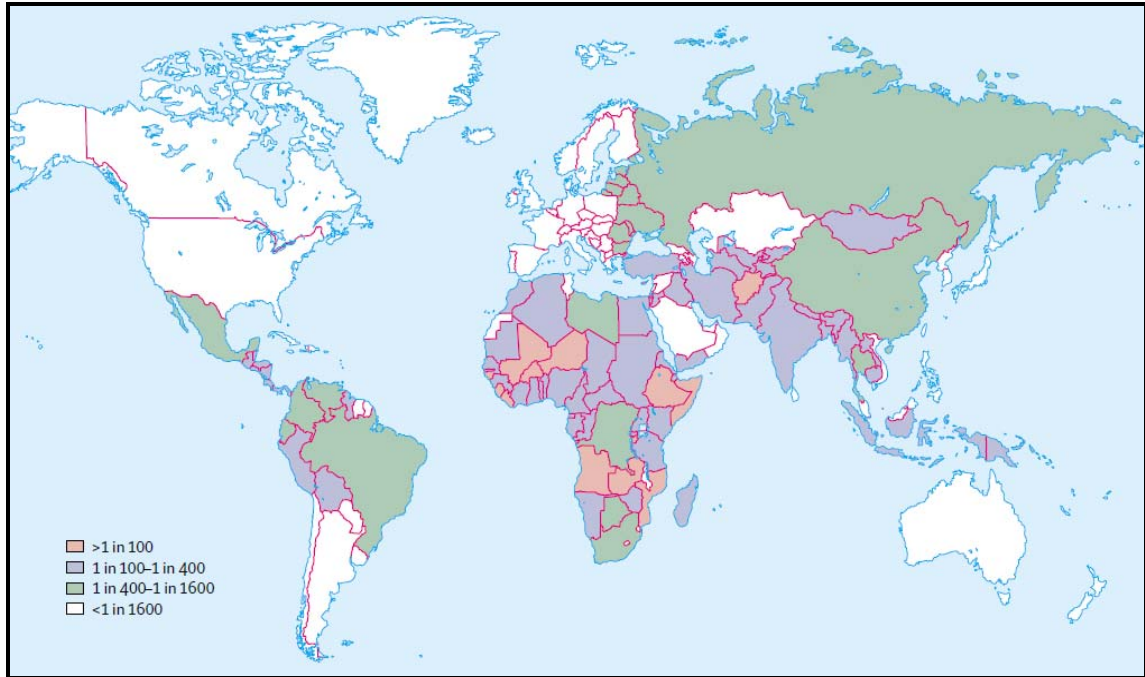


Figure 1.3 – The estimated rotavirus diarrhoea mortality of children younger than 5 across the world. Illustration taken from Glass et al., 2006.

Different strains occur in different geographical areas and can be a result of increased zoonotic transmission between human and animal rotaviruses. P1A[8]G1 strains occur less in Africa, Asia and South America, than in Australia, Europe and North America. The P[6]G9, G5 and G8 strains are, respectively, more frequent in India, Brazil and Africa. Outbreaks of rotavirus causing infections in both adults and children are rather rare (Angel *et al.*, 2007), since adults acquire immunity during childhood and most are not susceptible to certain rotavirus strain infections.

Over the past two decades the rotavirus genotypes G12 and G9 emerged worldwide. The latter genotype was specifically detected in the rotavirus strain G9P[6], which is prevalent in sub-Saharan Africa. Classification with the use of whole genome analyses, via pyrosequencing, yielded the identification of the genetic constellation and origin of G9P[6]. From the sequence analysis it was determined that the G9P[6] rotavirus strain, was a product of multiple reassortment events between the DS-1 and Wa-like strains. G9P[6] contained a DS-1-like genetic backbone with the substitutions of segment 9 (VP7) and segment 4 (VP4) as serotypes G9 and P[6] (Jere *et al.*, 2011). These two serotypes are not present in currently licensed rotavirus vaccines, which could result in a decrease in vaccine efficacy in sub-Saharan Africa.

1.6. Rotavirus pathogenesis

Rotaviruses can infect humans and animals at extremely low concentrations and are highly contagious. The virus can survive for months at room temperature in a stool sample or for days on surfaces found in the environment (Fischer *et al.*, 2004). The faecal-oral route often transmits the rotavirus from person to person, as well as fomites or countertops (Butz *et al.*, 1993). Infections are extremely hard to control and they often occur in nursing homes, day-care centres and hospitals. Practically all children are exposed to rotavirus infections prior to their third birthday, no matter the level of hygiene or food and water quality.

Rotavirus infections primarily occur in the enterocytes of the small intestines' jejunum. These differentiated enterocytes function to digest and absorb nutrients and water. Upon entry of the rotavirus into the enterocytes, the virion releases an exotoxin able to induce diarrhoea. The virus then obliterates the cells. The annihilation of these cells, lead to nutrient and water loss; which results in dehydration and malnutrition and can consequently result in death (Moon, 1994). Post-infection, large quantities ($10^9 - 10^{10}$ per gram) of shedded viruses can be detected in the stool of infected individuals.

Children suffer from a sudden onset of gastroenteritis, which lasts between 4 and 8 days. The clinical symptoms of children infected with rotavirus are nausea, vomiting, watery diarrhoea, dehydration, loss of appetite and abdominal pain (Staat *et al.*, 2002).

1.7. Rotavirus infectious cycle

The rotavirus infectious cycle cycle involves three steps: cell attachment, cell penetration and rotavirus replication. The entire infectious cycle of rotavirus is depicted in Figure 1.3. Rotavirus cell attachment is achieved with protease-sensitive VP4, which involves both an initial attachment and a post-attachment step. Trypsin protease cleavage of VP4 enhances the infectivity of the virus, since trypsinised viruses are able to enter cells more rapidly as opposed to non-trypsinised viruses (Kaljot *et al.*, 1988; Keljo *et al.*, 1988). As discussed in section 1.4.1.3, trypsin protease cleavage leads to the conformational change of VP4 to VP5* and VP8*. Receptors containing sialic-acid (SA) are involved in the initial attachment and interact with VP8*. Integrins interact with VP5* during the post attachment step (Coulson *et al.*, 1997; Guerrero *et al.*, 2000; Hewish *et al.*, 2000; Zarate *et al.*, 2000).

The cell entry of rotavirus is a multistep process which involves calcium-dependent endocytosis (Ruiz *et al.*, 1997): Prior to the infection of a host cell, the TLP needs to dissociate to a DLP, through the loss of the outer capsid (VP7). This is achieved by reduced concentration levels of calcium (discussed in section 1.4.1.3) in the endosomes. When dissociation has been completed, the virus particle can be lysed through the vesicle membrane, which leads to the escape of the DLP into the cytoplasm of the host cell (Ruiz *et al.*, 2000).

The replication of rotavirus occurs in three main stages. The first involves the translation and production of the structural and non-structural viral proteins. The replication, genome organisation and assembly of subviral particles (DLPs) occur in stage two. The assembly of mature virus particles in the endoplasmic reticulum and cell lysis concludes the third and final stage (Jayaram *et al.*, 2004). Both the replication and assembly steps occur in the viroplasm.

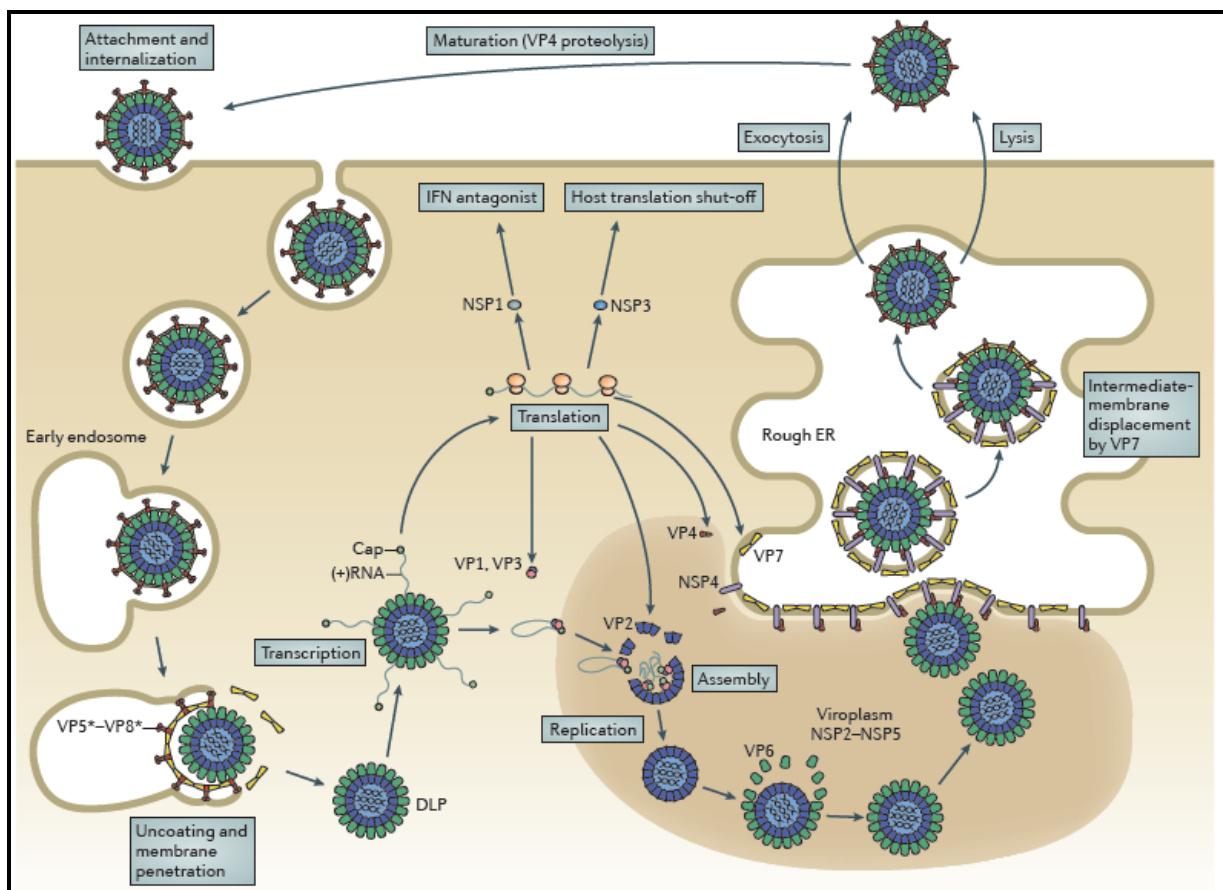


Figure 1.4 – The infectious cycle of rotavirus: Rotavirus attaches to the cell with the use of protease-sensitive VP4. As explained previously (section 1.4.1.3) VP4 converts to VP5* and VP8*, upon the cleavage of VP4 by trypsin protease. VP8* interacts with cell surface receptors that contain sialic-acid (SA), which binds rotavirus to the surface of the cell. With the use of endocytosis, rotavirus enters the cell where low calcium concentrations trigger the uncoating of the external layer (consisting of VP7)

after which VP5* penetrates the endosome membrane. With the DLPs present in the cytosol of the cell and the uncoating of the external layer the RNA dependant RNA polymerase complex is activated. The dsRNA genome segments are transcribed as capped positive-sense RNAs. Once transcribed these positive-sense RNAs are utilised to synthesise either the rotavirus viral proteins or negative-sense RNAs for genome segment replication. An interaction between NSP2 and NSP5 form viroplasm. These viroplasms sequester the components utilised during genome replication and subviral particle assembly. When the replication complex binds to the 3'ends of the positive sense RNAs the packaging of the genome segments begins. The synthesis of the dsRNA by VP1 is triggered by the assortment of VP2 around the replication complex. Thereafter VP6 assembles onto the internal layer to form the DLP. The assembly of VP7 onto the intermediate layer of the DLP is still vague, but a current assembly model proposes that NSP4 recruits the DLPs and VP4 to the surface of the endoplasmic reticulum (ER) membrane. These DLP-VP4-NSP4 complexes bud into the ER where VP7 (located in the ER) assembles onto the intermediate layer to form the TLP. When the TLPs are released into the gastrointestinal tract, these are once again exposed to the trypsin proteases which convert VP4 to VP5* and VP8*; and thus, completing the full circle of the rotavirus infectious cycle. Illustration taken from Trask *et al.*, 2012.

1.8. Host response upon natural rotavirus infection and correlates of protection

Upon natural infection, rotavirus elicits innate and acquired (humoral and cellular) immune responses.

1.8.1. Innate responses

Studies link rotavirus infections with innate immune responses, because of interactions of NSP1 with IFN regulatory factor 3 (Graff *et al.*, 2002). Although the effects of innate immune responses are unfamiliar in humans, this type of immunity acts as a modulator during *in vitro* rotavirus infection (Greenberg and Estes, 2009). Various *in vivo* and *in vitro* studies concerning the interferon (IFN)-induced antiviral effects of the innate immune response, have found that IFN types I and II (which have the ability to limit infection) levels increase when children and animals are infected with rotavirus (Wang *et al.*, 2007; Lecce *et al.*, 1990). Although administrations of these IFNs in cattle and pigs showed positive results of a reduction of diarrhoea associated with rotavirus infection (Schwers *et al.*, 1985), they had little effect on diarrhoea in mice (Greenberg and Estes, 2009). If and when IFN signalling is blocked or stopped, it amplifies the virulence of particular rotavirus strains and induces lethal diseases such as those found in the pancreas (Feng *et al.*, 2008).

1.8.2. Humoral responses

Primary rotavirus infections, resulting in severe gastroenteritis, protects against subsequent re-infections and rotavirus disease. Severe gastroenteritis was not associated with secondary

rotavirus infections. Although it was found that asymptomatic infections occur 3-4 times more frequently than symptomatic infections, both displayed similar degrees of protection. Chibo and co-workers (1986) reported on serotype-specific protection against rotavirus infection, which was related to the increased levels of neutralizing antibodies. Upon primary rotavirus infection, both homotypic and heterotypic antibody responses have been reported. These responses might indicate the presence of cross-reactive antibody epitopes. Immunoglobulin A (IgA) is a good correlate for protection as these neutralizing antibodies react with epitopes on rotavirus, thus providing heterotypic protection against rotavirus infection. During a study (Velazquez *et al.*, 2000) the authors found that children with a high level of serum IgA were protected against rotavirus infection as well as severe rotavirus diarrhoea, but those with a high level of serum immunoglobulin g (IgG) were only protected against rotavirus infection but not against severe diarrhoea. During a similar study, Hjelt and co-workers (1987) concluded that the total serum levels of IgA were linked with less severe disease, but IgG was not. Although the clinical significance of non-neutralizing antibodies, directed against VP2, VP6, NSP2 and NSP4, remains unclear, these antibodies are also correlated with protection. B-cells have been indicated as a local gut protective action against infection as they carry a gut specific homing receptor.

1.8.3. Cellular immune responses

After infecting adult mice with the murine rotavirus, T-cells demonstrated specific roles in generating immunity. CD8⁺ T-cells (also known as cytotoxic T cells) destroy specific cells, containing specific antigens, and aids in the resolutions of primary infections. CD4⁺ T-cells (also known as T-helper cells) assist in generating rotavirus-specific intestinal immunoglobulin A (IgA), and subsequently providing long-term protection against infection (Franco *et al.*, 1999).

1.9. Rotavirus vaccination

1.9.1. Vaccine history

The development of an effective rotavirus vaccine dates back to 1983, where Vesikari and others performed the first trial of the bovine-derived vaccine candidate, RIT 4237. Their findings established that the efficacy of live oral rotavirus vaccines against severe rotavirus diarrhoea and protection against human rotavirus strains was feasible with the use of animal derived strains. In addition, the protection efficacy of the vaccine was greater against severe disease as

opposed to mild disease. The vaccine development was, however, abandoned because of contradictory results regarding efficacy in developing countries (Vesikari *et al.*, 1984).

RotaShield was a human-simian reassortant rotavirus vaccine. It was developed in the 1990's by A. Z. Kapikian at the National Institutes of Health (Kapikian *et al.*, 1996). RotaShield contained four VP7 components, which are serotypically distinct from one another. The vaccine prevented severe diarrhoea in the US and Venezuela in young children. Its genome was derived from a heterologous simian host, which made it an attenuated vaccine. The vaccine was licensed in 1998 in the US, but an association between gut intussusceptions and vaccine administration was observed and the vaccine was subsequently withdrawn in 1999 (Murphy *et al.*, 2001). Intussusception is known as a pathological event during which the intestine will invaginate itself and becomes obstructed. The inability of the gut to absorb nutrients, at the site of obstruction, leads to malnutrition. This is followed by gut tissue's local necrosis (Angel *et al.*, 2007) and ultimately leads to the death of the patient.

1.9.2. Current vaccines

As mentioned previously, natural rotavirus infection studies indicated that although mild asymptomatic infections might take place, primary infections protect against consecutive severe gastroenteritis. Thus, early-life vaccination prevents most cases of severe rotavirus disease and consequently their complications, because these vaccinations mimic first natural infections (Parez, 2008).

Currently, there are two vaccines for rotavirus infections, licensed in Europe, USA and several other countries (Parez, 2008). RotaTeq and Rotarix are live, oral, attenuated viruses and were developed to accomplish broad immunity against the diverse rotavirus circulating strains.

The phenomenon of genetic reassortment has been beneficial to vaccine development, in particular the development of RotaShield and RotaTeq (Angel *et al.*, 2007). More particular, the hypothesis concerning host-range restriction (HRR), where animal hosts will attenuate in humans, is the basis of development of both of these vaccines (Pérez-Schael *et al.*, 1997).

1.9.1.1. RotaTeq

RotaTeq was developed by Merck Vaccines (Whitehouse Station, NJ, USA) and was licensed in 2006 in Europe and the United States of America (USA). It was prepared consisting of ten

genome segments from a parental bovine strain (W3C) and a single human rotavirus capsid encoding genome segment. The latter genome segment was selected from the most commonly occurring serotypes, namely G1, G2, G3, G4 and P1A. One of each of these genome segments was combined with the ten genome segments from W3C, to form the five reassortants, respectively (Heaton *et al.*, 2005), through various processes of continuing passaging and screening. Thus, RotaTeq is a pentavalent vaccine. Figure 1.4 illustrates the composition of RotaTeq. Children receive 3 doses at the age of 2, 4 and 6 months (Greenberg and Estes, 2009). RotaTeq provides 70% - 90% protection against severe diarrhoea (Angel *et al.*, 2007).

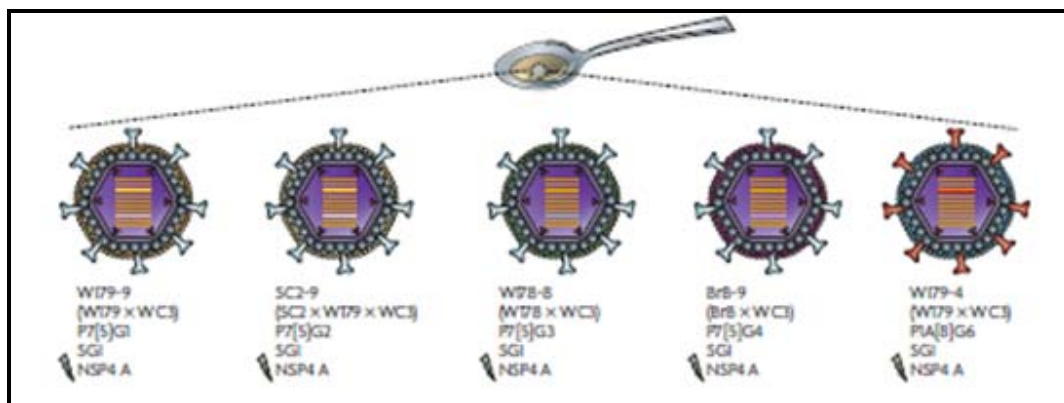


Figure 1.5. Composition of the existing live, oral, attenuated vaccine RotaTeq: The figure illustrates the five reassortant attenuated viruses occurring in the vaccine. Each of the reassortants contains ten genome segments from a parental bovine strain (W3C), and a single human rotavirus capsid encoding genome segment. This particular segment differs for each reassortant and was selected from the most commonly occurring serotypes (namely G1, G2, G3, G4 and G6); thus, resulting in five different attenuated rotavirus genome reassortants. Illustration taken from Angel *et al.*, 2007.

1.9.1.2. Rotarix

Rotarix or RIX 4414 was developed by GlaxoSmithKline (Rixensart, Belgium) and was licensed in 2006 in Europe and the United States of America (USA). The vaccine was derived from the 82-12 strain, which was a representative of one of the most commonly occurring human rotavirus serotypes (P1A[8]G1). The rotavirus strain was isolated from the stool sample of a naturally infected boy who suffered from gastroenteritis (Bernstein *et al.*, 1999). Rotarix was developed on the basis that a primary natural infection with a rotavirus strain efficiently prevents a secondary, more severe reinfection. Rotarix is a monovalent vaccine, which is illustrated in Figure 1.5. The vaccine is a virus capable of stimulating an immune response and creating immunity but not causing illness, known as a human attenuated vaccine. Children receive Rotarix in two doses at the age of 2 and 4 months (Greenberg and Estes, 2009). Rotarix provides 70% - 90% protection against any diarrhoea (Angel *et al.*, 2007).

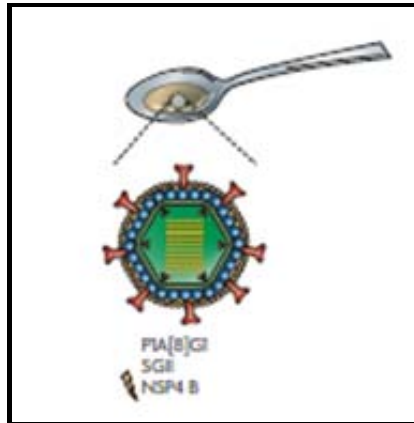


Figure 1.6. Composition of the existing oral, live, attenuated vaccine Rotarix: The figure illustrates the attenuated virus occurring in the vaccine, known as P1A[8]G1. Illustration taken from Angel et al., 2007.

1.9.1.3. Vaccine efficacy concerning RotaTaq and Rotarix

RotaTaq and Rotarix were licensed for their effective protection against severe diarrhoea and their reduction in hospitalization cases by more than 40%. The vaccines demonstrated no increased risk of intussusception (Ruiz-Palacios *et al.*, 2006; Vesikari *et al.*, 2006). In 2010, Madhi and colleagues determined a combined efficacy of approximately 61.2%, for Rotarix vaccine, in clinical trials involving South Africa and Malawi. The respective efficacies determined for South Africa and Malawi, were 76.9% and 49.4%.

Some drawbacks are associated with the use of oral attenuated live viruses and give rise to implementation boundaries in both developing and developed countries. Firstly, Payne and co-workers (2010) and Bucardo and co-workers (2012) reported on reassortments occurring between certain genome segments of the vaccine strain and wild-type virus strains. This phenomenon poses the risk of generating a more virulent virus and therefore may lead to infection. Secondly, current licensed vaccines are composed of strains occurring in developed countries. Thus, existing vaccines do not necessarily address the rotavirus strain diversity in developing countries. Thirdly, transmitted maternal antibodies (occurring in breast milk) have a potentially inhibitory effect on rotavirus vaccination in babies and can bind to the antigens of the virus, thus causing the antigens never to reach their location of interest (the enterocytes in the jejunum) (Perez, 2008).

In the case of the first dose administration of the RotaShield vaccine, the incidence of intussusception increased with an increase in age. Therefore RotaTeq and Rotarix cannot be administered before or after the ages of 6 and 26 weeks (Europe) or 6 and 32 weeks (USA) because whether these vaccines may induce intussusception, when the first dose is administered in older children, is unknown. In contrast, it has been proposed that the age restrictions on first dose vaccine administrations in developing countries should be lifted since the deaths caused by vaccine-associated intussusception will be far less than the lives saved by vaccination (Patel *et al.*, 2012). The development of non-replicating vaccines is of great importance; because they will not present the disadvantages associated with current vaccines (Parez, 2008).

1.9.3. Experimental vaccines

Some impediments concerning safety and production costs of the existing vaccines still remain. Non-replicating rotavirus vaccines are being considered as an alternative approach for vaccine development (Vieira *et al.*, 2005), as they do not propose the drawbacks associated with current vaccines. These alternative vaccines include the development of virus-like particle (VLP) vaccines and inactivated vaccines.

Virus-like particles (VLPs) have been used to unravel the structures of various viruses such as bluetongue, influenza, poliovirus, etc. VLPs have also been used to determine the roles of structural and non-structural proteins in viruses and for the examination of virus-host-interactions. These particles are an attractive alternative as non-live vaccine candidate for rotavirus vaccination, as the rotavirus-VLP system exhibits the equivalent antigen presentation of rotavirus (Parez, 2008), but is not associated with any of the side effects of the replication of the virus, since it does not contain the dsRNA genome of the virus. Thus, VLPs are excellent candidates for vaccination against rotavirus (Parez, 2008; Agnello *et al.*, 2006; Jiang *et al.*, 2006; O'Neil *et al.*, 1997; Parez *et al.*, 2006; Ciarlet *et al.*, 1998; Conner *et al.*, 1993; Crawford *et al.*, 1994). The assembly of the rotavirus-VLP includes the expression of the four major capsid proteins in insect cells (Crawford *et al.*, 1994), where three of these proteins contain antigenic properties. Out of all the structural proteins, only the intermediate (VP6) and external capsid (VP7 and VP4) proteins play an important role in the immune response of the host because they contain major antigenic properties that the others do not.

1.9.3.1. *Baculovirus expression vector system (BEVS)*

The baculovirus expression system was developed in the early 1980's by researchers at Monsanto. It has the ability of expressing a large number of proteins that imitate authentic viral proteins. This system enables the efficient and rapid production of recombinant baculoviruses. The BEVS used during this project was the Bac-to-Bac system from Invitrogen. The baculoviruses are specifically generated through the site-specific transposition of an expression cassette, containing the gene of interest, into a baculovirus shuttle vector (called a bacmid). This bacmid is propagated in DH10Bac *E. coli* bacterial cells. The production process, of recombinant baculoviruses, is demonstrated in Figure 1.6.

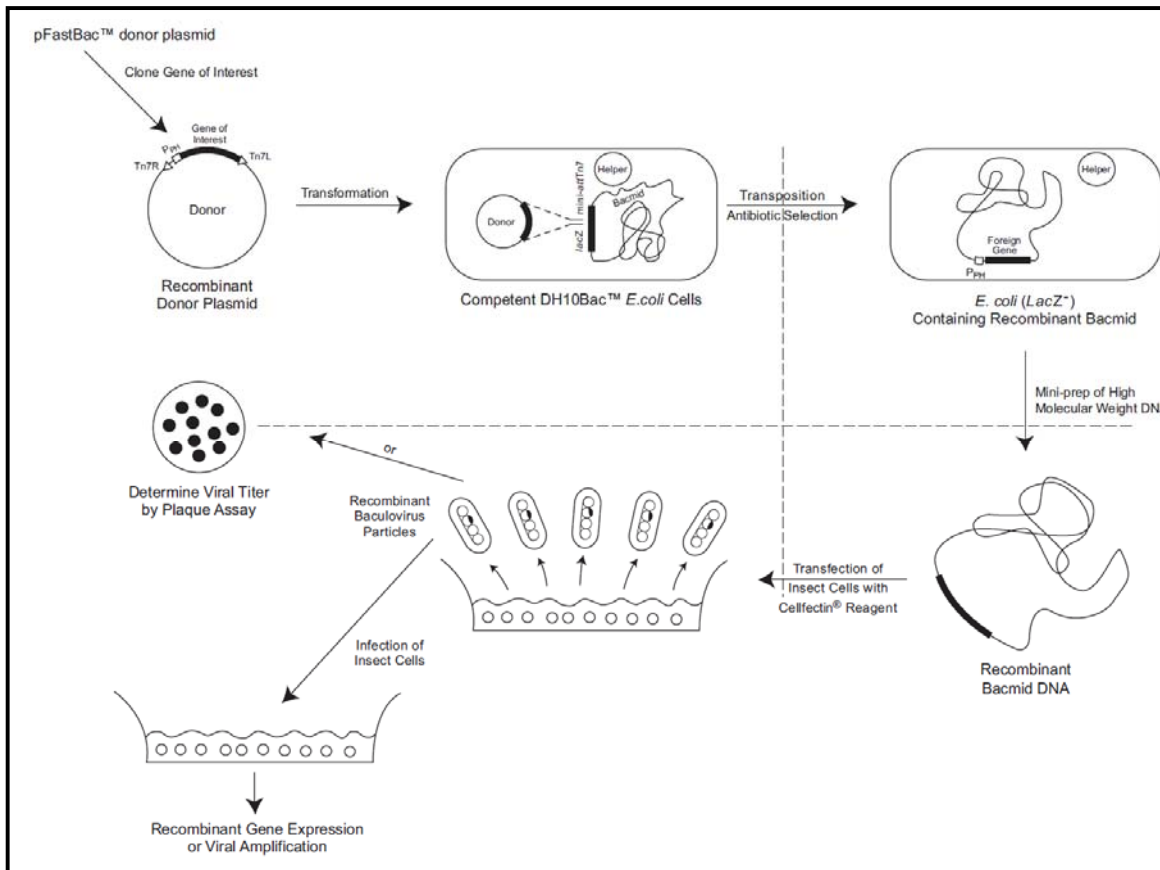


Figure 1.7 - The Bac-to-Bac system: The donor plasmid containing the gene of interest is propagated in ACC DH10Bac *E. coli*, which contains the baculovirus genome. Upon the transposition of the gene of interest (encoding a specific structural rotavirus protein) into the baculovirus genome, the recombinant bacmid is constructed. The recombinant bacmid DNA is transfected into Sf9 cells, which ultimately results in to the accumulation of certain recombinant rotavirus structural proteins. Illustration taken from Bac-to-Bac manual from Invitrogen.

There are many advantages in using the baculovirus expression system to produce VLPs. Firstly; the expression system contains no contaminants from mammalian sources. Secondly; the expression vectors are very flexible and easy to handle. Thirdly; there is a high recovery of antigens that have folded correctly, because of the production of bulk amounts of recombinant proteins in cell cultures (with high-density), generated in eukaryotic cells. Fourthly; the risk of culturing opportunistic pathogens is decreased, since the insect cells, used during the capsid assembly, are not dependent on supplements derived from mammalian cells. Fifthly; the host range of the baculovirus is very restricted and therefore does not represent any possible threat for the vaccinated individual (Noad and Roy, 2003). Next; cytoplasmic extracts are mainly used during the purification of most VLPs while the baculovirus is localized primarily in the nucleus of insect cells used during cell culture preparation and the baculovirus can be inactivated without difficulty through chemical treatment (Noad and Roy, 2003; Rueda *et al.*, 2000). Lastly; the baculovirus expression system can be used during extensive vaccine productions (Noad and Roy, 2003; Maranga *et al.*, 2002).

The baculovirus expression system was successful in expressing virus capsid proteins of, among others, rotavirus (Crawford *et al.*, 1994; Sabara *et al.*, 1991) with the capacity of forming VLPs (Roldao *et al.*, 2006). Different rotavirus proteins self-assemble into VLPs inside insect cells, which were co-infected with recombinant baculoviruses. These baculoviruses express a variety of rotavirus structural proteins (Parez, 2008). Crawford and co-workers (1994) and Labbe and co-workers (1991) stated that recombinant baculoviruses co-expressing VP2 and VP6 produce double-layered particles (DLPs) and when co-expressing VP2, VP6 and VP7 (in the absence or presence of VP4) triple-layered particles (TLPs) are produced.

1.9.3.2. Rotavirus-like particle (rota-VLP) production

The production of rotavirus-like particles is a multifaceted process (Figure 2.7), by which recombinant baculoviruses (expressing the structural proteins of interest) are used as transport vectors into host cells. These recombinant baculoviruses adsorb into cells by means of endocytosis. The nucleocapsids of the viruses (which contain the viral genes of interest) are released into the cytoplasm of the host cell, as a result of pH variation. Subsequently, the nucleocapsids migrate to the cell nucleus, where the viral genes of interest are presented. The replicated baculoviral DNA is, subsequently, transcribed into the corresponding mRNA by the RNA polymerase. After transportation of mRNA to the ribosomes, the viral proteins are produced. Upon their production, structural capsid proteins spontaneously assemble into

rotavirus-like particles, which in turn are released into the extracellular region (Roldao *et al.*, 2007).

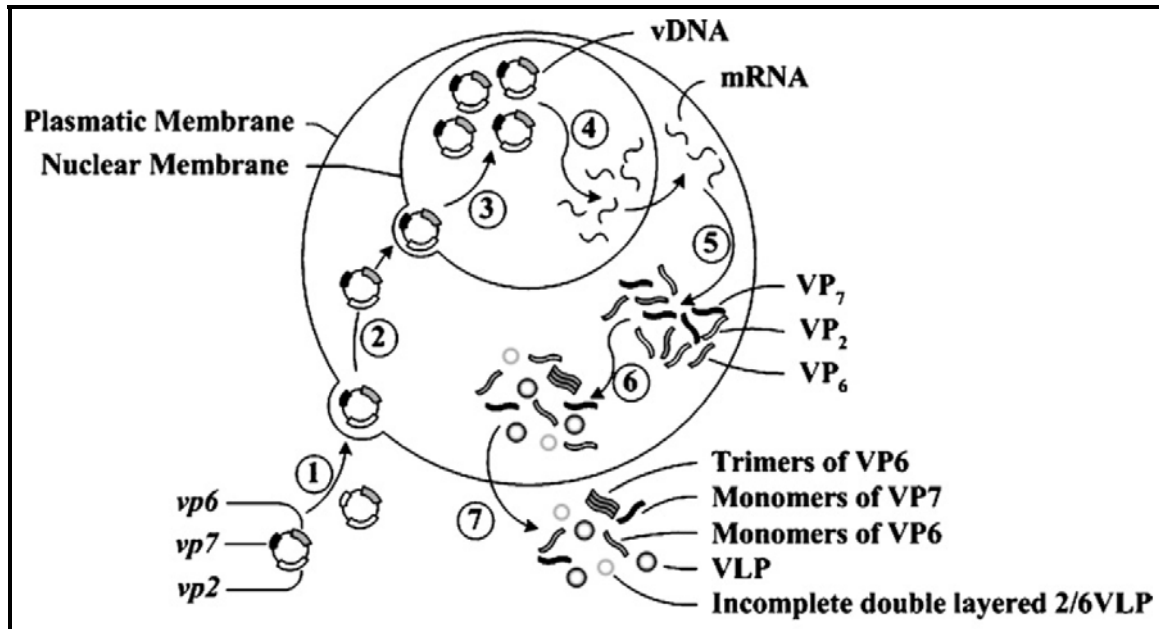


*Figure 1.8 - A schematic representation of the multifaceted rotavirus-like particle production process: 1) Adsorptive endocytosis of recombinant baculovirus expressing the genes of interest in the cell; 2) migration of the recombinant baculovirus to the nucleus of the cell; 3) the replication of the viral DNA; 4) the transcription of the viral DNA into the corresponding mRNA; 5) the synthesis of the expressed viral proteins, 6) the assembly of rotavirus-like particles with synthesised proteins; 7) the release of the rotavirus-like particles and unassembled protein structures into the extracellular medium. Illustration taken from Roldão *et al.*, 2007.*

Many determining factors and challenges influence the particle production process. The first and probably the most important factor is the quantity of expressed proteins in relation to each other. VP2 and VP6 have been shown to form structures, incapable of rotavirus virus-like particle (RV-VLP) assembly. VP2 forms an insoluble aggregate of SLPs and VP6 forms nanotubes of approximately 45nm. The authors of Mena and co-workers (2005) proposed a feasible method of efficient RV-VLP production, where the recombinant proteins are simultaneously expressed by all of the cells. This does, however, not refer to protein production quantity, as the production of high quantities of the recombinant proteins may lead to the formation of insoluble protein aggregates. Secondly, the transcription and translational rates of each individual recombinant protein plays a significant role, as the recombinant proteins differ in characteristics and size. Palomares and co-workers (2002) reported that the production rate is indirectly associated with the molecular weight of the protein. As the molecular weight of the protein increases, the production rate of the protein decreases. Thirdly, the primary drawback concerning the quantification and characterization of the rotavirus virus-like particles (RV-VLPs) is the

challenge of differentiating between the various particle types, due to the small difference in size. Fourthly, the location of intracellular accumulation also differs from protein to protein. These locations are displayed in table 1.2. In turn, the differences in accumulation locations propose setbacks of their own, concerning the purification of the various RV-VLPs.

Table 1.2 – The accumulation sites of various rotavirus-like particles

Rotavirus-like particles	Site of accumulation	References
SLPs	Intracellular region	Labbe <i>et al.</i> , 1991; Mena <i>et al.</i> , 2006
DLPs	Either intracellular or extracellular	Jiang <i>et al.</i> , 1998; Mena <i>et al.</i> , 2006; Castro-Acosta <i>et al.</i> , 2010; Benavides <i>et al.</i> , 2006
TLPs	Extracellular	Jiang <i>et al.</i> , 1998; Castro-Acosta <i>et al.</i> , 2010

1.9.3.3. Other expression systems

Various other systems could be considered when expression rotavirus recombinant proteins. Among these are: bacteria, yeast and mammalian cultured cells. The use of an expression system depends primarily on the properties of the protein of interest. Factors such as production cost and complexity of the protein should be considered.

- Bacteria

Bacteria expression systems propose numerous advantages such as the availability of various expression vectors, the low cost of culturing media and the suitable yield of recombinant proteins in a short period of time. Unfortunately, there has not been any success thus far in producing rotavirus-like particles in bacteria.

- Yeast

Due to the eukaryotic biosynthetic mechanisms, as well as easy handling and bacteria-like growth, yeast expression systems are attractive hosts for the expression of proteins that require post-translational processing. The production of VLPs in yeast has been reported by Rodrigues-Limas and co-workers (2011). The authors cloned rotavirus genome segments 2, 6 and 9 encoding VP2, VP6 and VP7 respectively, (using different plasmids with several promoter combinations) into four strains of *Saccharomyces cerevisiae*. TLPs were visualised with TEM. Of the virus-like particles obtained, only 41% were triple-layered, as a result of inefficient expression or assembly of VP7 onto the intermediate particles.

- Mammalian cells

Although this expression system is much more expensive than expression with yeast or bacteria, these cells are capable of producing glycoproteins, with the use of a glycosylation process, very close to the one utilised in humans. In higher mammals, glycosylation plays an important role in the recognition of foreign proteins. The latter is an important aspect concerning the immune system of the host. The production of DLPs in mammalian cells (CV-1) was reported by Gonzalez and Affranchino (1995). The production of DLPs and TLPs by mammalian cells, MA104, was reported by Trask and Dormitzer (2006).

1.9.3.4. Rota-VLP vaccine induced immune response studies

i. Animal models

Various animal models have been used to study the protective mechanisms against rotavirus infection and diarrhoea. Of these models, only two have been used during VLP immunisation studies. These animals include murine and neonatal gnotobiotic pig models. Each model presents some advantages and disadvantages. The murine or adult mice models are favoured for their small size and accessibility. Furthermore, several virulent rotavirus strains exist for mice and the immunological reagents, used to quantify and manipulate the model, are easily accessible. Mice are primarily infection resistance models, since they stay susceptible to rotavirus their entire life. Piglets are, however, the model of choice concerning rotavirus protection studies since they closely mimic human rotavirus pathogenicity. These models remain susceptible to infection for longer periods of time and can be infected symptomatically with virulent rotavirus strains from both humans and pigs (Greenberg and Estes 2009; Franco *et al.*, 1999).

ii. Immunisation studies

VLPs have been proven to stimulate effective B-cell mediated immune responses, CD4 proliferative responses and cytotoxic T lymphocyte responses (Schirmbeck *et al.*, 1996, Paliard *et al.*, 2000, Murata *et al.*, 2003).

Previous immunisation studies (Parez *et al.*, 2004) showed that the rotavirus intermediate capsid protein, VP6, interacts with a fraction of human naïve B-cells through the use of surface immunoglobulins. Protective immunity was obtained in, among other animal models, mice and gnotobiotic pigs. Furthermore, various reports state that immunisation with rotavirus DLPs induce protective immunity (Coste *et al.*, 2000; Fromantin *et al.*, 2001; Shuttleworth *et al.*, 2005; Gonzalez and co-workers (2004). Corthésy and co-workers (2006) reported that through an

intracellular antiviral effect, non-neutralizing IgA directed against the intermediate capsid protein (VP6) can mediate protection.

McNeal and co-workers (1998) showed that when VP4 and VP7 viral proteins corresponded with the serotype of the infected virus, TLPs were more efficient than DLPs. These results imply that neutralizing antibodies were not necessary during efficient immunity, even though they played a significant role in protection. In addition, non-neutralizing antibodies might be important during protection after non-living rotavirus vaccine immunization, since adult mice could not generate neutralizing antibodies, because the vaccines lacked the two viral surface proteins, VP4 and VP7 (Ward, 2008).

Immunisation with an engineered VLP containing a fused protein VP2-8, along with VP6 and VP7, obtained protective immunity against rotavirus infection in mice, with mucosal and systemic immune responses.

1.9.3.5. VLP vaccine advantages and disadvantages

These VLP vaccines offer many advantages. Firstly, they have reduced risks because the vaccine does not contain any infectious genetic material and therefore does not have the ability to replicate (Parez, 2008). Secondly, the production of these vaccines has an improved quality control, because production of the vaccine can be monitored more precisely. Thirdly, because these vaccines are not administered orally, maternal antibodies (present in the breast milk of babies) cannot bind to the antigens present on the VLPs, and prevent these antigens from reaching the enterocytes of the jejunum. Fourthly, the small size of VLPs enable simple uptake by dendritic cells. The structural epitopes located on the VLPs play an important role during dendritic B cell activation. Fifthly, foreign proteins may be inserted into the core of the VLP, which in turn may result to folding into highly immunogenic structures. Lastly, VLPs can provide a broader range of protection, since these particles can be engineered to contain structural proteins corresponding to different rotavirus strain serotypes (Crawford *et al.*, 1999).

VLP vaccines do however have drawbacks and higher concentrations of increased doses are often needed to comprise an equal protective effect as an attenuated virus vaccine would. As a result, these subunit vaccines are more expensive than an attenuated virus vaccine (Noad and Roy, 2003).

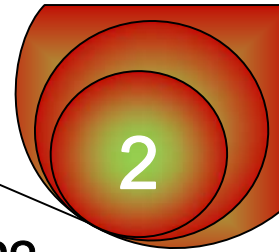
1.10. Motivation of the study

As discussed above, rotavirus infections are extremely problematic, causing hundreds of thousands of deaths of young children, worldwide. Current vaccines, addressing rotavirus infections, are questionable concerning their safety, specificity and cost in developing countries. A non-live vaccine approach at the NWU involves the development of a new generation VLP-vaccine that is not only safer but might also be more effective, since the vaccine is based on serotypes prevalent in sub-Saharan Africa. The vaccine addresses infections of the disease in developing countries and may potentially improve the socio-economical status of poor communities.

1.11. Aims of the study

The overall aim of this study is to engineer and optimise the expression of rotavirus-like particles in insect cells using a local South African G9P[6] rotavirus strain. The following objectives illustrate the specific focus areas of this M.Sc.:

1. Construct the G9P[6] rotavirus-like particle dVP2*8/6/7 (Chapter 2).
2. Verify the expression of several engineered rotavirus recombinant protein combinations (VP2/6, VP2/6/7, VP2/6/7/4, dVP2*8/6/7) in insect cells (Chapter 3).
3. Visualise rotavirus-like particles with transmission electron-microscopy (Chapter 3).



CHAPTER 2:

CONSTRUCTION AND EXPRESSION OF dVP2-8*/VP6/VP7 PARTICLES OF A SOUTH AFRICAN G9P[6] ROTAVIRUS STRAIN

2.1. Introduction

As described in Chapter 1, obtaining a high yield of VLPs that express the rotavirus surface spike protein VP4 is quite difficult. In addition, it has been reported that the VP4 spike protein is structurally very unstable (Parez *et al.*, 2006). Most of the VP4 neutralising linear B-cell epitopes are located on VP8*. This suggests a probability that VP8* may play a significant role in protective immunity (Larralde *et al.*, 1991; Padilla-Noriega *et al.*, 1995; Taniguchi *et al.*, 1988). Furthermore, Crawford and co-workers (1994) proposed a feasible method of expressing the epitopes of VP8* and VP4. They recommended expression of VP8* and VP4 in the presence of VP7 originating from the same strain.

The binding activity for both dsRNA and single-stranded RNA (ssRNA) is located within amino acids 1 -132 of VP2. When any number of amino acids is removed from this region, the RNA binding ability of VP2 is abolished (Labbé *et al.*, 1994). Further research was performed on the three dimensional (3D) structures of recombinant rotavirus-like particles, containing the protein VP2 with or without the N-terminal region. Findings showed that amino acids 1 – 92 were not necessary for the formation of recombinant VLPs (Lawton *et al.*, 1997). In the study of Charpilienne and co-workers (2001), the authors replaced the first 92 amino acids of VP2 with either 238-amino acid GFP or 249-amino acid DsRed protein (linked to dVP2 via a linker, SRGS or TCTAGAGGATCC), testing their hypothesis that the chimeric VLP would tolerate much larger inserts. Double and triple layered particles were obtained, and cryo-electron microscopy (cryo-EM) investigations showed that the VLP assembly was not altered.

Parez and co-workers (2006) proposed a method to avoid VP4 protein instability for VLP production. The authors took advantage of the fact that amino acids 1 – 92 were dispensable during VLP formation and replaced them with the VP4 cleaved product, VP8*. When expressing

the dVP2/8* fusion protein along with VP6 and VP7, VLPs were obtained. These VLPs induced protective immunity in mice (Istrate *et al.*, 2008).

The aim of the work reported in this chapter was to generate a dVP2-8*/6/7 VLP with a similar approach as that followed by Charpilienne and co-workers (2001) and Perez and co-workers, (2006). The linker (TCTAGAGGATCC) reported by Charpilienne and co-workers (2001), was used to fuse dVP2 and VP8* together (as proposed by Perez and co-workers (2006)). These proteins were expressed in insect cells, using the Bac-to-Bac baculovirus expression system (BEVS; Invitrogen), along with VP6 and VP7, to produce rotavirus G9P[6] dVP2-8*/6/7 TLPs.

2.2. Materials and Methods

All the reagents and kits used during the study are listed in Table 1 in Appendix 1, along with their catalogue numbers and manufacturers. The preparation of all the solutions and buffers utilised in the study, is described in Appendix 2.

2.2.1. Virus strain, bacterial strains and cell lines

In 1999, the Diarrhoeal Pathogens Research Unit (DPRU) at the University of Limpopo, Medunsa Campus, obtained a stool sample of a South African neonate suffering from rotavirus infection. The rotavirus infection was typed as G9P[6]. The double-stranded RNA (dsRNA), isolated directly from the stool sample, was amplified as complementary DNA (cDNA) with the use of a sequence-independent genome amplification method. The consensus nucleic acid sequence of the viral genome was obtained by pyrosequencing (Potgieter *et al.*, 2009). Synthetic genome segments, encoding the four major structural rotavirus capsid proteins, were optimized for expression in insect cells and purchased from Genart. These codon-optimised genome segments, were used to construct a clone expressing dVP2-8*/6/7.

The *Escherichia coli* (*E.coli*) bacterial strains, used during the preparation of the recombinant bacmid through recombination, were competent *E. coli* and ACC DH10Bac cells. The *E. coli* cells (Invitrogen) had a competency of 2.7×10^7 colonies/ μ g DNA and were obtained from a fellow student, Mr. Chris Badenhorst. *E. coli* cells are optimized to give high yields of recombinant plasmid. ACC DH10Bac *E. coli* cells (containing the baculovirus genome) were used during the construction of the recombinant bacmids. The significance of these cells is described in Kaba and co-workers (2004), where the authors made modifications to the

baculovirus expression system by deleting the chitinase and v-cathepsin genes from the baculovirus genome. As a result, the level of foreign protein expression and transportation increased. Furthermore, many recombinant proteins (secreted from the cells) exhibited an increased integrity and were protected against degradation.

Spodoptera frugiperda 9 (Sf9) cells were used during the expression experiments in this study. These cells are monolayer insect cells that have been adapted to grow in suspension as well. These cells were used in both monolayer and suspension and were maintained in TC100 medium supplemented with 10% fetal bovine serum (FBS), 1% penicillin/streptomycin and 2.5 µg/ml Amphotericin B/Fungizone. The concentration of the cells was determined with the use of a haemocytometer and a 0.4% trypan blue solution (Appendix 2). Cells were seeded according to the recommendations of the Bac-to-Bac manual (Invitrogen). All insect cell expression experiments were performed in the sterile environment of a tissue culture laboratory. The analysis of protein expression was performed in a Biosafety level 2 (BSL-2) molecular biology laboratory.

2.2.2. Cloning vector

A uniquely engineered pFastBacquad (pFBq) cloning vector was used throughout this study. The original multiple cloning site of pFastBac, was modified by Dr. A.C. Potgieter (Deltamune) to include the multiple cloning site of pBACgus4x1 (Novagen). Therefore, the pFBq contains 2 polyhedron and 2 p10 promoters permitting the expression of up to 4 genes simultaneously. The pFBq is depicted in Figure 2.1.

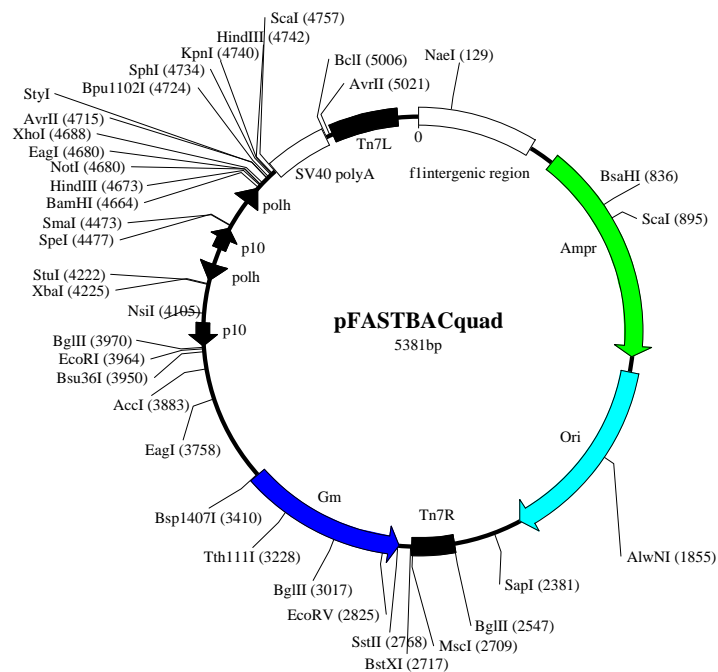


Figure 2.1 - The plasmid map of pFastBACquad (pFBq): The plasmid map illustrates the various properties of pFBq. Several restriction enzyme (RE) sites, which have multiple recognition sites in the plasmid are indicated. pFBq contains 2 polyhedron and 2 p10 promoters, indicated by black arrows, in the multiple cloning site (MCS), permitting the expression of up to four genes. There are two transposon regions flanking the MCS which facilitate the transposition of the cloned genes of interest into the baculovirus genome of the ACC DH10Bac *E.coli* cells. The dark blue and green arrows represent segments encoding resistance against gentamycin and ampicillin, respectively. The light blue arrow represents the origin of replication (Ori) which determines host range and facilitates with the replication of the plasmid. The SV40 polyA signal region functions in transcription termination and polyadenylation.

The pFBq cloning vector, containing rotavirus genome segment 2 encoding VP2 (pFBqVP2), was used during the amplification of the fused construct (dVP2-8*) where the 5'-end of the truncated region of genome segment 4 (encoding VP8*) was linked to the 3'-end of the truncated region of genome segment 2 (encoding dVP2) (section 2.3.2). The pFBq cloning vector, containing genome segments 6 and 9 (encoding VP6 and VP7, respectively) were used during the generation of the pFBqdVP2-8*/6/7 construct (section 2.3.3).

2.2.3. Oligonucleotides

The oligonucleotides used in this study are listed in Appendix 3.

2.2.4. Recombinant DNA techniques

The general recombinant DNA techniques used throughout this study are described in the subsequent sections (2.2.4.1 – 2.2.4.11). These techniques are described in detail in Sambrook and Russell (2001).

2.2.4.1. Polymerase chain reaction (PCR) amplification of the coding regions of interest

With the use of PCR, the codon-optimised rotavirus truncated genome segments 2 (encoding deltaVP2 (dVP2)) and 4 (encoding VP8*) were amplified. The amplification was performed with the use of a BioRad™ thermocycler in order to yield large quantities of amplicon encoding dVP2 and VP8*. These coding regions were amplified separately in reaction mixtures that contained 1 × Ex-Taq buffer, 5 units/μl Ex-Taq polymerase, 0.25 mM dNTP mixture, 0.5 mM DELTAVP2FOR/VP8FOR, 0.5 mM VP2REV/VP8REV and molecular grade water. The final reaction volumes were 50 μl. Thirty cycles of amplification were performed. Each cycle consisted of 30 s denaturation at 95 °C followed by 30 s annealing at 56 °C and 2 min extension at 72 °C. Prior to the first cycle of amplification, the samples were denatured for 1 min at 95 °C and after the last cycle of amplification the samples were kept at 72 °C for 15 min. The amplicons were analysed with electrophoresis (using a 1% agarose gel containing 0.6 μg/ul ethidium bromide – section 2.2.4.2) to separate according to fragment size. The electrophoresis was performed for 60 min at 80 V.

2.2.4.2. Agarose gel electrophoresis

Agarose gel electrophoresis was used to analyse PCR products and restriction enzyme digestion products, as well as to isolate and purify genome segments for further experiments. DNA samples were separated according to varying fragment size. Unless stated otherwise, 1% agarose gels were used during this study. These gels were prepared with 1 × TAE buffer (Appendix 2). The gel mixture contained 0.6 μg/μl ethidium bromide to facilitate the visualisation of DNA with ultraviolet (UV) light. Express DNA Ladder was used as a size marker for DNA fragments. Biorad Fermentas orange loading dye was added to the samples to, among other functions, track migration. Electrophoresis was done using a BioRad™ system at a constant

voltage of 80 V for 60 min (unless stated otherwise). Gel photographs were obtained with a Syngene ChemiGenius Bio-Imaging system and GeneSnap software.

2.2.4.3. Purification of PCR products

PCR amplicons were excised from the agarose gels using a sterile stainless-steel blade, weighed, transferred into a clean tube and purified with a Nucleospin Extract II kit (Macherey-Nagel) according to the manufacturer's protocol. The appropriate volume NT buffer (Macherey-Nagel) was added to the tube with the gel pieces. The gel pieces were then dissolved at 50 °C. As a result of chaotropic salts present in the NT buffer, DNA bound to the silica membrane of the Nucleospin Extract II column. The column was centrifuged to remove any impurities, such as agarose and salts, as they do not bind to the column. Thereafter, the column was washed with NT3 buffer (Macherey-Nagel), which contains ethanol to remove any remaining contaminants. After the removal of small quantities of remaining NT3 buffer (by brief centrifugation for 2 min at 11.6×1000 rpm), the column was placed within a clean 1.5 ml centrifuge tube. DNA was eluted from the column with 30 μ l of Elution Buffer NE (Macherey-Nagel) by centrifugation for 1 min at 11.6×1000 rpm.

2.2.4.4. Spectrophotometric analysis of DNA

The concentrations of the DNA samples were determined using a Nanodrop ND1000 Spectrophotometer (NanoDrop Technologies, Inc.). The spectrophotometer determines the yield of DNA as well as the purity of the DNA in question. The instrument utilises the principle that one absorbance unit at 260 nm corresponds to 50 ng/ μ l of dsDNA. Subsequently, the yield of dsDNA can be determined. DNA purity is calculated at a ratio of A_{260}/A_{280} , as proteins absorb at 280 nm. The spectrophotometer was blanked with the appropriate buffer.

2.2.4.5. Restriction enzyme digestion

Restriction enzyme digestions were used to prepare specific DNA fragments for cloning, as well as to screen for the correct cloning of the VP8* and dVP2 coding regions into the cloning vector of interest. Generally for DNA preparation and cloning screening purposes, respective final reaction volumes of 60 μ l and 20 μ l were used. Digestions were performed with 5 units/ μ l EcoRI, 2.5 units/ μ l BamHI and 2.5 units/ μ l XbaI enzyme. Each reaction mixture contained 2 \times Tango Buffer (containing BSA), molecular grade water and specific enzymes, where EcoRI was

used together with either BamHI or XbaI. These samples were digested at 37 °C for approximately 10 h. The digested samples were analysed with agarose gel electrophoreses (section 3.5.2) and purified (section 3.5.3).

2.2.4.6. DNA ligation reaction

DNA fragments to be ligated were prepared by PCR and/or restriction enzyme digestion. Three DNA fragments were digested: the pFBq containing genome segment 6 (VP6) and genome segment 9 (VP7); the amplicon encoding dVP2 and the amplicon encoding VP8*. Reaction mixtures had a final volume of 20 µl, containing the DNA, 1 × T4 DNA Ligase Buffer, 1.25 Weiss u/µl T4 DNA Ligase and molecular grade water. Samples were ligated for 72 h at 4 °C.

2.2.4.7. Electroporation of dsDNA vector and inserts (pFBqdVP2-8*/6/7) into competent *E. cloni* cells

Prior to electroporation, 100 µl of electrocompetent *E. cloni* cells (section 2.2.1) were thawed on ice. A volume of 10 µl of the ligated DNA (section 2.2.4.6) was added to the cells. Electroporation was performed with a BioRad™ electroporator. With the use of an electrical discharge, electropores were momentarily produced in the cell membranes, allowing the transportation of the ligated construct DNA into the cells. Electroporation was performed within a sterile 1 mm Gene Pulser Cuvette with a voltage, capacitance and resistance of 1800 V, 25 µF and 200 Ohm, respectively. The transformed cells were supplemented with super optimal broth, with catabolite repression, (SOC) medium (Appendix 2)), to a final sample volume of 1 ml. The cells were incubated for 1 h at 37 °C and plated out onto agar plates (containing 100 µg/ml ampicillin). A volume of 100 µl was plated out onto two individual plates and the remainder of the sample on a third plate. The preparation of these agar plates are described in Appendix 2. The plates were incubated at 37 °C, for approximately 12 h.

2.2.4.8. Mini plasmid extraction

Prior to the plasmid extraction, several picked colonies of transformed *E. coli* (*E. cloni*) bacterial cells (section 2.2.4.7.) were inoculated in 3 ml sterile LB medium, with the use of a sterile toothpick. A reference agar plate was prepared along with inoculations. The cultures were grown at 37 °C for 10 h at 200 rpm. Plasmid extraction was performed with the STET boiling lysate miniprep protocol. After the amplification of the transformed cells, the clarified cells were resuspended in STET buffer (8% sucrose, 5% TritonX-100, 50 mM EDTA, 50 mM Tris)

containing lysozyme (1 mg/ml). The preparation of STET buffer is described in Appendix 2. These reagents weaken the cell walls. When the temperature of the sample is increased to 100°C, the cells are lysed. The increase in temperature simultaneously facilitates the degradation of contaminants such as the bacterial cells' proteins and chromosomal DNA. This does, however, not affect the plasmid DNA, since these closed circular strands of dsDNA exhibit intertwined phosphodiester backbones. After boiling the samples, centrifugation was performed at 13.2×1000 rpm and the pellet was removed by use of a sterile toothpick. Plasmid DNA was precipitated by the addition of 250 μ l isopropanol and subsequently pelleted by centrifugation at 13.2×1000 rpm for 8 min. The plasmid DNA pellet was vacuum-dried with the Speedy-vac for 15 minutes to remove the isopropanol. Plasmid DNA was resuspended with 20 μ l Tris-chloride EDTA (TE) buffer (Appendix 2) and incubated at 68 °C for 10min. A DNA sample volume of 1 μ l was used to screen plasmid DNA minipreps for the correct insertion of the coding regions (VP8* and dVP2) into the cloning vector of interest (pFBqVP6/7). Screening consisted of restriction enzyme digestions (as previously stipulated in section 2.2.4.5). One of the samples contained 1 μ l pFBqVP2/6/7 as a positive control. After the digestion, 5 μ l of RESTOP (loading buffer containing RNase A – Appendix 2) was added to the samples. The samples were incubated at 37 °C for 10min, to digest contaminating traces of RNA, and subsequently centrifuged. Digestion fragments were analyzed with agarose gel electrophoresis, as discussed in section 2.2.4.2.

2.2.4.9. Long-term storage of the bacteria containing plasmids of interest in glycerol

Stocks of the bacterial cells containing pFBqdVP2-8*/6/7 were stored in 15% glycerol in volumes of 1 ml each. These clones were stored at -80 °C.

2.2.4.10. Preparation of plasmids for sequencing

Prior to the plasmid extraction, the selected bacterial colonies were inoculated from the reference plate into 50 ml LB medium (containing 100 μ g/ml ampicillin) and incubated at 37 °C for 12 h while shaking at 200 rpm. Extraction was performed according to the manufacturers' protocol of the PureYield™ Plasmid Midiprep System (Promega). The cells were pelleted for 10 min, in a 50 ml centrifuge tube, at 8×1000 rpm. After resuspension of the cells with 3 ml Cell Resuspension Solution (Promega), the cells were lysed for 3 min with 3 ml of Cell Lysis Solution (Promega). The lysis solution contains properties such as a high pH and the presence of

sodium dodecyl sulphate (SDS), which allows the dissociation of contaminants such as the bacterial cells' proteins and chromosomal DNA. With the addition of 5 ml of Neutralization Solution, these contaminants are precipitated in the presence of acetate-acetic acid buffer and the high pH is neutralised. With the use of a PureYield™ Clearing column (Promega), the dissociated contaminants are removed by centrifugation for 5 min at 2.6×1000 rpm. The cleared lysate was placed on a PureYield™ Binding column (Promega), which binds the plasmid DNA. The latter column was washed twice, first with 5 ml Endotoxin Removal Wash and then 20 ml Column Wash Solution (Promega), with centrifugation in-between. After the removal of small quantities of remaining washing buffer (by centrifugation for 10min at 2.6×1000 rpm), the column was placed within a clean 50 ml centrifuge tube. Plasmid DNA was eluted from the column with 600 μ l of nuclease-free water by centrifugation for 5 min at 2.6×1000 rpm. The plasmid DNA concentration was determined with the use of the Nanodrop 1000 Spectrophotometer (section 2.2.4.4).

2.2.4.11. DNA sequencing

The extracted recombinant plasmid DNA (section 2.2.4.10) was sequenced by the Central DNA Sequencing Facility (Stellenbosch University). Automated Sanger sequencing was performed using the oligonucleotides indicated in Appendix 2. Sequence analysis was performed with the use of FinchTV and DNAMan (Version 4.13) computer software. An *in silico* sequence was designed prior to the cloning of the construct, with DNAMan using the rotavirus G9P[6] consensus nucleic acid sequences of genome segments 2 and 4. The constructed *in silico* sequence was used as a reference sequence to facilitate the screening of unwanted mutations.

2.2.5. Baculovirus expression vector system (BEVS)

2.2.5.1. Bacmid DNA construction

The construction of the bacmid DNA was performed according to the Bac-to-Bac BEVS from Invitrogen. ACC DH10Bac *E. coli* cells contain the baculovirus genome, were used during the construction of the recombinant bacmids. These cells have been discussed in section 2.2.1. Approximately 500 ng of isolated pFBqdVP2-8*/6/7 DNA (section 2.2.4.10) was transformed into the bacterial cells. A transformation of pFBq, containing no gene inserts, was included as a negative control. After the addition of the DNA to the cells, these were incubated for 2 h on ice. Samples were briefly incubated at 42 °C for 45 s and re-incubated on ice for 2 min. The cells

were supplemented with 700 µl SOC medium. Transposition occurred within the at 37 °C for 4 h, shaking at 200 rpm. Cultures were plated out in a 10 and 40 percentile fashions using LB medium, onto agar plates (containing kanamycin (0.05 mg/ml), tetracycline (0.02 mg/ml), gentamycin (0.007 mg/ml), X-gal (0.2 mg/ml) and IPTG (0.04 mg/ml)). The preparation of these plates is described in Appendix 2. The plates were incubated at 37 °C, for approximately 48 h.

2.2.5.2. Bacmid DNA isolation

Prior to the isolation, the colonies obtained from the bacmid construction (section 2.2.5.1) are inoculated, from the transformed plates, into separate vials containing 2 ml LB medium (Appendix 2) with gentamycin (0.007 mg/ml), kanamycin (0.05 mg/ml) and tetracycline (0.02 mg/ml). The isolation of the recombinant bacmid DNA was performed according to the manufacturers' protocol of the Bac-to-Bac BEVS from Invitrogen with one minor alteration. The alteration involved the use of the Glucose Tris-chloride EDTA (GTE) buffer. This isolation is performed on the same principle (section 2.2.4.10) without the use of filtering and DNA binding columns. DNA is precipitated with the addition of isopropanol and pelleted by centrifugation. In addition, the precipitated DNA pellet is washed with 500 µl 70% ethanol, to further purify the DNA. Afterwards, the ethanol was removed without disrupting the DNA pellet and the pellet was air dried for approximately 10 min. The pellet was dissolved in 30 µl nuclease-free water. The DNA concentration was determined (section 2.2.4.4).

2.2.5.3. Screening for appropriate recombinant bacmids

To evaluate successful transposition of the gene of interest into the baculovirus shuttle vector, the recombinant bacmids were amplified (section 2.2.4.1) with minor changes. These changes involved amplification with an EppendorfTM thermocycler in the presence of 0.25 mM M13FOR and M13REV primers, using an annealing temperature of 58 °C for 30 s. The M13 primers are indicated in Appendix 3. The screening process was completed with agarose gel electrophoresis (section 2.2.4.2). The recombinant bacmid DNA concentrations were determined (section 2.2.4.4) and the desired recombinant bacmid clones were stored (section 2.2.4.9).

2.2.5.4. Transfection of Sf9 cells with bacmid DNA

Sf9 cells, used during the procedure, were described in section 2.2.1. Prior to the transfection, sterile wells of 6-well plates (Nunc) were seeded at 1×10^6 cells/well using supplemented TC100 medium (section 2.2.1). These cells were incubated for 1 h at 28 °C to achieve cell monolayer formation. DNA complex solutions of 100 µl volumes were set up, separately. These complexes contained bacmid DNA (section 2.2.5.2), Fugene 6 reagent and non-supplemented TC100 medium. The DNA complexes were incubated at room temperature for 1 h. After the cells were washed and re-supplemented with 2 ml non-supplemented TC100 medium, DNA complexes were added to their corresponding wells in a drop-wise fashion. The transfection reactions were incubated at 28 °C, for about 8 h, to achieve the introduction of bacmid DNA into the cells. The transfections were performed in the absence of foetal bovine serum (FBS) and antibiotics, as these supplements may interfere with the transfections. A mock transfection, containing no DNA complex, was included as a negative control. After the 8 h incubation period, the medium (containing the DNA complexes) was removed and replaced with supplemented TC100 medium. The cells were re-incubated for approximately 72 h at 28 °C. Six DNA complexes of the positive recombinant were prepared and used for transfection purposes. A negative control containing a bacmid with no recombinant insert (FB) was included during the transfection procedure.

2.2.5.5. Preparation of P1 viral stocks

The P1 viral stock was isolated from the transfected cells according to the manufacturer's protocol. The medium, containing the baculovirus, was removed from the transfected cells and placed into a separate 15 ml centrifuge tube. The samples were then centrifuged for 5 min at 1600 rpm in order to remove any remaining cells and large debris. The supernatant, known as the P1 viral stock, was transferred to a separate tube and stored at 4 °C (protected from light). The pellet of Sf9 cells was discarded.

2.2.5.6. Infection of Sf9 cells with recombinant baculovirus, expressing the genes of interest

As described in section 2.2.5.4, Sf9 cells were seeded in supplemented TC100 medium, in sterile wells of 6-well plates, prior to infection. Alternatively each well contained a concentration of 8×10^5 cells/well. Cells were infected with isolated P1 viral stock (section 2.2.5.5). The cells were initially infected with 200 µl supplemented TC100 medium and 300 µl of the P1 viral stock.

After an incubation of 1 h at room temperature, shaking, another 1.5 ml supplemented TC100 medium was added to the infected cells. The infections were incubated at 28 °C for 96 h or until the cytopathic effect (CPE) reached approximately 90-95%.

2.2.5.7. Harvesting of the recombinant baculovirus and cells

When cells reached the appropriate CPE they were harvested by centrifugation for 5 min at 1600 rpm. The baculovirus-containing medium, known as the P2 viral stock was collected (section 2.2.5.5). The cell pellet was washed thoroughly with 1 ml of 1×Phosphate buffered saline (PBS) (Appendix 2), followed by centrifugation, to remove any contaminating substances from the remaining maintenance medium. After the PBS had been removed, the pellet was resuspended in 200 µl lysis buffer (10 mM Tris, 0.1 mM EDTA and 1% SDS). The lysis buffer functions to release the contents of the cells and dissolve the proteins of interest. The protein samples were stored at -20 °C.

2.2.5.8. SDS-PAGE

Using sodium-dodecyl-sulphate polyacrylamide gel electrophoresis or SDS-PAGE, protein expression was evaluated. The method was used as described previously by Laemmli (1970) and Sambrook and Russell (2001). It relies on the protein dissociation into individual polypeptide subunits, with minimal aggregation. The buffer system used during this experiment is discontinuous, as the pH and ionic strength of the stacking and separating gels are different. This increases the resolution of the gel, by concentrating the sample complexes into a smaller volume.

A 10% gel was generally prepared and consisted of a separating and stacking gel. The separating gel consisted of 10% acryl-amide (0.27% bisacrylamide), 376 mM Tris-Cl (pH8.8), 0.1% SDS, 0.1% APS (ammoniumperoxodisulphate) and 0.008% TEMED (Tetramethylethylenediamine). The separating gel was left for polymerisation for 1 h after isopropanol was added to the surface of the gel. The isopropanol was thoroughly removed and the stacking gel was added. The stacking gel consisted of 3.72% acryl-amide (0.1% bisacrylamide), 372 mM Tris-Cl (pH6.8), 0.1% SDS, 0.1% APS and 0.008% TEMED. The stacking gel was polymerized in the presence of a 10-well comb, to facilitate sample application.

Samples of 38 μ l were prepared consisting of 2 μ l 20% reducing agent, 28 μ l sample (section 2.2.5.7) and 8 μ l 4 \times Dual color Protein loading buffer and heated to 98 $^{\circ}$ C for 5 min. Upon completion of polymerisation of the stacking gel, 20 μ l of the prepared samples was loaded onto the gel. As a size and migration reference, 5 μ l of PageRuler (plus prestained protein ladder) (Fermentas) was included in one of the sample wells.

The gels were electrophoresed with the BioRadTM system at constant 30 mA for 60 min (unless stated otherwise) in the presence of 1 \times TGS (25 mM Tris, 2 M Glycine, 0.1% SDS) buffer. Afterwards, the gels were stained for 8 h with 45% (v/v) methanol, 10% (v/v) acetic acid and 0.4% (w/v) Coomassie brilliant blue R250, while shaking. The gel was destained for 1 h with 45% (v/v) methanol and 10% (v/v) acetic acid destaining solution. When the proteins of interest were visible, the gel was documented by scanning and subsequently dried for 1 h at 60 $^{\circ}$ C. The preparation of the TGS buffer, the staining and destaining solution is described in Appendix 2.

2.3. Results and Discussion

As pointed out in section 2.1, this Chapter focused on the construction and expression of dVP2-8*/6/7 TLPs of a South African G9P[6] rotavirus strain. The cloning strategy used to generate the fused construct of pFBqdVP2-8*/6/7 is illustrated in Figure 2.2. The first step in the construction was to generate the fused construct of dVP2-8*. This was achieved by amplifying the coding regions of VP8* and dVP2 from the genome segments 4 and 2, respectively. Amplification (section 2.2.4.1) was performed with complementary designed primers (section 2.3.1). The second step consisted of restriction enzyme digestion of the VP8* and dVP2 coding regions for cloning (section 2.2.4.5). The pFBq containing the coding regions of VP6 and VP7 (pFBqVP6/7) was included during the preparation. The pFBqVP6/7 was constructed, prior to this study by Dr. H.G. O'Neill. The third and final step of the construction was to ligate the two amplified coding regions (VP8* and dVP2), along with pFBqVP6/7, in a three-part ligation (section 2.2.4.6). The amplified coding regions were connected at the 3'-end of VP8* and 5'-end of dVP2. The ligation yielded the fused construct of pFBqdVP2-8*/6/7.

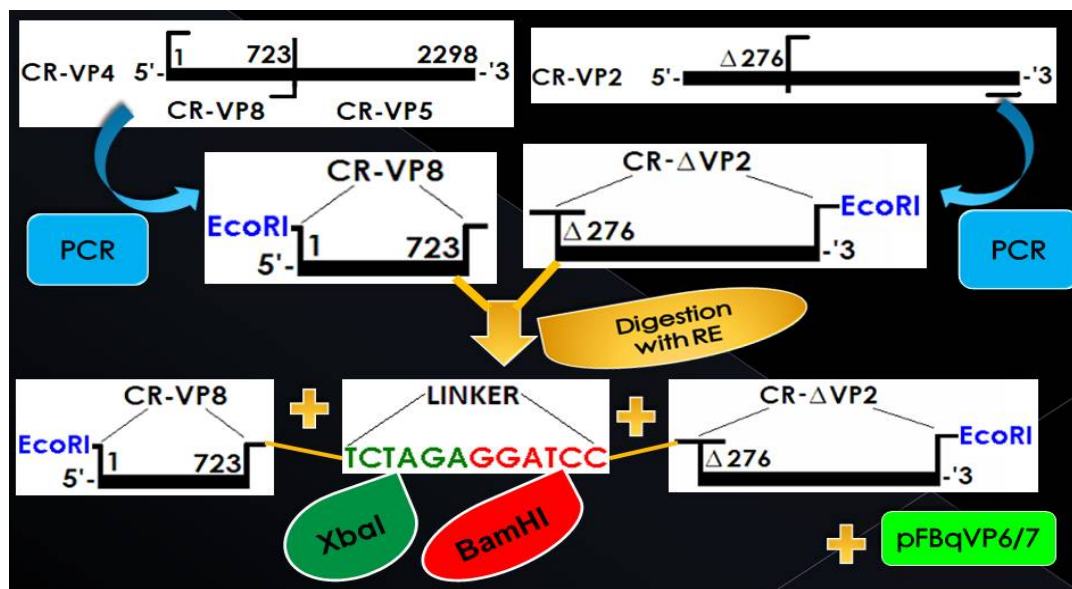


Figure 2.2 – A schematic representation of the construction of pFBqdVP2-8/6/7: Polymerase chain reaction (PCR) was used to amplify the coding regions of VP8* (732bp) and dVP2 (2388bp) from genome segment 4 (VP4) (2298bp) and genome segment 2 (VP2) (2765bp) coding regions, respectively. Thereafter these two coding regions, as well as the plasmid, were digested with restriction enzymes (BamHI, XbaI and EcoRI). Lastly the VP8* and dVP2 coding regions were ligated together with the plasmid containing the coding regions of VP6 and VP7. The two coding regions were connected between the 5'-end of the truncated region of genome segment 4 (encoding VP8*) and the 3'-end of the truncated region of genome segment 2 (encoding dVP2) with the linker (containing the restriction enzyme recognition sites of BamHI and XbaI) in between to produce the fused construct (dVP2-8*).*

2.3.1. Design of primers used during the amplification of genome segments encoding dVP2 and VP8*

The amplification of the codon-optimised rotavirus genome segments 2 (encoding VP2) and 4 (encoding VP4), required complementary primers. These primers were designed with the use of DNAMAN (version 4.13, Lynnon) computer software. As described in the introductory section of Chapter 2, basepairs 1 – 276 of genome segment 2; or rather amino acids 1 - 92 of rotavirus VP2 were not necessary for the conformation of recombinant VLPs. The design of dVP2 was previously described by Charpilienne and co-workers (2001) and Labbe and co-workers (1991). Multiple alignments of amino acid sequences of VP2 were performed, using representative type A rotavirus sequences. The alignments were used to locate the annealing position of the forward primer (representing the SRGS linker) (Charpilienne *et al.*, 2001) to form dVP2, from VP2. Figure 3.3.1(a) represents the alignment of multiple RV serotype A VP2 amino acid sequences, of which the first sequence represents the rotavirus G9P[6] sequence used during this study. The rest of the sequences were obtained from GenBank. The GenBank sequence

identity numbers are as follows: RV A (Ro1845) - EU708891.1; RV A (HCR3A) - EU708902.1; RV A (N155) - EU200794.1 and RV A – DQ480724.1. All of the sequences aligned with G9P[6] at amino acids 92-93. This demonstrates the conservation of the coding region, VP2, sequence among human type A rotaviruses. In addition, according to the alignment, the G9P[6] VP2 sequence has one amino acid less in comparison with the rest of the sequences (indicated with the full stop). From the alignments, the location of ligation between the C-terminal of VP8* and the N-terminal of dVP2 was determined to be between amino acids 92Q and 93K (illustrated in red).

```

RV A G9P6 MAYRKRGARREANLNNNDRMQEKID.EKQDSNKIQLSDKVLSKKEEIVTDSHEEVKVTDE 59
RV Ro1845 MAYRKRGARREANLGNNDRMQEEKDNEKQDSNKMQLSDKVLSKKEEVVTDSEQEEVKIADE 60
RV HCR3A MAYRKRGARREANLGNNDRMQEEKDNEKQDSNKMQLSDKVLSKKEEVVTDSEQEEVKIADE 60
RV A N155 MAYRKRGARREANINNNDRMQEKDDEKQDQNNRTQLADKVLSKKEEVVTDSEQEEIKITDE 60
RV A MAYRKRGARREANINNNDRMQEKDDEKQDQNNRMQLSDKVLSKKEEVVTDSEQEEIKIADE 60

RV A G9P6 LKKSTKEESKQLLEVLKTKKEEHQKEIQYEILQKTIPTTFEPKETILRKLEDIQPELAKKQT 119
RV Ro1845 VKKSTKEESKQLLEVLKTKKEEHQKEIQYEILQKTIPTTFEPKETILKKLEDIKPEQAKKQT 120
RV HCR3A VKKSTKEESKQLLEVLKTKKEEHQKEIQYEILQKTIPTTFEPKETILKKLEDIKPEQAKKQT 120
RV A N155 VKKSTKEESKQLLEVLKTKKEEHQKEIQYEILQKTIPTTFEPKESILKKLEDIKPEQAKKQT 120
RV A VKKSTKEESKQLLEILKTKKEEHQKEIQYEILQKTIPTTFEPKESILKKLEDIKPEQAKKQT 120

```

Figure 2.3 – Multiple alignment of the partial VP2 amino acid sequences of selected type A rotaviruses to that of G9P[6]. Amino acids 92 and 93 are indicated in red by QK, showing the location of ligation between the C-terminal of VP8 and the N-terminal of dVP2 to yield dVP2-8*.*

The primers used to amplify the regions of genome segments encoding VP8* and DELTAVP2 (dVP2) were designed to contain the restriction enzyme recognition site (EcoRI) and the linker, as described by Charpilienne and co-workers 2001. VP8FOR contains a restriction enzyme recognition site for EcoRI at the 5'-end. VP8REV and DELTAVP2FOR contain the linker, which in turn contains the restriction enzyme recognition sites of BamHI and XbaI. The positions of these restriction enzyme recognition sites are different for the two primers. For VP8REV the BamHI and XbaI sites are located at the 5'-end and 3'-end, respectively. For DELTAVP2FOR the XbaI and BamHI sites are located at the 5'-end and 3'-end, respectively. These and other primers are indicated in Appendix 3. These primers were ordered from Eurofins MWG Operon. The VP2REV primer was previously designed by Dr. H.G. O'Neill and contains the restriction enzyme recognition site for EcoRI at the 5'-end.

As determined from the alignment, the first 92 amino acids, or 276 basepairs were removed and the sequence (TCTAGAGGATCC) encoding the linker (SRGS) was fused to amino acid 93; or rather basepair 277, to amplify the truncated region of genome segment 2 (VP2) encoding dVP2. Figure 2.4 illustrates the DNA sequence of genome segment 2 (VP2) which shows the annealing position of the DELTAVP2FOR primer. The corresponding amino acid composition of VP2 is also indicated.

1	ATGGCTTACCGCAAGCGTGGTGCCTCGTCGCGAGGCTAACCTGAACAACAACGACCGTATG
1	M A Y R K R G A R R E A N L N N N D R M
61	CAGGAAAAGATCGACGAGAAGCAGGACTCCAACAAGATCCAGCTGTCCGACAAGGTGCTG
21	Q E K I D E K Q D S N K I Q L S D K V L
121	TCCAAGAAGGAAGAAATCG TCACCGACTCCCACGAGGAAGTCAAGGTACCCGACGAGCT
41	S K K E E I V T D S H E E V K V T D E L
181	GAAGAAGTCCACCAAGGAAGAATCCAAGCAGCTGTTGGAGGTGCTCAAGACTAAGGAAGA
61	K K S T K E E S K Q L L E V L K T K E E
	DELTAVP2FOR
241	ACACCAGAAGGAAATCCAGTACGAGATCCTGCAAG GATCTAGAGGATCCAAGACCATCCCC
81	H Q K E I Q Y E I L Q SRGS K T I P
301	ACCTTCG AGCCCAAGGAAACTATCCTGCGCAAGTTGGAGGACATCCAGCCCGAGCTGGCT
101	T F E P K E T I L R K L E D I Q P E L A
361	AAGAAGCAGACCAAGCTGTTCCGTATCTTCGAGCCTAAGCAGCTGCCATCTACCGTGCT
121	K K Q T K L F R I F E P K Q L P I Y R A
421	AACGGCGAGCGGAGCTGCGTAACCGTTGGTACTGGAAGTTGAAGAAGGATACCCTGCCC
141	N G E R E L R N R W Y W K L K K D T L P
481	GACGGCGACTACGACGTGCGCGAGTACTTCCTGAACCTGTACGACCAGGTGCTGACCGAG
161	D G D Y D V R E Y F L N L Y D Q V L T E
541	ATGCCCGACTACCTGCTGCTGAAGGACATGGCTGTGGAGAACAAGAAGTCCCCTGACGCT
181	M P D Y L L L K D M A V E N K N S R D A
601	GGCAAGGTGGTGGACTCCGAGACTGCTTCCATCTGCGACGCTATCTTCCAGGACGAGGAA
201	G K V V D S E T A S I C D A I F Q D E E
661	ACTGAGGGTGCCTGTGCGTCGTTTCATCGCTGAGATGCGTCAGCGTGTGCAGGCTGACCGT
221	T E G A V R R F I A E M R Q R V Q A D R
721	AACGTGGTCAACTACCCCTCC
241	N V V N Y P S

Figure 2.4 – Partial DNA sequence of genome segment 2 (VP2), showing the annealing position of the primer designed for the amplification of the truncated region of genome segment 2 encoding dVP2: The forward primer (DELTAVP2FOR) for the amplification of the region of genome segment 2 encoding dVP2 is indicated in yellow. The unamplified region of

genome segment 2 (VP2) (basepairs 1 - 276), is located at the 5' end of DELTAVP2FOR. The truncated region of genome segment 2 encoding dVP2, is located at the 3' end (following DELTAVP2FOR).

As mentioned in section 1.4.1.3, amino acids 1-241 of VP4, is cleaved to produce two proteins, VP5 and VP8*, upon trypsin protease exposure. With the latter in mind, the SRGS-linker was inserted between amino acids 241 and 242 of VP4, to produce VP8*. VP8FOR and VP8REV primers were designed to facilitate the amplification of coding region VP8* from genome segment 4 (encoding VP4). The annealing positions of these primers are indicated in Figure 2.5.

VP8FOR

```

1      CCGAATTCATGGCTTCCCTGATCTACCGTCAGCTGCTGACCAACTCCTACACCGTGGAGC
1      EcoRI  M A S L I Y R Q L L T N S Y T V E

53     TGTCCGACGAGATCAACACCATCGGTTCCGAGAAGTCCCAGAACGTGACCATCAACCCCG
18     L S D E I N T I G S E K S Q N V T I N P

113    GTCCCTTCGCTCAGACCAACTACGCTCCCGTGACCTGGTCCCACGGCGAGGTCAACGACT
38     G P F A Q T N Y A P V T W S H G E V N D

173    CCACCACCATCGAGCCCCTGCTGGACGGTCCCTACCAGCCCACCAACTTCAAGCCCCCCA
58     S T T I E P V L D G P Y Q P T N F K P P

233    ACGACTACTGGATTCTGCTGAACCCACCAACCAGCAGGTGGTGTGGAGGGCACCAACA
78     N D Y W I L L N P T N Q Q V V L E G T N

293    AGACCGACATCTGGGTGGCCCTGCTGCTGGTTCGAGCCCAACGTGACCAACCAGTCCCGTC
98     K T D I W V A L L L V E P N V T N Q S R

353    AGTACACCCTGTTCGGCGGAGACTAAGCAGATCACCGTGGAGAACAACACCAACAAGTGA
118    Q Y T L F G E T K Q I T V E N N T N K W

413    AGTTCTTCGAGATGTTCCGCTCCAACGTGAACGCTGAGTTCAGCACAAGCGTACCCTGA
138    K F F E M F R S N V N A E F Q H K R T L

473    CCTCCGACACCAAGCTGGCTGGTTTCATGAAGTTCTACAACCTCCGTGTGGACCTTCCACG
158    T S D T K L A G F M K F Y N S V W T F H

533    GCGAGACTCCCCACGCTACCACCGACTACTCCTCCACCTCCAACCTGTCCGAGGTGGAGA
178    G E T P H A T T D Y S S T S N L S E V E

593    CTGTGATCCACGTGGAGTTCTACATCATCCCCCGTTCCCAAGAATCCAAGTGCTCCGAGT
198    T V I H V E F Y I I P R S Q E S K C S E

653    ACATCAACACCGGCCTGCCCCCATGCAGAACACCCGTAACATCGTGCCCGTGGCTCTGT
218    Y I N T G L P P M Q N T R N I V P V A L

```

VP8REV

```

713    CCTCCCGTTCCTCTAGAGGATCCGTGACCTACCAGCGTGTCTCAGGTCAACGAGGACATCA
238    SRGS      V T Y Q R A Q V N E D I

773    TCATCTCCAAGACCTCCCTGTGGAAGGAAATGCAGTACAACCGCGACATCATCATCCGCT

```

258 I I S K T S L W K E M Q Y N R D I I I R
 833 TCAAGTTCAACAACAGCATCGTGAAGCTGGGTGGCCTGGGTTACAAGTGGTCCGAGATCT
 278 F K F N N S I V K L G G L G Y K W S E I
 893 CCTTCAAGGCTGCCAACTACCAGTACTCCTACCTGCGTGACGGCGAGCAGGTACCCGCTC
 298 S F K A A N Y Q Y S Y L R D G E Q V T A
 953 ACACCACCTGCTCCGTGAACGGTGTCAACAACCTTCTCCTACAACGGTGGTTCCCTGCCCA
 318 H T T C S V N G V N N F S Y N G G S L P
 1013 CCGACTTCTCCGTGTCCCGTTACGAGGTCAATCAAGGAAAACCTCCTACGTCTACGTGGACT
 338 T D F S V S R Y E V I K E N S Y V Y V D
 1073 ACTGGGACGACTCCCAGGCTTTCCGTAACATGGTGTACGTGCGCTCCCTGGCTGCTAACC
 358 Y W D D S Q A F R N M V Y V R S L A A N
 1133 TGAAGTCCGTTGAAGTGTCCGTTGGCAACTACAACCTCCAGATCCCCGTGGGCGCTTGGC
 378 L N S V K C S G G N Y N F Q I P V G A W
 1193 CCGTGATGTCCGGTGGTGTGTGTCCCTGCACTTCGCTGGTGTACCCTGTCCACCCAGT
 398 P V M S G G A V S L H F A G V T L S T Q
 1313 TCACCGACTTCGTGTCCCTGAACTCCCTGCGTTTCCGTTTCTCCCTGACCGTGGAGGAAC
 418 F T D F V S L N S L R F R F S L T V E E
 1373 CCCCCTTCTCCATCCTGCGTACCCGCGTGTCCGGCCTGTACGGCCTGCCCGCTTTCAACC
 438 P P F S I L R T R V S G L Y G L P A F N
 1253 CCAACAACGGCCACGAGTACTACGAGATCGCTGGTTCGCTTCTCCCTGATCTCTCTGGTGC
 458 P N N G H E Y Y E I A G R F S L I S L V
 1313 CCTCCAACGACGACTACCAGACCCCCATCATGAACTCCGTACCGTGCCTGAGGACTTGG
 478 P S N D D Y Q T P I M N S V T V R Q D L
 1373 AGCGTCAGCTGGGTGACCTGCGTGAGGAGTTCAACTCCCTGTCCCAAGAAATCGCTATGA
 498 E R Q L G D L R E E F N S L S Q E I A M
 1433 CCCAGCTGATCGACCTGGCTCTGCTGCCCTGGACATGTTCTCTATGTTCTCCGGCATCA
 518 T Q L I D L A L L P L D M F S M F S G I
 1493 AGTCCACCATCGACGTGGCTAAGTCTATGGTCACCAAGGTCATGAAGAAGTTCAAGAAGT
 538 K S T I D V A K S M V T K V M K K F K K
 1553 CCGGCCTGGCTACCTCCATCTCCGAGCTGACCGGTTCCCTGTCCAACGCTGCTTCCCTCCG
 558 S G L A T S I S E L T G S L S N A A S S
 1613 TGTCCAGGTCCTCCTCCATCCGTTCCAACATCTCCTCCATCTCTGTGTGGACCGACGTGT
 578 V S R S S S I R S N I S S I S V W T D V
 1673 CCGAGCAGATCGCTGGCTCCTCCGACTCCGTGCGTAACATCTCCACCCAGACCTCCGCTA
 598 S E Q I A G S S D S V R N I S T Q T S A
 1733 TCTCCAAGCGTCTGCGTCTGCGTGAGATCACCAACCAGACTGAGGGCATGAACTTCGACG
 618 I S K R L R L R E I T T Q T E G M N F D
 1793 ACATCTCCGCTGCTGTGCTCAAGACCAAGATCGACCGTTCCACCCACATCTCCCCGACA

```

638      D I S A A V L K T K I D R S T H I S P D
1853     CCCTGCCTGACATCATCACCGAGTCCTCCGAGAAAGTTCATCCCCAAGCGTGCTTACCGTG
658     T L P D I I T E S S E K F I P K R A Y R
1913     TGCTGAAGGACGACGAGGTCATGGAGGCTGACGTGGACGGCAAGTTCCTTCGCTTACAAGG
678     V L K D D E V M E A D V D G K F F A Y K
1973     TCGGCACCTTCGAGGAAGTGCCCTTCGACGTGGACAAGTTCGTGGACCTGGTCACCGACT
698     V G T F E E V P F D V D K F V D L V T D
2033     CCCCCGTGATCTCCGCTATCATCGACTTCAAGACCCTGAAGAACCTGAACGACAACCTACG
718     S P V I S A I I D F K T L K N L N D N Y
2093     GTATCACCCGCTCCCAGGCTCTGGACCTGATCCGTTCCGACCCCCGTGTGCTGCGTGACT
738     G I T R S Q A L D L I R S D P R V L R D
2153     TCATCAACCAGAACAACCCCATCATCAAGAACCGTATCGAGCAGCTGATCCTGCAGTGCC
758     F I N Q N N P I I K N R I E Q L I L Q C
2213     GTCTGTAATGA
778     R L * *

```

Figure 2.5 – The DNA sequence of G9P[6] genome segment 4 (VP4), showing the annealing positions of primers designed for the amplification of the region of genome segment 4 encoding VP8.* The primers, used to amplify the region of genome segment 4 encoding VP8*, are indicated in green and yellow and represented by VP8FOR and VP8REV, respectively. The region, located between the two primers, represents the region of the genome segment encoding VP8*. The region located after the VP8REV primer represents the region of the genome segment encoding VP5.

2.3.2. Polymerase chain reaction (PCR) amplification of the regions of genome segments 2 and 4 encoding dVP2 and VP8*, respectively

PCR was used to amplify the regions of genome segments 2 and 4 encoding dVP2 and VP8*, respectively. Amplicons were analysed (section 2.2.4.2) and are displayed in Figure 2.6(a)-(b). The coding region of VP8* was amplified successfully at 741 bp in lane 3 of Figure 2.6(a). This was, however, not the case with the coding region of dVP2, as no amplification could be detected in Figure 2.6(a) lane 5 at 2388 bp. Further optimization of the amplification conditions were performed for dVP2. These factors included the use of another DNA template, as well as the annealing temperature for the amplification of dVP2. The DNA template pGA15VP2 (used during the previous amplifications) was substituted with pFBq plasmid containing VP2 coding region (pFBqVP2). The pFBqVP2 construct was previously generated by Dr. H.G. O'Neill. The pFBqVP2 DNA template was used during subsequent annealing temperature optimisation experiments. Initially, an annealing temperature of 60°C was used for the amplification of both

coding regions. During the optimisation of the annealing temperatures, a temperature gradient (ranging from 55°C - 59°C) was used. All the temperatures utilised showed successful amplification of dVP2 from pFBqVP2 (results not displayed). The amplicon yields were compared (section 2.2.4.2) with the conclusion that 56°C was the optimal annealing temperature for amplification of dVP2. The temperature of 56°C was used during subsequent amplifications of dVP2.

The amplification results of these two altered factors are displayed in Figure 2.6(b). As a control, the previously used pGA15VP2 was included during the analyses. The fragment of dVP2 (pFBqVP2) was clearly visible at 2388bp in lane 3 (Figure 2.6(b)), but a light smear of dVP2 (pGA15VP2) was visible in lane 4. This suggested that the DNA template of pGA15VP2 might have been degraded.

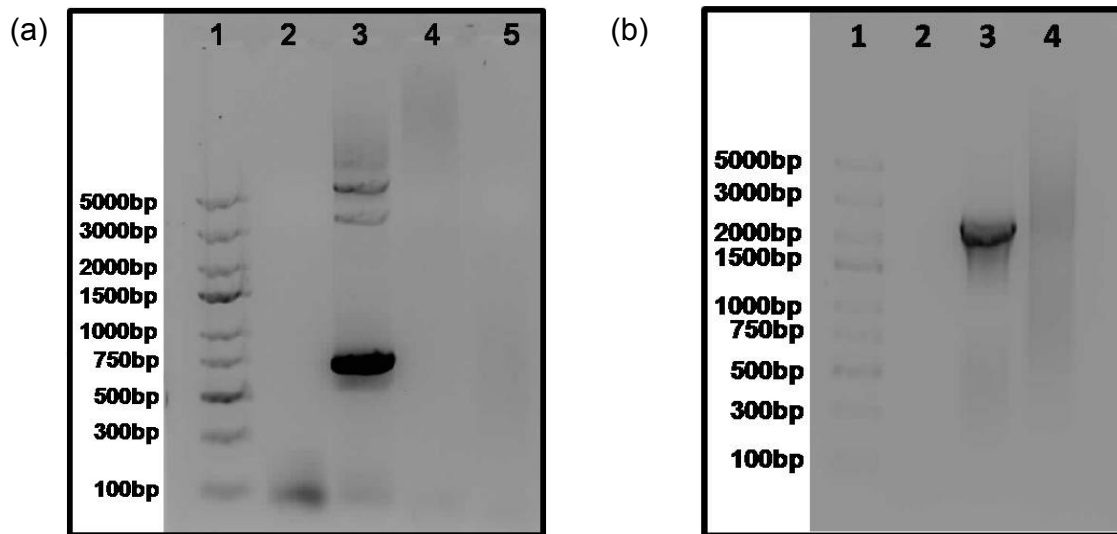


Figure 2.6 – 1% Agarose gel analysis of amplification of the regions encoding VP8 (of genome segment 4) and dVP2 (of genome segment 2): (a) Lanes 1, Express DNA ladder (Fermentas); 2, no template control of VP8* coding region; 3, VP8* coding region; 4, negative no template control of dVP2 coding region; 5, dVP2 coding region. (b) Amplification of dVP2 coding region using different DNA templates: Lanes 1, Express DNA ladder; 2, no template control of dVP2; 3, dVP2 coding region (pFBq VP2); 4, dVP2 coding region (pGA15VP2).*

2.3.3. Cloning of the truncated regions of genome segments 2 and 4 encoding dVP2 and VP8*, respectively, into pFBq containing the coding regions of VP6 and VP7

Following the successful amplification of the regions encoding dVP2 and VP8*, these two amplicons were gel purified (section 2.2.4.3), digested with certain restriction enzymes (section 2.2.4.5) and ligated (section 2.2.4.6) together with the pFBq plasmid, containing the coding regions of VP6 and VP7 (pFBqVP6/7). The coding region samples of dVP2 and VP8*, which were both digested with BamHI, were combined in the same ligation reactions. Likewise, the XbaI digested coding region samples of dVP2 and VP8*, were combined in the same ligation reactions. The ligation reactions were optimized, using the following calculation:

$$\text{Concentration/Total bp} = \text{Concentration of DNA (ng/}\mu\text{l)} / \text{Base pair length (bp)}$$

The ligation samples were set up according to the calculations. The ligation procedure (section 2.2.4.6) was performed in ratios of 1:1:1 and 1:3:3, for pFBqVP6/7:d92VP2:VP8*. The pFBqdVP2-8*/6/7 construct was transformed into competent *E.coli* (*E. cloni*) bacterial cells (section 2.2.1). The cells contained displayed a relatively good degree of competency at 2.7×10^7 colonies/ μg DNA. The three-part ligation (with ratio 1:3:3) was successful and 23 colonies were obtained. Following extraction of plasmid DNA of potential positive clones (section 2.2.4.8), restriction enzymes (BamHI, EcoRI and XbaI) were used to screen for the positive insertion of the amplicons encoding both dVP2 and VP8* into the multiple cloning site of pFBqVP6/7 (section 2.2.4.5).

Prior to the digestions, *in silico* generated schematic representations (of the expected fragments) were constructed with DNAMan (Version 4.13, Lynnon) computer software. These predicted representations are illustrated in Figure 2.7 (a) and (b). A possible cloning orientation error could be attributed to the fact that the fused construct contains an EcoRI enzyme recognition site on both the 5' and 3'-ends. Thus, the fused coding regions could be cloned into the pFBqVP6/7 in the correct (5'-end to 3'-end) and incorrect (3'-end to 5'-end) orientation. For correctly and incorrectly orientated cloning, BamHI digestion would yield fragments of 2640bp and 8017bp, and 4281bp and 6376bp, respectively. There are two digestion sites, as there is an additional BamHI recognition site in the linker located in the fused construct between the 5'-end of the truncated region of genome segment 4 (encoding VP8*) and the 3'-end of the truncated region of genome segment 2 (encoding dVP2). Figure 2.7(a) illustrates BamHI digestion after

correctly orientated cloning and Figure 3.7(b) illustrates BamHI digestion after incorrectly orientated cloning.

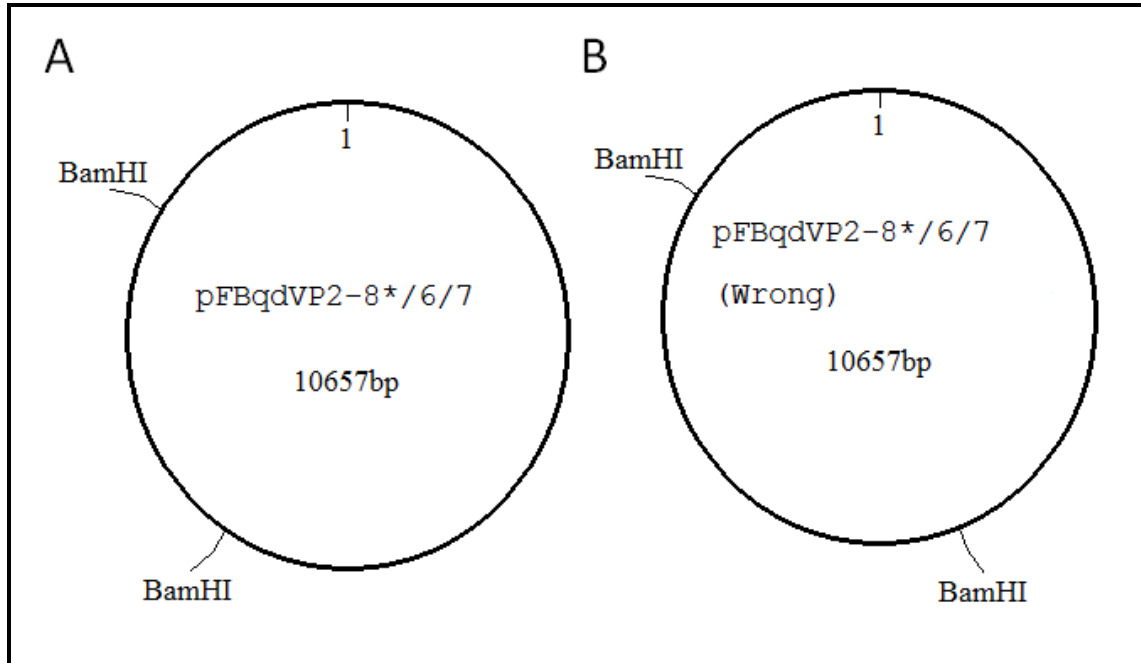


Figure 2.7 – In silico BamHI digestion of pFBqdVP2-8/6/7: (A) Represents the digestion with BamHI if pFBqdVP2-8*/6/7 had been cloned in the correct orientation, with fragments of approximately 2640bp and 8017bp. (B) Represents the digestion with BamHI if pFBqdVP2-8*/6/7 had cloned in the wrong orientation, with fragments of approximately 4281bp and 6376bp.*

Agarose gel electrophoretic analysis of the digestions was performed (section 2.2.4.2) and the results are shown in Figure 2.8. As a negative control, pFBqVP2/6/7 was included during the analyses. Results showed 8 (4, 6, 9, 10, 11, 12, 15 and 21) of the 23 colonies contained plasmids with correctly orientated inserts. Colonies depicted in Figure 2.8.

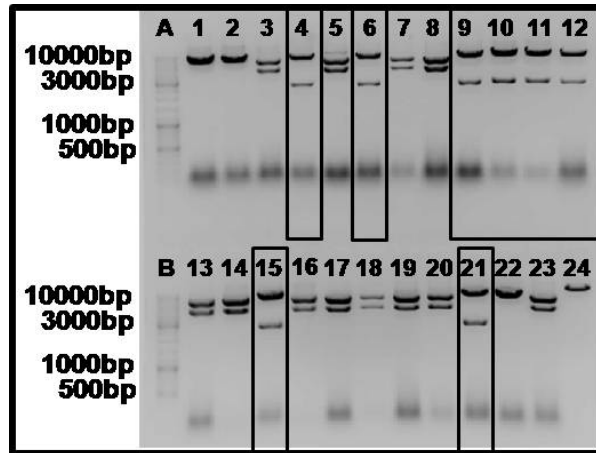


Figure 2.8 – 1% Agarose gel analyses of BamHI digestion of possible pFBqdVP2-8/6/7 plasmid:* Lanes A and B: DNA Ladder Mix. Lanes 1 to 23, the digested miniprep DNA of 23 plasmids; 24, a control pFBqVP2/6/7. All the positive clones with fragments of approximately 2640bp and 8017bp are boxed in the Figure.

Two additional confirmatory restriction enzyme digests were performed on positive plasmids. The one was with EcoRI. Since there was an EcoRI site on both sides of the cloned fragment, no distinction could be made between correctly and incorrectly orientated cloning. Expected fragments, yielded after digestion, were 3100bp and 7557bp (no schematic shown). An additional digestion with XbaI would give the following fragments of correctly orientated cloning: 990bp, 1205bp and 8462bp. There are three digestion sites, as there is an additional XbaI recognition site in the linker located in the fused construct between the 5'-end of the truncated region of genome segment 4 (encoding VP8*) and the 3'-end of the truncated region of genome segment 2 (encoding dVP2). These fragments are illustrated in Figure 2.9 (a). The fragments that were expected, if the fused construct had cloned in the incorrect orientation, were 1205bp, 2643bp and 6809bp. These fragments are illustrated in Figure 2.9 (b).

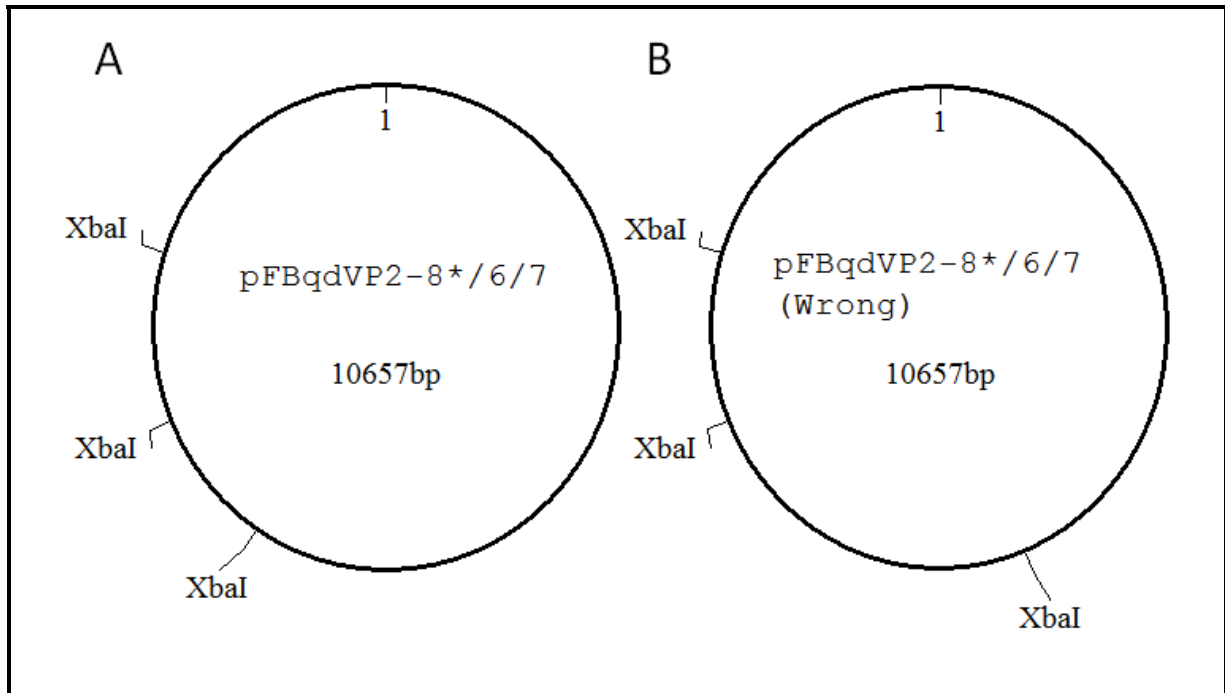


Figure 2.9 - In silico XbaI digestion of pFBqdVP2-8/6/7: a) Represents the digestion with XbaI if pFBqdVP2-8*/6/7 was cloned in the correct orientation, with fragments of 990bp, 1205bp and 8462bp. b) Represents the digestion with XbaI if pFBqdVP2-8*/6/7 was cloned in the wrong orientation, with fragments of 1205bp, 2643bp and 6809bp.*

Digestions with EcoRI and XbaI on the 8 plasmids had the correct orientation according to the previous BamHI digestion (in Figure 2.8(a)). The analyses of these digestions are illustrated in Figure 2.10. All 8 clones yielded the expected fragments after digestion, with 3100bp and 7557bp for EcoRI and 990bp, 1205bp and 8462bp for XbaI. These colonies were stored (section 2.2.4.9). Colony number 15 was selected at random and prepared for sequencing purposes (section 2.2.4.10).

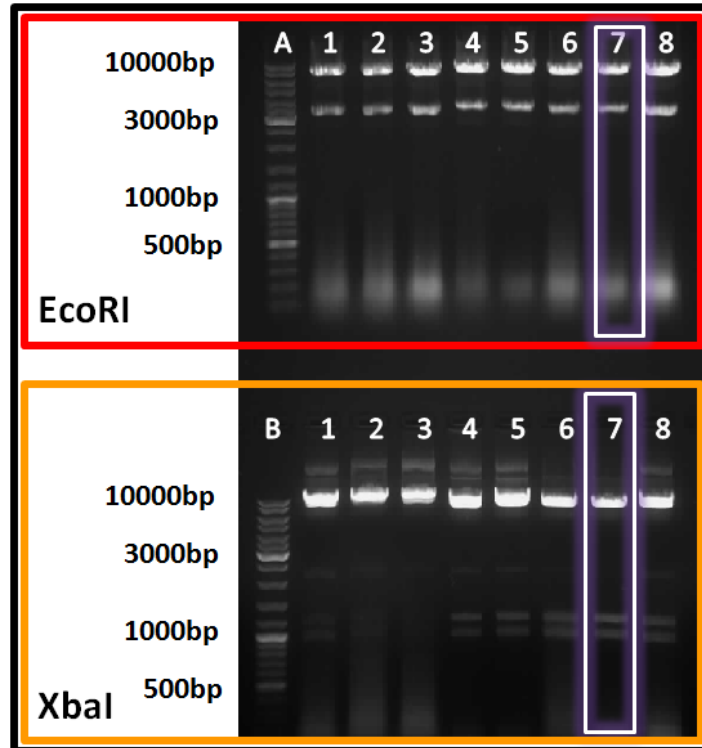


Figure 2.10 – 1% Agarose gel analyses of EcoRI and XbaI digestion of possible pFBqdVP2-8/6/7 plasmid:* Lanes A and B: the DNA Ladder Mix. Lanes: 1 – 8, digestions of positive clones 4, 6, 9, 10, 11, 12, 15 and 21, respectively. Positive clone in lane 7 was randomly selected and prepared for sequencing purposes.

2.3.4. Molecular characterisation of the pFBqdVP2-8*/6/7

An *in silico* sequence of the pFBqdVP2-8*/6/7 clone was designed, prior to the cloning of the construct, with DNAMan (version 4.13) computer software to facilitate the screening of unwanted mutations, occurring in the construct. These unwanted mutations may alter the structure of the translated recombinant proteins. Prior to sequencing, the DNA of plasmid 15 was isolated (section 2.2.4.10). Plasmid 15 was sequenced to ensure that it contained the coding regions of interest (dVP2, VP8*, VP6 and VP7). The primers, used for sequencing, were described in section 2.2.3. The sequence was manually checked and edited with the use of FinchTV. The assembly of the construct was confirmed by aligning it with the *in silico* sequence.

pFBqdVP2-8*67	ACAAAAAACCAACACACAGTTCTAATGAAAATAAAGAACTTTTATTATGAATTC	TTATTA	3960
VP2intF1/F2	-----		12
VP2intR1	-----		0
pFBqdVP2-8*67	CAGCTCGTTCATGATGCGCATGTTGTGCGAAAGCGACAGCGTTGATGGGCTCCACGGTGTC		4020
VP2intF1/F2	-----		72
VP2intR1	-----		0
pFBqdVP2-8*67	AGCGGACACGAAAGCCAGCAGGTCGGAGTACACGGTGAAGGTCAGGTTGGAGGTCAGCAT		4080
VP2intF1/F2	-----		132
VP2intR1	-----		0
pFBqdVP2-8*67	CTGCATGGAGTTACGGGAAGTCGAACTGCTGGGGCACCTGCTTGTACACCTTGGTGGTGGGA		4140
VP2intF1/F2	-----		192
VP2intR1	-----		0
pFBqdVP2-8*67	GGTGGGCACCCAGTCGTAGTTAGCCACCAGGTAGAAGTCGTTGGAGTCGGAGTTGATCTT		4200
VP2intF1/F2	-----		252
VP2intR1	-----		0
pFBqdVP2-8*67	GTACAGGATGGGCTTCAGGGTGTCCACCTTCCTCAGCTTCACGATCTGAGCGAACACGGT		4260
VP2intF1/F2	-----		312
VP2intR1	-----		0
pFBqdVP2-8*67	GGCGTCCAGCTTGGCGATCAGGGAGATGACGGAAGAGTCGGTGATGAAGGGCAGAGCACC		4320
VP2intF1/F2	-----		372
VP2intR1	-----		0
pFBqdVP2-8*67	CACGAGAGCCACGGGCTGGTTGTTTCAGCAGCATGTTGGTGATCTGAGCGTAGTCGCCAGA		4380
VP2intF1/F2	-----		432
VP2intR1	-----		0
pFBqdVP2-8*67	ACGCATCAGCTCCTCCAAGTTGATCTGCTGGAAACCTCCAAGTTACGAGCGATGTTTAC		4440
VP2intF1/F2	-----		492
VP2intR1	-----		0
pFBqdVP2-8*67	GTAACCGTACATCTCGTACAGCTCCAAGTGCATGTCACGGTAAGCGATGATGACACCCTG		4500
VP2intF1/F2	-----		552
VP2intR1	-----		0
pFBqdVP2-8*67	AGCGATCTTGTCGGAAGCACGCTCGATCTGGTCCATGTTTCATCAGGATCAGGTTGAAGAT		4560
VP2intF1/F2	-----		612
VP2intR1	-----		0
pFBqdVP2-8*67	GTCCAGACGACGGATCTCCACGGGCAGCAGGCGCAGACGGTCACGCAGACGGTACATCTG		4620
VP2intF1/F2	-----		672
VP2intR1	-----		0
pFBqdVP2-8*67	CTCGTCGGGCACACGGGACACGTCGAAGATGTACAGGCGCTTGAGGAAGTCTCTCGACGAT		4680
VP2intF1/F2	-----		732
VP2intR1	-----		0
pFBqdVP2-8*67	AGCCTTCATCTTCTTTTGGTAGAGGTTTAGGCGGTTAGCAGCGGTGATGATAGCCACAGC		4740
VP2intF1/F2	-----		792
VP2intR1	-----		0

pFBqdVP2-8*67	CTCGTTGATACGCTCGTTGTAGTTGCTGTGGAAGTTCACGTTACGTTGTAGTAGTGAA	4800
VP2intF1/F2	-----	852
VP2intR1	0
pFBqdVP2-8*67	CAGGGTCTGAGGGGAGGGGATCACGGTAGCGTTGCCGATCAGCATGCACAGGGAGGTCAC	4860
VP2intF1/F2	-----	912
VP2intR1	0
pFBqdVP2-8*67	GGAGGTCAGCTGCAGCTTCTCGGTGGTCAGGGTCTGCACGTGCTGCATGTTTCATGGTGAT	4920
VP2intF1/F2	-----	972
VP2intR1	0
pFBqdVP2-8*67	GCAAGCCATCAGAGTCTCGTAGTTGTAAGCCAGCAGACGGGTCAGGTCCACGAGCTGGCC	4980
VP2intF1/F2	-----	1032
VP2intR1	0
pFBqdVP2-8*67	CAGACGGTTGGACAGCAGCAGGATACCACGCTGGATGGAACGCTTGTAGTCGATAGGCAT	5040
VP2intF1/F2	-----	1092
VP2intR1	0
pFBqdVP2-8*67	GGTGGGGAAGTCTGACGGGACAGCTGCATCAGAGCCTCCATCAGCTGGTTGATCACGTG	5100
VP2intF1/F2	-----	1152
VP2intR1	0
pFBqdVP2-8*67	ACCGTTACGGATGTTGTCGTTACAGACCTGGTTACAGGACACCGTCGATCACAGCCTGACC	5160
VP2intF1/F2	-----	1212
VP2intR1	0
pFBqdVP2-8*67	GAAGTGGTTGTTGTTGACGAAGTGCAGCCAGTTGGCCACCTGGAAGTTCTGGATCTGCTG	5220
VP2intF1/F2	-----	1272
VP2intR1	0
	VP2intF2	
pFBqdVP2-8*67	CTCGGCGATCTGGAAGGGGGTCTGGGGTTCGCCGTTACGGTAGTGCATACGCTGCATGCC	5280
VP2intF1/F2	-----	1332
VP2intR1	0
pFBqdVP2-8*67	GAAAGCGGGGTAGATGATGGTGTTCACGATAGCCAGCTGGCAAGCCACCAGGGACTCGCG	5340
VP2intF1/F2	-----	1392
VP2intR1	0
pFBqdVP2-8*67	GATGAACATGTCGTTAGGCACCACGGTCAGCAGCCACATGCCGAGATCAGGGACATGTA	5400
VP2intF1/F2	-----	1452
VP2intR1	0
pFBqdVP2-8*67	GTTGGTGGTCACGAAGTCCAGGGACATGGTACGCTGGGACAGCATAGCAGCGATCAGGGT	5460
VP2intF1/F2	-----	1512
VP2intR1	0
pFBqdVP2-8*67	CTTGAAGCAGTCGTTAGCAGCCTGGGAGTTGATACCGGTCAGGAAGTCTGAGTCTCGGACTG	5520
VP2intF1/F2	-----	1572
VP2intR1	0
pFBqdVP2-8*67	GATGGTCAGAGCCTCCAAGTGCAGGTCCTGGGACATCTTCTGGATCTGAGCCTCGGTGCT	5580
VP2intF1/F2	-----	1632
VP2intR1	0

pFBqdVP2-8*67	GACCAGTTCCTTCAGGTCGGGCACCACGGAACGAGCGAGGATGTAGTTGGAGGTGGTGAT	5640
VP2intF1/F2	-----	1692
VP2intR1	0
pFBqdVP2-8*67	GGTGTCCACAGGGACTCGAAGTTGTCGTGGAGGTTTCAGACGGTCCTGCAGCAGGTTGGG	5700
VP2intF1/F2	-----	1752
VP2intR1	0
pFBqdVP2-8*67	ACGGATGTAACGAGCGGTGGAGGGCAGGTTACGGTCCATGTTTCAGGATGTAGTTCACGTC	5760
VP2intF1/F2	-----	1812
VP2intR1	0
pFBqdVP2-8*67	GTTACGGATACGCTCGGGGATGTAGTTGAAGATGATGTTCGTTTCAGGGGCTCGACCAG	5820
VP2intF1/F2	-----	1872
VP2intR1	0
pFBqdVP2-8*67	CTGGTCTGGAGGAAGTACTCGTTGAAAGCGTAGTCGATGGGGTGCAGGATGGAGGGTA	5880
VP2intF1/F2	-----	1932
VP2intR1	0
pFBqdVP2-8*67	GTTGACCACGTTACGGTCAGCCTGCACACGCTGACGCATCTCAGCGATGAAACGACGCAC	5940
VP2intF1/F2	-----	1992
VP2intR1	0
	VP2intF1	
pFBqdVP2-8*67	AGCACCTCAGTTTCTCGTCCTGGAAGATAGCGTCGCAGATGGAAGCAGTCTCGGAGTC	6000
VP2intF1/F2	-----	1995
VP2intR1	0
pFBqdVP2-8*67	CACCACCTTGCCAGCGTCACGGGAGTTCTTGTCTCCACAGCCATGTCCTTCAGCAGCAG	6060
VP2intF1/F2	-----	1995
VP2intR1	0
	VP2intR1	
pFBqdVP2-8*67	GTAGTCGGGCATCTCGGTCAGCACCTGGTCGTACAGGTTCAGGAAGTACTCGCGCACGTC	6120
VP2intF1/F2	-----	1995
VP2intR1	0
pFBqdVP2-8*67	GTAGTCGCCGTCGGGCAGGGTATCCTTCTTCAACTTCCAGTACCAACGGTTACGCAGCTC	6180
VP2intF1/F2	-----	1995
VP2intR1	-----	54
pFBqdVP2-8*67	GCGCTCGCCGTTAGCACGGTAGATGGGCAGCTGCTTAGGCTCGAAGATACGGAACAGCTT	6240
VP2intF1/F2	-----	1995
VP2intR1	-----	114
pFBqdVP2-8*67	GGTCTGCTTCTTAGCCAGCTCGGGCTGGATGTCTCCTCCAAC TTGCGCAGGATAGTTTCTTT	6300
VP2intF1/F2	-----	1995
VP2intR1	-----	174
pFBqdVP2-8*67	GGGCTCGAAGGTGGGGATGGTCTTGGATCCTCTAGAGGAACGGGAGGACAGAGCCACGGG	6360
VP2intF1/F2	-----	1995
VP2intR1	-----	234
pFBqdVP2-8*67	CACGATGTTACGGGTGTTCTGCATGGGGGGCAGGCCGGTGTGATGTACTCGGAGCACTT	6420
VP2intF1/F2	-----	1995
VP2intR1	-----	294

pFBqdVP2-8*67	GGATTCTTGGGAACGGGGGATGATGTAGAACTCCACGTGGATCACAGTCTCCACCTCGGA	6480
VP2intF1/F2	1995
VP2intR1	-----	354
pFBqdVP2-8*67	CAGTTGGAGGTGGAGGAGTAGTCGGTGGTAGCGTGGGGAGTCTCGCCGTGGAAGGTCCA	6540
VP2intF1/F2	1995
VP2intR1	-----	414
pFBqdVP2-8*67	CACGGAGTTGTAGAACTTCATGAAACCAGCCAGCTTGGTGTCTGGAGGTCAGGGTACGCTT	6600
VP2intF1/F2	1995
VP2intR1	-----	474
pFBqdVP2-8*67	GTGCTGGAACCTCAGCGTTCACGTTGGAGCGGAACATCTCGAAGAACTTCCACTTGTGGT	6660
VP2intF1/F2	1995
VP2intR1	-----	534
pFBqdVP2-8*67	GTTGTTCTCCACGGTGATCTGCTTAGTCTCGCCGAACAGGGTGTACTGACGGGACTGGTT	6720
VP2intF1/F2	1995
VP2intR1	-----	594
pFBqdVP2-8*67	GGTCACGTTGGGCTCGACCAGCAGCAGGGCCACCCAGATGTCGGTCTTGTGGTGCCTC	6780
VP2intF1/F2	1995
VP2intR1	-----	654
pFBqdVP2-8*67	CAACACCACCTGCTGGTTGGTGGGGTTCAGCAGAATCCAGTAGTCGTTGGGGGGCTTGAA	6840
VP2intF1/F2	1995
VP2intR1	-----	714
pFBqdVP2-8*67	GTTGGTGGGCTGGTAGGGACCGTCCAGCAGGGCTCGATGGTGGTGGAGTCGTTGACCTC	6900
VP2intF1/F2	1995
VP2intR1	-----	774
pFBqdVP2-8*67	GCCGTGGGACCAGGTACGGGAGCGTAGTTGGTCTGAGCGAAGGGACCGGGTTGATGGT	6960
VP2intF1/F2	1995
VP2intR1	-----	834
pFBqdVP2-8*67	CACGTTCTGGGACTTCTCGGAACCGATGGTGTGATCTCGTCCGACAGCTCCACGGTGTA	7020
VP2intF1/F2	1995
VP2intR1	-----	894
pFBqdVP2-8*67	GGAGTTGGTCAGCAGCTGACGGTAGATCAGGGAAGCCATGAATTCAGATCTGTGATTGTA	7080
VP2intF1/F2	1995
VP2intR1	-----	954

Figure 2.11 - The multiple alignment of the partial in silico sequence (pFBqdVP2-8*/6/7) and the sequenced data of the region encoding dVP2-8*: The alignment shows the partial pFBqdVP2-8*/6/7 in silico sequence, depicting only the inserted coding regions of dVP2 and VP8*. The VP2intF1/F2 sequence was obtained through combining the sequence data obtained from the primers VP2intF1, VP2intF2. The sequence VP2inR1 was obtained from the primer with the corresponding name. The restriction enzyme recognition sites are in colour: EcoRI (red), BamHI (yellow) and XbaI (green). The regions encoding dVP2 and VP8* are indicated in pink and dark blue, respectively. The part of the sequence that was not sequenced coloured in turquoise.

The multiple alignment (of the sequenced data with the *in silico* sequence) showed that there were no base changes in pFBqdVP2-8*/6/7. There is a part of the sequence (5944-6126 bp) that was not sequenced. This might be related to the limit in read length due to the polymerase used in the sequencing reaction or the maximum read length that can be obtained with the sequencing approach used. However, it was decided to continue with further experiments without the full confirmation that the coding regions of dVP2 and VP8* were correctly cloned into pFBqVP6/7, since the rest of the sequenced data seemed to be reliable.

2.3.5. Expression of dVP2-8*/6/7 in insect cells

Recombinant bacmids were prepared in ACC DH10Bac *E. coli* cells (section 2.2.1) containing the baculovirus genome. Recombinant bacmids were obtained through a transposition process (section 2.2.6.1) as illustrated in Figure 2.12. Two types of colonies will be present white and blue. White colonies indicate successful transposition of the gene of interest since no functional β -galactosidase could be formed. β -galactosidase reacts with X-Gal to form a blue colour as with what is found in blue colonies. These blue colonies do thus not contain the transposed gene of interest. Eleven white colonies were inoculated, bacmid DNA extracted (section 2.2.6.2) and screened with PCR (section 2.2.6.3) for the insertion of the coding regions of dVP2-8*, VP6 and VP7 into the baculovirus genome. The concentrations of the bacmid DNA obtained were measured (as explained in section 2.2.4.4) and are shown in Table 2.1.

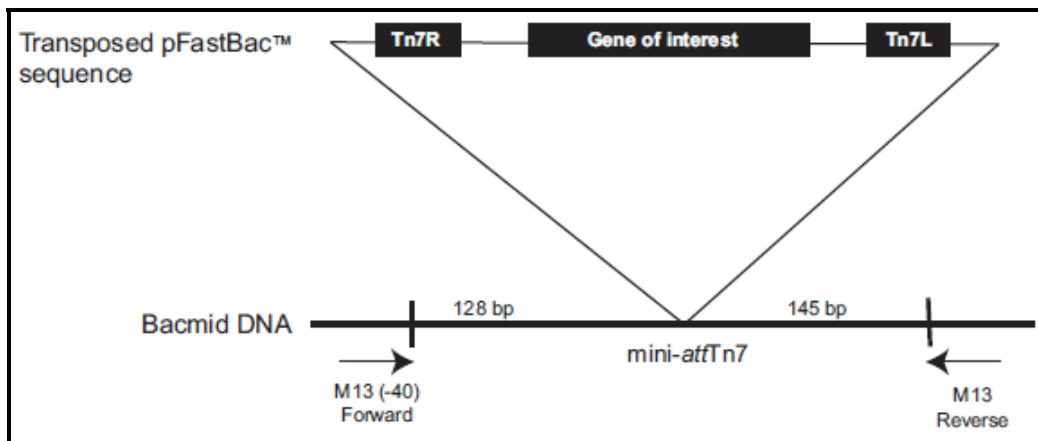


Figure 2.12 – Strategy to analyse recombinant bacmids: Bacmid contains the M13 Forward and Reverse primers that anneal to sites flanking the mini-attTn7 site (within the lacZ α -complementation region) to facilitate the PCR analyses. Illustration taken from the Bac-to-Bac manual from Invitrogen.

Table 2.1 – DNA concentrations of recombinant bacmids

Number of colony	Concentration
1	18.2 ng/μl
2	59.5 ng/μl
3	11.3 ng/μl
4	26.1 ng/μl
5	65.7 ng/μl
6	12.5 ng/μl
7	51.0 ng/μl
8	5.9 ng/μl
9	9.0 ng/μl
10	30.8 ng/μl
11	11.5 ng/μl
12	25.5 ng/μl
13	66.4 ng/μl

(control – pFBq)
(control – pFBq)

Ideally the concentration should have ranged between 1 - 4 μg DNA. The concentration of the bacmids extracted in this study ranged between 10 and 70 ng/μl. Despite the low DNA concentrations (table 2.1), PCR was performed to screen for the recombinant bacmid (section 2.2.5.4). The expected size of the amplicon for the recombinant bacmid was 8438bp. A blue colony was included in the analyses as a negative control, since it does not contain any transposed coding regions. The expected size of the amplicon of the blue colony was 300bp. Another negative control was included in the analysis, known as FB, in lanes 12 and 13 (Figure 2,13). The FB recombinant bacmid was transposed from an empty pFBq, The expected size of the amplicon of the FB recombinant bacmid was 3100 bp. The amplicons obtained were analysed (section 2.2.4.2). The results are shown in Figure 2.13. The amplification of the recombinant bacmid DNA was successful, as a DNA fragment of 8438bp was visible in eight samples (1, 2, 5, 6, 8, 9, 10 and 11). These desired recombinant bacmid clones were stored as described in section 3.2.4.9. Lanes 3, 4 and 7 (Figure 2.13) did not contain any amplicons. This could probably be attributed to drying the bacmid DNA longer than necessary. Due to the extensive drying, the recombinant bacmid DNA could not be resuspended or dissolved for PCR analysis resulting in no amplicons.

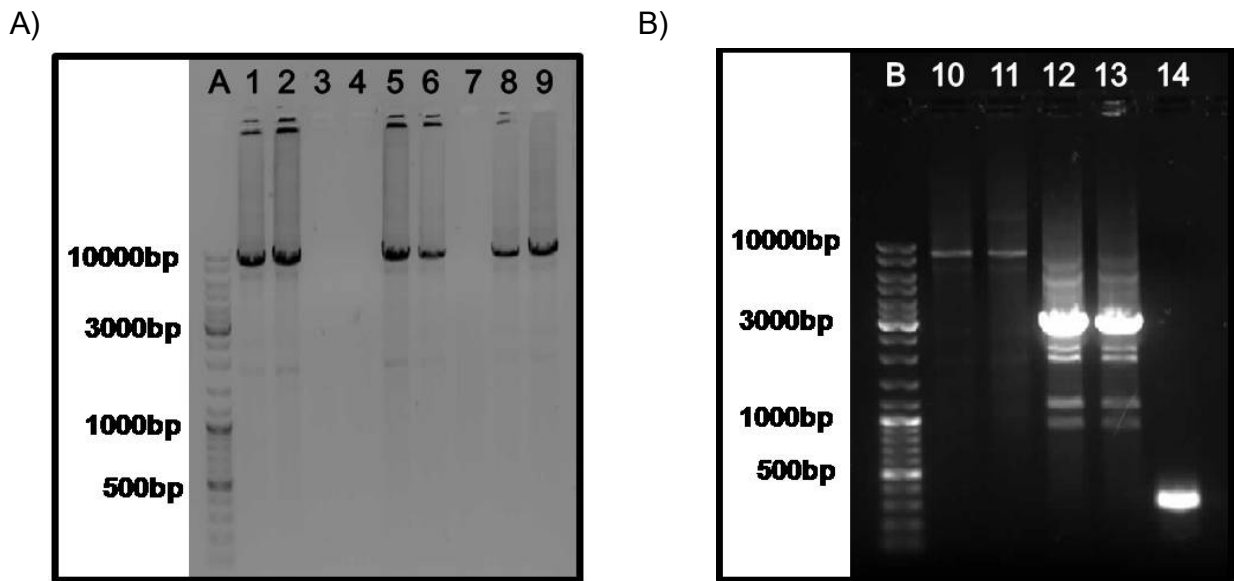


Figure 2.13 – 1% Agarose gel analyses of the recombinant bacmids: Lanes: A and B, 9 μ l Express DNA ladder; 1 to 11, 20 μ l amplified, constructed recombinant bacmid DNA; 12 and 13, 20 μ l amplified, constructed recombinant bacmid DNA generated from the empty pFBq cloning vector; 14, 20 μ l blue colony as a negative control.

Some of the parameters of the bacmid DNA isolation procedure (section 2.2.5.2) were optimised, in order to yield higher bacmid DNA concentrations. These parameters included doubling all of the incubation and centrifuge times. The volume of water used to resuspend the bacmid DNA pellet, was decreased to 30 μ l. In preparation for transfection, the colonies containing the recombinant bacmid DNA were streaked out onto agar plates and incubated. The recombinant bacmid DNA was isolated under sterile conditions (section 2.2.5.3). The concentration of bacmid DNA obtained (section 2.2.4.2), are displayed in table 2.3. The concentrations were high enough and the DNA could be used for the transfections. The bacmid DNA obtained was screened (section 2.2.5.4) and results are displayed in Figure 2.14. These results were positive. As before (Figure 2.13) the recombinant bacmid was present in all the colonies at approximately 8438bp.

Table 2.2 - The isolated recombinant bacmid DNA prepared for transfection

Number of colony	Concentration
1	2.6 µg/µl
2	1.8 µg/µl
5	3.8 µg/µl
6	3.4 µg/µl
8	1.6 µg/µl
9	2.8 µg/µl

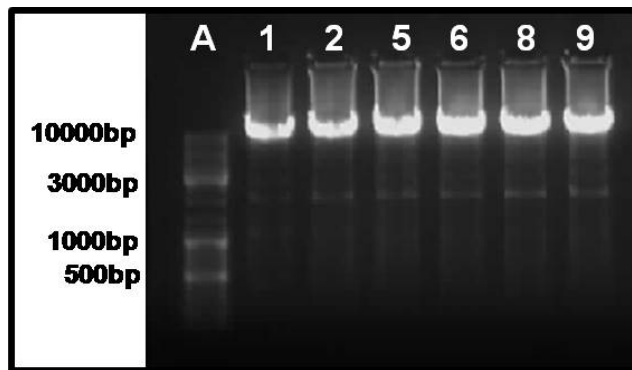


Figure 2.14 - 1% Agarose gel analyses of the recombinant bacmids prepared for transfection:
Lane A: 9µl Express DNA ladder. Lanes 1, 2, 5, 6, 8, 9: 20ul amplified, constructed recombinant bacmid DNA.

Transfections were performed (section 2.2.5.5) with all six the recombinant bacmid DNA constructs, displayed in Figure 2.14. The cytopathic effect (CPE) of the cells was monitored after transfection. At 96 h post-transfection CPE was completed. The transfection supernatant (P1 viral stock) was harvested as described in section 2.2.5.6.

This supernatant was expected to contain the recombinant baculovirus, expressing the rotavirus construct dVP2-8*/6/7. In order to evaluate the expression of the protein construct, a secondary infection was performed (section 2.2.5.7). The cells and supernatant (known as P2 viral stock) were harvested separately (section 2.2.5.8) and the total protein content (of soluble and insoluble proteins) were evaluated for expression using SDS-PAGE (section 2.2.5.9).

Expression of the fused protein dVP2-8* was observed at 106,7 kDa (Figure 2.15 lanes 3, 4, 5, 6, 7, and 8). This compares well with the expression of the fused protein (dVP2-8*) reported by Perez and co-workers (2006). The expected sizes for VP6 and VP7 are 44,9 kDa and 37 kDa, respectively. The wild type (FB) baculovirus was included as a negative control during the

expression analysis. The FB negative control originated from the transformation of the transposon region of an empty pFBq (containing no cloned coding region inserts) into the baculovirus genome within the ACC DH10Bac cells. This “empty” isolated recombinant bacmid was transfected into Sf9 cells along with the rest of the recombinant bacmids. The wild type (FB) baculovirus does not express dVP2-8*, VP6 or VP7. Furthermore, the recombinant baculovirus expressing VP2 (102,7 kDa), VP6 and VP7, functioned as a comparison to the new recombinant baculovirus construct. Although the recombinant protein bands are very faint, expression of some of the proteins could still be visualised. It was unclear whether VP7 was expressed at all, since no clear distinction could be made from the gel. We expected VP7 expression at 37 kDa in the dVP2-8*/6/7 and VP2/6/7 constructs, but the FB negative control also contained a band of that particular size. Three possible explanations could be formulated: one, these protein bands are from baculovirus origin and are not VP7; two, these protein bands are from Sf9 insect cell origin and are not VP7; or three, the negative control was contaminated with VP7 prior to the expression analysis. Bands of VP2, dVP2-8*, and VP6 proteins were visible (Figure 2.15). It was concluded that the expression of dVP2-8* was successful with the BEVS from the expression analysis.

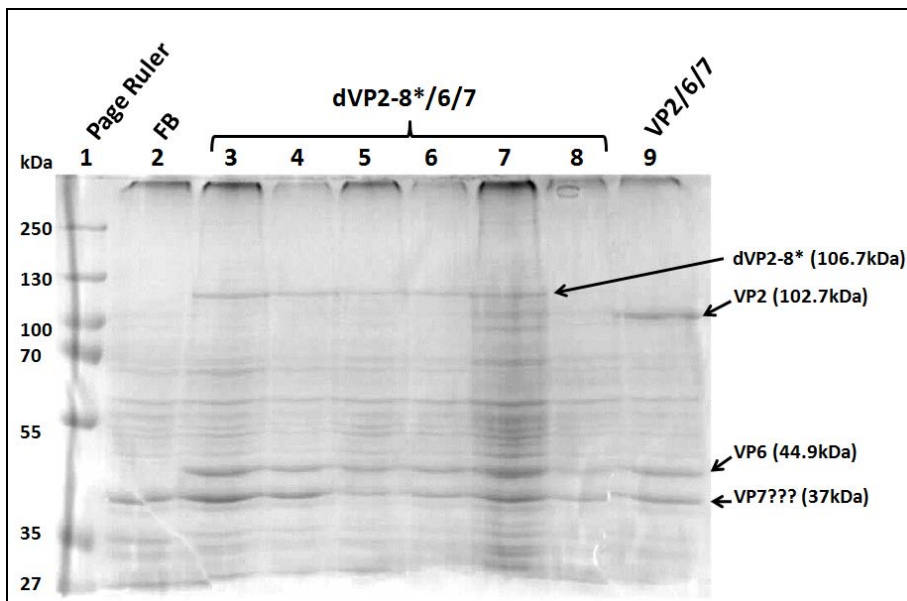


Figure 2.15 – 10% SDS-PAGE analyses of the expression of dVP2-8/6/7:* Lanes: 1, 9 μ l PageRuler (Fermentas); 2, 20 μ l wild type (FB) baculovirus as a negative control; 3-8, 20 μ l expressed fused recombinant construct d92VP2-8*/6/7; and 9, 20 μ l expressed recombinant construct VP2/6/7.

2.3.6. Investigation of protein solubility of recombinant dVP2-8*/6/7

SDS-PAGE can be used to evaluate the solubility of proteins. Solubility often correlates with biological activity and correctly presented epitopes that induce protective immunity. A test was performed using the dVP2-8*/6/7 construct, to compare the effects of three different lysis buffers on protein solubility. The lysis buffers that were used are the following:

1. Phosphate buffer solution (PBS) containing 0.5% nonyl phenoxy-polyethoxy-ethanol (NP40)
2. 10 mM Tris containing 0.1 mM EDTA, 1% dissolved organic carbon (DOC), 0.1% SDS
3. 10 mM Tris containing 0.1 mM EDTA, 1% SDS

These buffers will be referred to as buffer 1, 2 and 3 for the remainder of the study. Buffer 1 was previously used in the laboratory. Alternatively, buffers 2 and 3 were published by Labbe and co-workers (1991), who reported that VP2 was 75% soluble in buffer 2 and 100% soluble in buffer 3. The solubility percentage was determined from the remainder of VP2 in the supernatant subsequent to centrifugation. All of the lysis buffers were supplemented with the Complete, Mini, EDTA-free protease inhibitor cocktail solution (Roche) containing serine and cysteine protease inhibitors. These inhibitors prevented protein degradation. The infection procedure and harvesting of the infected cells, was performed as described in section 2.2.5.7 and 2.2.5.8, respectively. Cells were resuspended in 100 µl of the listed lysis buffers. The soluble and insoluble fractions (of the samples) were separated through centrifugation at 13.2×1000 rpm. The samples resuspended in buffers 2 and 3, were centrifuged immediately. Alternatively, the sample resuspended in buffer 1 was incubated at room temperature for 30 min, prior to the centrifugation. The insoluble fractions were discarded. The presence of proteins in the soluble fractions, were evaluated using SDS-PAGE (section 2.2.5.9). The expression results are displayed in Figure 2.16. A wild type (FB) baculovirus was included as a negative control during the expression analysis and was dissolved with all three of the buffers, independently. As explained previously, this virus does not express dVP2-8*, VP6 or VP7. According to the results obtained, the only buffer which dissolved dVP2-8* and VP6 was buffer no. 3. The presence of VP7 expression still remains a debatable factor, since the protein band was present all of the soluble fractions along with the FB negative controls. The other two buffers (no. 1 and 2) precipitated the proteins, which were discarded along with the insoluble fractions. Thus, no protein expression of dVP2-8* and VP6 (with VP7 as a possible exception)

were visible (Figure 2.16) for buffers 1 and 2. dVP2-8* (106,7kDa), VP6(44,9kDa) and possibly VP7 (37kDa) are only visible in lane 7 (Figure 2.16).

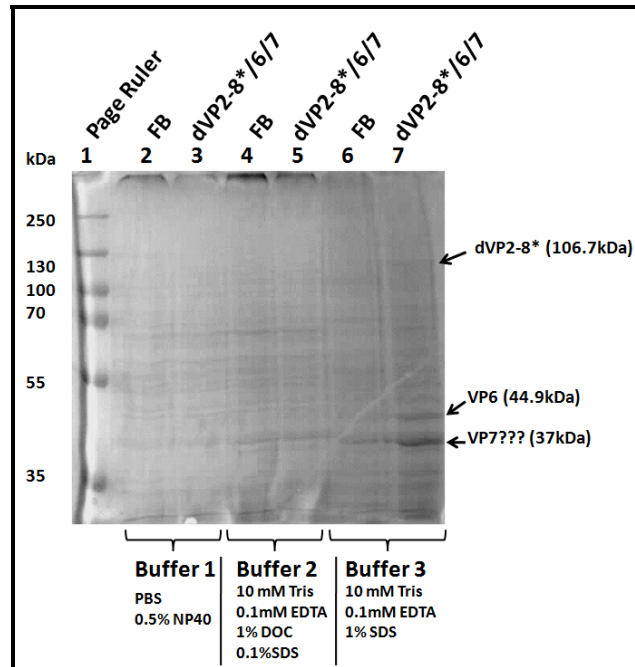
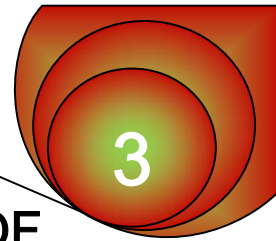


Figure 2.16 – 10% SDS-PAGE analyses of the expression of dVP2-8*/6/7 resuspended in three separate buffers: Lanes: 1, 5µl of PageRuler (Fermentas); 2, 20µl of FB as a negative control (suspended in buffer no. 1); 3, 20µl of expressed fused recombinant construct dVP2-8*/6/7 (suspended in buffer no. 1); 4, 20µl of FB as a negative control (suspended in buffer no. 2); 5, 20µl of expressed fused recombinant construct dVP2-8*/6/7 (suspended in buffer no. 2); 6, 20µl of FB as a negative control (suspended in buffer no. 3); and 7, 20µl of expressed fused recombinant construct dVP2-8*/6/7 (suspended in buffer no. 3).

2.4. Summary

Oligonucleotides were designed (section 2.3.1) for the successful amplification of the regions encoding dVP2 and VP8* from genome segments 2 and 4, respectively (section 2.3.2). These two truncated regions were ligated and subsequently cloned into the pFBq vector, which already contained the coding regions of VP6 and VP7 (sections 2.3.3 - 2.3.4). The pFBqdVP2-8*/6/7 was sequenced by the Central DNA Sequencing Facility (Stellenbosch University). The sequenced data of pFBqdVP2-8*/6/7 was compared to the *in silico* sequence constructed with DNAMAN (section 2.3.4). Although there was a small part of the sequence not characterised (5944-6126 bp) it was decided to continue with subsequent experiments without the full confirmation that the coding regions of dVP2 and VP8* were correctly cloned into pFBqVP6/7. The MCS of pFBqdVP2-8*/6/7 was transposed into the baculovirus genome contained within

the ACC DH10Bac *E.coli* cells. Recombinant bacmids were isolated and screened for correct transposition of the coding regions dVP2-8*, VP6 and VP7. Positive recombinant bacmid clones were used during transfection experiments with Sf9 cells. The expression of dVP2-8* and VP6 with recombinant baculoviruses, were evaluated with SDS-PAGE (section 2.3.5). The expression of dVP2-8* and VP6 were successful. The expression of VP7 still needs to be verified as no clear distinction could be made between the protein bands seen in the dVP2-8*/6/7 construct and the negative control. An investigation was performed to compare the effect of different buffers on the solubility of the dVP2-8*, VP6 and VP7 proteins (section 2.3.6). Suspension of the proteins with buffer 3 (10 mM Tris containing 0.1 mM EDTA, 1% SDS) exclusively yielded the soluble fraction of the expressed dVP2-8* and VP6.



CHAPTER 3:

ANALYSIS OF VARIOUS RECOMBINANTS OF ROTAVIRUS VP2, VP6, VP4, VP7 AND dVP2-8* OF G9P[6] BACULOVIRUS EXPRESSION AND PARTICLE FORMATION

3.1. Introduction

Roldáo *et al.*, (2006) reported the determining factors for the synthesis of recombinant rotavirus structural proteins. These factors include the concentration of intracellular rotavirus viral DNA (vDNA), the size of the protein, codon usage and maturation time of the rotavirus particle. The formation of the glycoprotein (VP7) takes approximately 30 minutes longer, than the rest of the proteins (VP2, VP6 and VP4) (Lodish *et al.*, 1986).

In this chapter of my study I focused on the verification of expression of all the engineered rotavirus recombinant proteins. These recombinant constructs were expressed by the BEVS in Sf9 insect cells suspended in Excell Titre High medium and were the following: VP2/6, VP2/6/7, dVP2-8*/6/7 and VP2/6/4/7. The production of the various rotavirus-like particles was evaluated with transmission electron microscopy (TEM). In addition, the expression of the recombinant proteins was evaluated and compared in two different cell lines; Sf9 and Sf9 mimic cells.

3.2. Materials and methods

3.2.1. Extraction of baculovirus DNA (gDNA) from insect cells

Prior to the Bac-gDNA isolation, the recombinant baculoviruses expressing genome segments 2, 4, 6 and 9 encoding VP2, VP4, VP6 and VP7, respectively, were used to infect Sf9 cells (section 2.2.5.6) separately. The recombinant baculovirus expressing genome segments 6 and 9 encoding VP6 and VP7 along with the truncated genome region encoding dVP2-8* (Chapter 2), was also used. The suspension medium and cells containing the various recombinant baculoviruses, were harvested (section 2.2.5.7) separately with minor alterations. The cell pellet was, resuspended in 200 µl 1×PBS. The Bac-gDNA was isolated with the ZR Insect & Tissue DNA Kit-5 (Zymo research). Cells were added to ZR BashingBead™ Lysis tubes (Zymo

research), containing 750 µl lysis solution. The tubes were shaken with a beadbeater (Rentsch, model MM400) at 30 Hz for 10 min to release the contents of the cells. Cell debris was pelleted by centrifugation and the supernatant was transferred onto a Zymo-Spin™ IV Spin Filter (Zymo research), fitted inside a collection tube. Bac-gDNA containing supernatant was passed through the filter to remove any remaining cell debris. Bac-gDNA was lysed by 1200 µl Genomic Lysis buffer. Bac-gDNA was adhered to a Zymo-Spin™ IC Column (Zymo research) with the same principle as described in section 2.2.4.3. Bac-gDNA was washed with pre-wash- and wash-buffer, prior to centrifugation, to remove any remaining contaminants. Bac-gDNA was eluted from the column by the addition of 15µl elution buffer and subsequently centrifuged. The concentration and purity of the Bac-gDNA was determined (section 2.2.4.4). The isolated DNA was used to amplify (section 2.2.4.1) genome segments 6 and 9 encoding VP6 and VP7, using primers (Appendix 2) with minor alterations. The primers were annealed for 30 s at 58 °C. The DNA amplicons were analysed as described in section 2.2.4.2.

3.2.2. Western blot assay

The SDS-PAGE gel containing separated proteins was electro-transferred onto a nitrocellulose membrane (Whatman) for 1 hour at 100 V in the presence of transfer buffer. The transfer buffer consisted of 0.025 M Tris, 0.2 M Glycine and 20% methanol (pH 8.4). Protein transfer was verified with Ponceau S solution (Fluka Biochemika). After the transfer verification, the staining solution was removed and the nitrocellulose membrane washed with distilled water. In order to prevent non-specific binding of the antibodies to the proteins, the membrane was soaked in blocking buffer containing 5% skim milk, 0.1% Tween-20, 0.2 M NaCl and 0.05 M Tris-HCl (pH 7.4) for approximately 8 h. The membrane was, subsequently, incubated with the primary Goat polyclonal anti-rotavirus antibody (Abcam) in a 1:1000 dilution ratio for 8 h. The primary and secondary antibodies were diluted in blocking buffer. Afterwards the membrane was rinsed with washing buffer containing 0.1% Tween-20, 0.2 M NaCl and 0.05 M Tris-HCl (pH 7.4). The secondary antibody, which was specific to the primary antibody used, was Donkey anti-Goat IgG (Abcam). The membrane was incubated in the secondary antibody in a 1:500 dilution ratio for 1 hour. In addition, the secondary antibody contained a covalently attached horseradish peroxidase enzyme. Following the secondary antibody incubation, the membrane was rinsed once more with the washing buffer. After the removal of any traces of remaining antibody, the membrane was developed with the Pierce ECL Western Blotting Substrate (Pierce). The substrate contained a 1:1 ratio of Detection reagent 1 (Peroxide solution) and Detection reagent 2 (Luminol enhancer solution). The substrate binds to the horseradish peroxidase enzyme

which in turn leads to the decay of oxidised luminal radicals and results in light emission that can be captured onto Kodak Biomax X-ray film (Sigma). The film was exposed to Ilford Phenisol developing solution (Ilford) until protein bands were visible. Subsequently, the film was fixed for 5 min with Ilford Rapid Fixer solution (Ilford).

3.2.3. Amplification of virus-stock

According to the Bac-to-Bac manual (Invitrogen), if the titre of the recombinant baculovirus stock (or P2 viral stock) has not been determined, the titre may be assumed to range between 1×10^6 pfu/ml and 1×10^7 pfu/ml. For amplification purposes, it was assumed that the recombinant baculovirus stock (or P2 viral stock), contained a titre of 1×10^6 pfu/ml. The recombinant baculovirus stock expressing the genome segments was used to infect Sf9 cells (section 2.2.5.6) with minor alterations. The cells were seeded in a 75 cm³ flask (Nunc) containing 1.5×10^7 cells covered with Excell Titre High medium (SAFC Biosciences). The preparation Excell Titre High medium (SAFC Biosciences) did not include the use of FBS, and was described in Appendix 2. After the formation of the cell monolayer, cells were infected with the appropriate recombinant expressing baculovirus at an MOI of 0.1, determined from the assumed titre of 1×10^6 pfu/ml. Initially, 1.5 ml of the P2 viral stock was diluted to 7 ml with Excell Titre High medium (SAFC Biosciences). The diluted virus was used to infect the cells which were then rocked for 1 hour. Before incubation at 28 °C, a further 8 ml Excell Titre High medium (SAFC Biosciences) was added to the flask. The CPE was monitored, until reaching approximately 95-100%. Cells and 15 ml P3 viral stock was harvested (section 2.2.5.7).

Another blind amplification was performed with a multiplicity of infection (MOI) of 0.1 using 10 ml of the P3 viral stock. A 100 ml suspension culture (including the 10 ml viral stock) was used containing 1×10^6 cells/ml in Excell Titre High medium (SAFC Biosciences). The CPE was monitored by counting the number of live cells with the use of a haemocytometer (Nunc) in the presence of 0.4% trypan blue solution, until reaching approximately 95-100%. Cells and P4 viral stock were harvested (section 2.2.5.7).

3.2.4. Viral plaque assay

The assay was used to determine the titre of the amplified P4 viral stock (section 3.2.3). Prior to infection cells were seeded (section 2.2.5.4) in a six-well plate (Nunc). Log dilutions of the P4 viral stock were prepared in TC100 medium (Sigma), ranging from 10^{-1} to 10^{-8} . These dilutions

were then layered on top of the cell monolayer and incubated for 1 hour at 28°C. After the incubation, the dilutions were removed starting at the highest dilution (10^{-8}) and ending with the lowest (10^{-1}). The dilutions were replaced with 2 ml of plaquing medium, which consisted of 1% low melting point agarose gel (Sigma) prepared in Grace's medium (Invitrogen) containing 10% FBS, 5% Penicillin / Streptomycin and 5% Amphotericin. The agarose gel overlay was allowed to polymerise for about 20 min. Subsequently, the plates were incubated at 28°C for 7-8 days. A mock infection was included as a control during the analyses, to monitor cell growth.

After the control monolayer of cells was approximately 100% confluent, the cells were stained with yellow coloured 0.1% Thiazolyl Blue Tetrazolium Bromide (MTT) (Sigma) for 8 h. MTT is converted by mitochondrial dehydrogenases of living cells to form a MTT formazan of dark blue/purple colour. The preparation of the MTT was described in Appendix 2.

3.2.5. Infection of Sf9 cells with recombinant baculovirus

The titred P4 recombinant baculovirus stock (section 3.2.4) was used to infect Sf9 cells (section 2.2.5.6). For infection purposes, an MOI of 1.5 was used. A volume of 20 ml P4 viral stock was diluted to a final volume of 100 ml suspension culture, containing 1×10^6 cells/ml. The cells were suspended in Excell Titre High medium (SAFC Biosciences). Cell viability was observed with the use of a haemocytometer (Nunc) in the presence of 0.4 % trypan blue solution. When CPE of approximately 95 % was achieved (120 hpi), the cells and supernatant were harvested by centrifugation at $3000 \times g$ for 15 min at 4 °C.

3.2.6. Sucrose gradient purification of rotavirus-like particles

The cells and recombinant baculovirus expressed protein containing medium (section 3.2.5), were purified and analysed separately. The cell pellet was resuspended in 10 ml lysis buffer (containing 10 mM Tris, 0.1 mM EDTA, 1% DOC, 0.1% SDS and protease inhibitors) and centrifuged at $3000 \times g$ for 15 min, to remove cell debris. The latter lysis buffer was mentioned earlier (section 2.3.6) where it was referred to as lysis buffer 2. Although the results (Figure 2.16) showed little protein solubility, this buffer was utilised based on reports by Labbe and co-workers (1991). The authors used buffer 2 during the purification of VLPs, and reported optimal results depicting intact purified DLPs. The 100 ml clarified supernatant was layered on top of 5 ml 40% sucrose cushions (prepared in $1 \times$ PBS). Ultracentrifugation was performed with the Sorvall GX ultracentrifuge, unless stated otherwise. The samples were centrifuged for 2 h at 27

000 rpm at 4 °C, with the Sorvall Surespin 630 rotor. Subsequently, the supernatant was discarded and the pellets were resuspended in 400 µl 1×PBS. Volumes of 100 µl and 300 µl of the medium and cell protein samples were loaded on top of discontinuous sucrose gradients (10% - 60%), prepared in 1×PBS. The samples were centrifuged for 1 hour at 28 000 rpm in a Sorvall TH-660 rotor at 4 °C. After centrifugation, gradients were carefully placed on the Instrument Gradient Station fractionator (Biocomp). The fractionator was programmed to collect fractions of 220 µl in 1.5 ml centrifuge tubes from the top of the gradient. Thus fraction 1 was the top fraction and fraction 16 was the bottom fraction. These fractions were analysed independently.

3.2.7. Bicinchoninic (BCA) assay for protein quantification

The protein quantity of the sucrose gradient fractions (obtained in section 3.2.6), were determined with the use of the BCA assay (Sambrook and Russell, 2001). During this assay, Cu^{2+} is reduced to Cu^+ in the presence of aromatic amino acids. Bicinchoninic acid (BCA) reacts with Cu^+ and gives rise to an intense purple colour, with a maximum absorption at 562nm. A volume of 1 µl of the protein sample was diluted with 9 µl ddH₂O (10×) in a 96-well plate. This 10 µl protein dilution was then mixed with 200 µl of a 50:1 v/v ratio solution of BCA:CuSO₄.5H₂O (Sigma). Bovine serum albumin (BSA) (Sigma) was used for the preparation of a standard range, during the quantification. The BSA standard range ranged from 0 – 10 µg/µl, with intervals of 2 µg/µl. All reactions were prepared in duplicate. The microplate was incubated at 37 °C for 20 min. The absorbance of each sample was measured at 562 nm with a Biotek Synergy HT plate reader (BioTek Instruments). The protein quantity of each fraction was quantified using the standard curve from the bovine serum albumine (BSA) (Sigma) standard range, with Gen5 (version 1.11) automated software (BioTek Instruments).

3.2.8. Transmission electron microscope (TEM) visualisation of rotavirus particles

The fractions exhibiting the highest level of expression of the recombinant proteins (VP2, VP4, VP6, VP7 and dVP2-8*) of each rVLP was prepared for TEM visualisation. The fraction was layered on top of approximately 4.2 ml 1 × PBS (Appendix 2). The sample was centrifuged for 1 hour at 28 000 rpm in a Sorvall TH-660 rotor at 4 °C in order to remove any traces of sucrose, which might influence the visualisation of the particles. The supernatant was, subsequently, discarded and the pellet was resuspended in 50 µl 1 × PBS (Appendix 2).

The integrity and morphology of the rotavirus-like particles were observed with the use of TEM. TEM utilises electrons that pass through a sample for image capturing. A drop (5 µl) of protein sample, described above, was adsorbed onto a 3.05 mm diameter, 0.85% formvar coated, 400 mesh copper grid (Agar Scientific) for 60 s. A drop (5 µl) of 1% uranyl acetate (Merck) was used to stain the grid for 30 s, before air drying and examination. Various, independently prepared, grids were examined with one of three TEMs (Table 3.1).

Table 3.1 – TEM models used for the visualisation of rVLPs

Number	TEM model	Location	Operator
1	Philips CM10	Electron Microscopic Unit, North-West University Potchefstroom campus	Mrs. W. Pretorius
2	Jeol JEM-1200 Ex Mk-I	Agricultural Research Council - Onderstepoort Veterinary Institute (ARC-OVI)	Mr. J. Putterill
3	Philips CM10	Faculty of Veterinary Science Electron Microscopic Unit, University of Pretoria	Mrs. E van Wilpe

For the first and second TEMs, the micrographs were developed on film. The third TEM made use of AnalySIS i-TEM (SIS – Soft Image Systems) software for the digital imaging and measurements of the particles. The microscopes were all operated at approximately 80 kV.

3.3. Results and Discussion

3.3.1. Generation of a pFBq-based recombinant baculovirus control

During expression analysis experiments (Figure 2.15), it was unclear whether the expression of VP7 was successful, since the protein band (suspected to be VP7) was also present in the recombinant baculovirus negative control (FB). As mentioned earlier (section 2.3.5) three possible explanations for this occurrence could be formulated, where this protein band originated either from the baculovirus itself, the insect cells or by contamination of the negative control with VP7. To eliminate the possibility of VP7 contamination of the baculovirus (FB) negative control, a new negative control was generated to re-evaluate whether VP7 was being expressed or not.

To verify that the newly isolated (2.2.4.10) pFBq DNA (section 2.2.2) did not contain any contaminating traces of genome segment 9 (encoding VP7), pFBq DNA was amplified (section

2.2.4.1) with VP7FOR and VP7REV primers (Integrated DNA Technologies) complimentary to segment 9 (encoding VP7). Amplification alterations entailed the use of denaturing and annealing temperatures at 96 °C and 65 °C, respectively. Amplification results were analysed (section 2.2.4.2) and are displayed in Figure 3.1. The size of the expected amplicon of segment 9 (encoding VP7) was 977 bp. The newly isolated and previously used (old) pFBq cloning vector (lanes 3 and 4, respectively, Figure 3.1) did not contain an amplicon of segment 9 (VP7). Thus, the newly isolated pFBq DNA was not contaminated with traces of segment 9 and could be used during subsequent experiments. The previously used pFBq DNA was not contaminated either, which meant that potential contamination might have occurred on a later stage in the generation of the negative control. A DNA sample of pFBq containing segments 4 (VP4) and 9 (VP7) was included as a positive control during the amplification analyses. Segment 9 was amplified successfully in the positive control, as a fragment was clearly visible at 977 bp (lane 6 – Figure 3.1). There was another band present at approximately 3500 bp (lane 3 – Figure 3.1) in the new pFBq control. The presence of this band was probably due to contamination during the preparation of the amplification samples so it was decided to continue with further experiments nonetheless. An amplicon of approximately 977 bp was obtained in the negative control of pFBq containing segments 6 (VP6) and 2 (VP2). This meant that the pFBqVP2/6 DNA was contaminated with traces of segment 9 (VP7) DNA. Although this contamination was present on a DNA level, it was uncertain if it was also present on a protein level. Thus, it was decided to evaluate whether the recombinant baculovirus expressing recombinant rotavirus VP2/6 (generated from transposition with the pFBqVP2/6 in question) contained contaminating traces of VP7 (section 3.3.3).

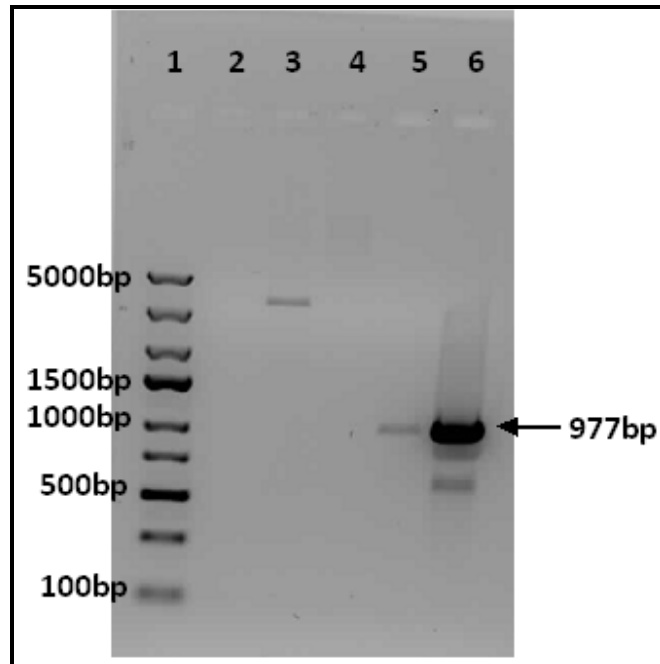


Figure 3.1 – 1% Agarose gel analysis of the amplification of new pFBq plasmid DNA using segment 9 (VP7) primers: Lanes: 1, 6 µl Express DNA ladder (Fermentas); 2, 20 µl negative no template control; 3, 20 µl newly isolated pFBq plasmid DNA; 4, 20 µl previously used (old) pFBq plasmid DNA; 5, 20 µl VP2/6 coding regions; 6, 20 µl VP4/7 coding regions.

The newly isolated pFBq DNA was used for the construction of a new wild type baculovirus negative control. Bacmid construction and isolation was performed as described previously (sections 2.2.5.1-2.2.5.2). The transposition process used for bacmid construction was illustrated in Figure 2.12. The generated recombinant bacmid DNA was screened with PCR for the transposition of FB into the baculovirus genome (section 2.2.5.3). The expected fragment for FB was 3100 bp. As a negative control, blue colonies were isolated and analysed alongside the white colonies obtained. The expected fragment for the blue colony was 300 bp. The amplicons were analysed (section 2.2.4.2) and are illustrated in Figure 3.2. The fragment of 3100 bp was present in lanes 3-8 and 10-12 (Figure 3.2), thus transposition was successful in these colonies. The fragment of the negative control was present at 300 bp in lanes 13-16 (Figure 3.2), where no transposition occurred. In lane 17 both fragments related to the negative control (300 bp) and those expected for successful transposition are present. This is related to the fact that the colony picked for amplification was a mixture of cells containing the empty bacmid and recombinant bacmid. This colony was probably not purely blue neither white but rather grey. Some non-specific amplified fragments are present in the new recombinant bacmid samples, located in lanes 3-8 and 10-12 (Figure 3.2). The recombinant bacmid colonies, located in lanes 3, 6, 8, 10 and 11, were stored (section 2.2.4.9).

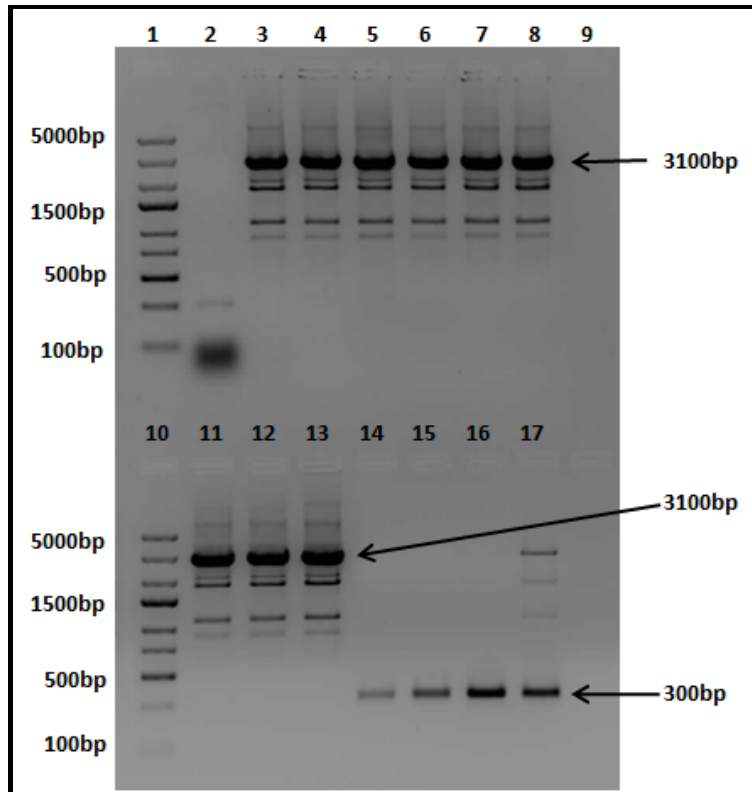


Figure 3.2– 1% Agarose gel analyses of recombinant FB bacmids: Lanes: 1 and 10, 3 μ l Express DNA ladder (Fermentas); 2-8 and 11-13, 20 μ l constructed recombinant bacmid DNA; 9, 20 μ l no template control and lane 14-17, 20 μ l blue colony as a negative control.

For transfection purposes the colonies containing recombinant bacmid DNA were streaked out onto agar plates and grown prior to inoculation. The recombinant bacmid DNA was isolated under sterile conditions (section 2.2.5.2). The concentrations of DNA obtained were analysed (section 2.2.4.4) and are displayed in Table 3.2. These concentrations obtained were low and not optimal for transfection purposes, but were used nonetheless. A possible explanation for the low DNA concentrations could be attributed to the isolated DNA being air-dried too long, leading to the difficulty of DNA resuspension.

Table 3.2– Concentrations of the isolated recombinant bacmid DNA of FB negative control

Number of clone	Concentration
3	82.5 ng/μl
6	72.0 ng/μl
8	70.3 ng/μl
10	47.5 ng/μl
11	67.9 ng/μl

Transfections were performed (section 2.2.5.4) with the five new control recombinant bacmid DNA constructs, displayed in Figure 3.2. The CPE of the cells were monitored after transfection. At 96 h post-transfection CPE was completed. The transfection supernatant (P1 viral stock) containing the baculovirus expressing the new FB negative control, was harvested (section 2.2.5.7). In order to evaluate the expression of the new FB control a secondary infection was performed (section 2.2.5.6) and CPE was monitored. The cells and supernatant (known as P2 viral stock) was harvested at 96 h post-infection (hpi) (section 2.2.5.7). The expression of the proteins, were evaluated (section 2.2.5.8).

The SDS-PAGE analysis results are shown in Figure 3.3. Although no clear and sharp bands were obtained during the SDS-PAGE analyses, it was still possible to evaluate expression. All the FB baculovirus constructs still expressed the protein band (speculated to be VP7) at 37kDa (lanes 2-6 – Figure 3.3) when compared to the results obtained in Figure 2.15. This raised the question of whether VP7 was being expressed at all. Assuming that the band at 37 kDa was not VP7, it was concluded to be of either baculovirus or insect cell origin. Furthermore, the negative control does not express any of the other recombinant proteins (VP2, VP4, VP6, VP7 and dVP2-8). In addition, when comparing the expression results obtained in Figure 2.15 with that of Figure 3.3, similar prominent bands are visible in both - for example the band located just below the 70 kDa marker line. Thus, concluding that the first FB negative control was not contaminated with traces of recombinant baculovirus expressing VP7 after all. From the expression analysis, it was concluded that the expression of the new FB control (FB) was successful with the BEVS. Sample FB (F2) #8 (lane 5 – Figure 3.3) was selected at random for subsequent expression experiments.

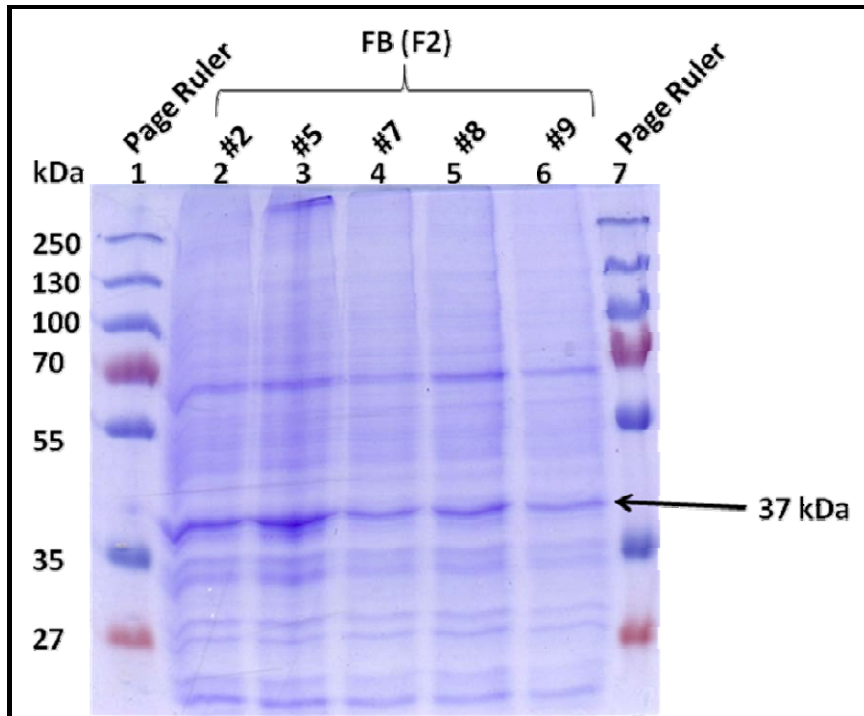


Figure 3.3 – 10% SDS-PAGE analyses of the expression of recombinant baculovirus negative control (FB): Lanes: 1 and 7, 5 μ l PageRuler (Fermentas); 2 to 6, 20 μ l of the respective new FB controls.

3.3.2. Description of baculoviruses used for expression of various combinations of rotavirus proteins VP2, VP4, VP6, VP7 and dVP2-8*

Several recombinant baculoviruses were engineered to express recombinant rotavirus capsid proteins in the following combinations: VP2/6, VP2/6/7, dVP2-8*/6/7 and VP2/6/4/7. The dVP2-8*/6/7 baculovirus expressed construct was generated during this study and was described in Chapter 2. The other three recombinant baculoviruses were prepared by Dr. H.G. O'Neill. This section focused on the evaluation of expression of all of the recombinant proteins.

As described in section 2.3.5, some drawbacks have been experienced concerning the verification of expression of rotavirus G9P[6] glycoprotein (VP7). The molecular weight of VP7, determined by the amino acid sequence, is 37.4 kDa. However, according to SDS-PAGE analysis, the apparent molecular weight (MW_{app}) of VP7 is 34 kDa (Mellado *et al.*, 2008). The difference in size can be attributed to the bicistronic nature of VP7, as it contains two conserved in-frame initiation codons (Chan *et al.*, 1986 and Stirzaker *et al.*, 1987).

3.3.3. Analysis of protein expression with SDS-PAGE

The Sf9 cells were infected independently with recombinant baculoviruses expressing VP2/6, VP2/6/7, dVP2-8*/6/7 and VP2/6/4/7, respectively (section 2.2.5.6). In addition, the newly generated FB control (section 3.3.1) was included. CPE of the cells were monitored after infection and was completed at approximately 96 hpi. The supernatant (P2 viral stock) and cells were harvested (section 2.2.5.7). The expression of the recombinant proteins was evaluated with the use of SDS-PAGE (section 2.2.5.8). SDS-PAGE protein fragment sizes expected for all recombinant protein expression experiments were dVP2-8* (106.7 kDa), VP2 (100 kDa), VP4 (84 kDa), VP6 (44.9 kDa), and VP7 (34 kDa). SDS-PAGE showed the expression of all of the proteins (Figure 3.4) at their approximate sizes, with the exception of VP7. As before, the protein fragment of VP7 expected at 34 kDa was also detected in the baculovirus negative control (FB). Furthermore, when examining the SDS-PAGE analysis results the band thought to be VP7 was also present in the recombinant baculovirus expressing VP2/6, which could also mean a contamination of VP7 in this recombinant baculovirus construct (section 3.3.1). However, all of the recombinant baculovirus constructs (FB, VP2/6, VP2/6/7, VP2/6/4/7 and dVP2-8*/6/7) in lanes 2-6 (Figure 3.4) contained the band thought to be VP7 (34kDa). Thus, it was not entirely confirmed whether this band was VP7 (34kDa), since the VP7 could have been expressed at a very low level and was not clearly detected following Coomassie staining. Further expression analyses would be required for full confirmation (section 3.3.5).

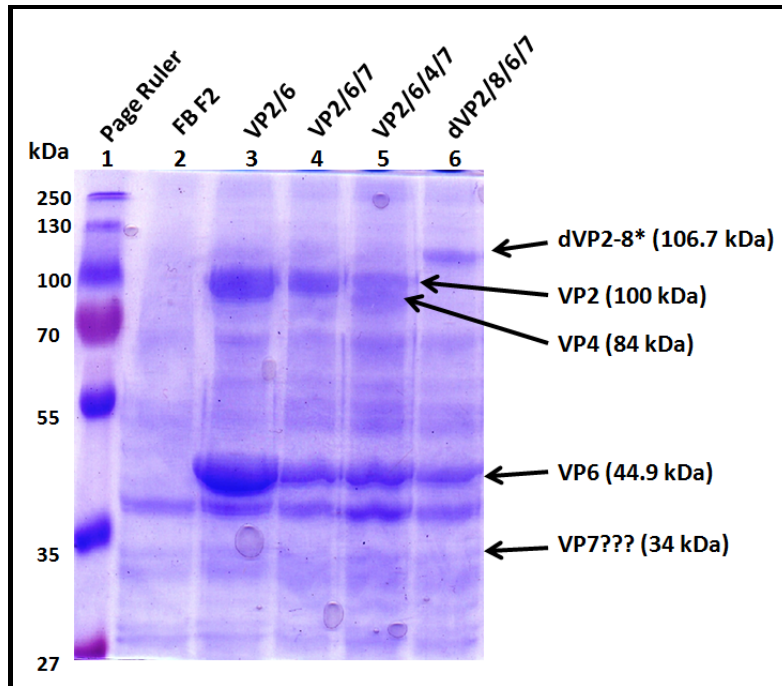


Figure 3.4 – 10% Coomassie blue stained SDS-PAGE analyses of the baculovirus expression of recombinant rotavirus VP2, VP4, VP6, VP7 and dVP2-8:* Lanes: 1, 5 μ l PageRuler (Fermentas); 2, 20 μ l of the newly constructed FB control; 3, 20 μ l of recombinant baculovirus VP2/6 expressed proteins; 4, 20 μ l of recombinant baculovirus VP2/6/7 expressed proteins; 5, 20 μ l of recombinant baculovirus VP2/6/4/7 expressed proteins; 6, 20 μ l of recombinant baculovirus dVP2-8*/6/7 expressed proteins.

3.3.4. The verification of the presence of coding region of genome segments 9(VP7) and 6(VP6) in DNA isolated from baculoviruses expressing combinations of VP2/6, VP2/6/7, VP2/6/4/7 and dVP2-8*/6/7, respectively

In order to verify expression of VP7, it was important to determine whether recombinant baculoviruses, used to infect Sf9 cells, contained the transposed region of the genome segment 9 (VP7). Baculovirus genomic DNA (Bac-gDNA) was isolated (section 3.2.1) from the Sf9 insect cells and amplified (2.2.4.1) with the use of genome segment 9 (VP7) and genome segment 6 (VP6) primers (Appendix 3). The amplification results are shown in Figure 3.5. Three sets of genome segment 9 (VP7) primers were used. The first set (VP7FOR and VP7REV) yielded an amplicon fragment of 940 bp, shown in lanes 3, 5 – 7 and 10 (Figure 3.5). A second set (VP7FOR2 and VP7REV2) yielded an amplicon fragment of 992 bp, shown in lane 8 (Figure 3.5). The third and final set (VP7FOR and VP7REV2) yielded a fragment of approximately 1100 bp, shown in lane 9 (Figure 3.5). Amplification with the VP6 primers yielded an amplicon of 840

bp, shown in lanes 13, 15 – 18 (Figure 3.5). A no template control (lanes 1 and 12 – Figure 3.5) was included during the analysis along with a negative control (FB) in lanes 4 and 14 (Figure 3.5). In addition, the positive control (pFBqVP4/7) as template for genome segment 9 (VP7) was included in lane 3 (Figure 3.5) along with the positive control (pFBqVP2/6) as template for genome segment 6 (VP6) in lane 13 (Figure 3.5). All of the samples yielded fragments of the approximate correct size. Therefore, it was possible to conclude that the recombinant baculoviruses expressing the combinations of VP2/6/7, VP2/6/4/7 and dVP2-8*/6/7, used during infection experiments, contained the transposed region of genome segment 9 (VP7). Furthermore, the recombinant baculoviruses expressing the combinations of VP2/6, VP2/6/7, VP2/6/4/7 and dVP2-8*/6/7 also contained the transposed region of genome segment 6 (VP6).

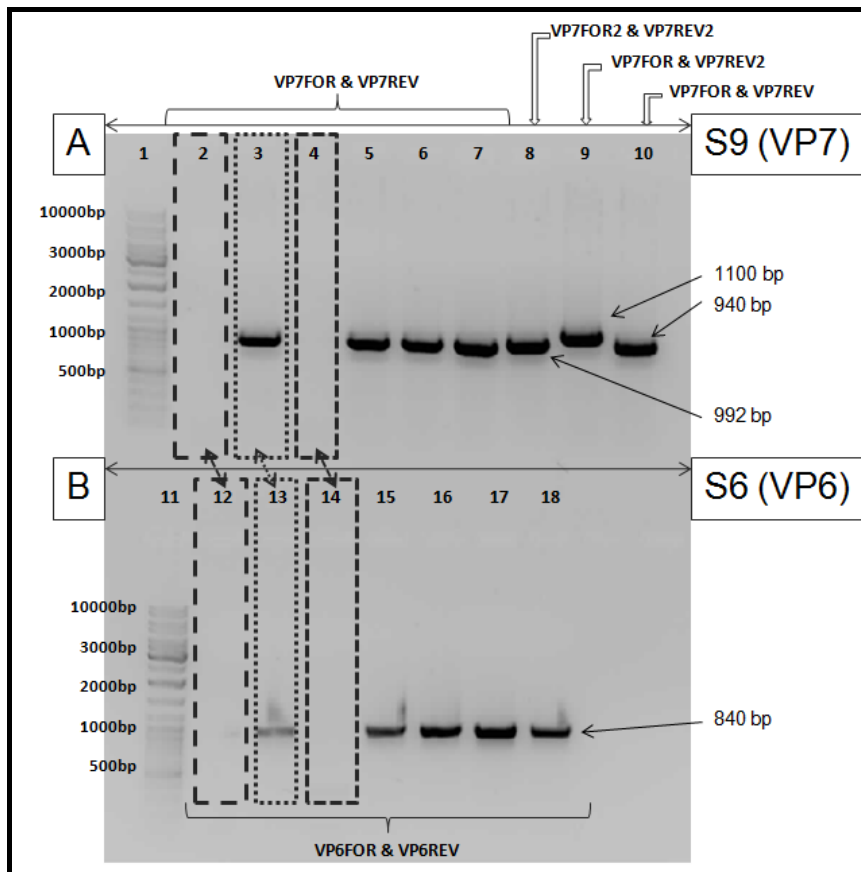


Figure 3.5 – 1% Agarose gel analyses showing the verification of the presence of coding regions of genome segments 9 (VP7) and 6 (VP6) in DNA isolated from baculoviruses expressing combinations of VP2/6, VP2/6/7, VP2/6/4/7 and dVP2-8/6/7, respectively: Lanes: 1 and 11, 3µl Express DNA ladder (Fermentas); 2 and 12, 20 µl no-template controls of the respective amplifications (A and B); 3 and 13, 20 µl positive controls pFBqVP4/7 and pFBqVP2/6 as templates of A and B, respectively; 4 and 14, 20 µl DNA from the baculovirus negative FB control; 5, 20 µl DNA from the recombinant baculovirus (expressing VP2/6/7); 6,*

20 µl DNA from the recombinant baculovirus (expressing VP2/6/4/7); 7, 20 µl DNA from the recombinant baculovirus (expressing dVP2-8*/6/7); 8, 20 µl DNA from the recombinant baculovirus (expressing dVP2-8*/6/7); 9, 20 µl DNA from the recombinant baculovirus (expressing dVP2-8*/6/7); 10, 20 µl DNA from the recombinant baculovirus (expressing VP4/7); 15, 20 µl of DNA from the recombinant baculovirus (expressing VP2/6); 16, 20 µl DNA from the recombinant baculovirus (expressing VP2/6/7); 17, 20 µl DNA from the recombinant baculovirus (expressing VP2/6/4/7); 18, 20 µl DNA from the recombinant baculovirus (expressing dVP2-8*/6/7). The baculovirus DNA in lanes 2-7 and 10 were amplified with VP7FOR and VP7REV primers. The baculovirus DNA in lane 8 was amplified with VP7FOR2 and VP7REV2 primers. The baculovirus DNA in lane 9 was amplified with VP7FOR and VP7REV2 primers. The baculovirus DNA in lanes 13-18 were amplified with VP6FOR and VP6REV primers.

3.3.5. Verification of VP7 expression in recombinant baculoviruses expressing combinations of VP2/6/7, VP2/6/4/7 and dVP2-8*/6/7, respectively

Further expression analyses were performed with the use of western blot analysis (section 3.2.2). Mellado and co-workers (2008) detected a high expression level of VP7 with the use of a polyclonal goat primary antibody during a western blot assay. This antibody was raised against rotavirus NCDV (Nebraska calf diarrhoea virus). Due to its polyclonal nature, the antibody can detect a variety of epitopes and all the structural proteins expressed can be detected. During the western blot analysis, the recombinant protein samples were subjected to SDS-PAGE (section 2.2.5.8). As a reference to the western blot analysis, two identical SDS-PAGE gels were analysed. One of the two was stained and documented as described in section 2.2.5.8. The approximate protein fragment sizes expected were as follow: dVP2-8* (106.7 kDa); VP2 (100 kDa); VP4 (84 kDa); VP6 (44.9 kDa); and VP7 (34 kDa). The results of the SDS-PAGE (A) and the western blot (B) analysis are shown in Figure 3.6. The FB control was included in the western blot analyses to be able to determine whether there was any non-specific protein binding. Unfortunately the FB control (lane 2 – Figure 3.6) in the SDS-PAGE analysis was smudged, due to a small piece of unwanted gel located in the well it was loaded into. The expression of rotavirus recombinant VP2, VP6, VP4 and dVP2-8* was verified with SDS-PAGE analysis (A – Figure 3.6). As before, VP7 expression was not visible in any of the recombinant baculoviruses expressing VP2/6/7, VP2/6/4/7 or dVP2-8*/6/7, with SDS-PAGE analysis. VP7 expression was finally detected with the western blot assay in lanes 3-6 (B – Figure 3.6). The expression of rotavirus recombinant VP6 was also detected with the western blot assay. The expression of VP4, VP2 and dVP2-8* could not be verified with the western blot assay, but it was confirmed with SDS-PAGE (A)(Figure 3.6). The expression of VP4, VP2 and dVP2-8* was visible in lanes 4; 2-4; and 5-6, respectively. This was probably due to the fact that the antibody

was raised against rotavirus NCDV and the variation in epitopes between the calf and the G9P[6] strain could result in no detection. In addition, a comparison of expression was done between two baculoviruses, both expressing dVP2-8*/6/7, resuspended in two different buffers. The two buffers used were 20 mM Tris-HCl pH 7.5 and 1 × PBS. This data was shown in lanes 5-6 of Figure 3.6, respectively. No difference in expression could be seen between the two buffers used. Two bands of VP7 were detected with the western blot assay in some of the samples (lanes 4, 5 and 6 – Figure 3.6). This phenomenon has been reported previously by Chan and co-workers (1986) and Stirzaker and co-workers (1987) and was attributed to the bicistronic nature of VP7 as it contains two conserved in-frame initiation codons. Furthermore, VP7 was not detected in the recombinant baculovirus expressing VP2/6, thus concluding that this construct was only contaminated with genome segment 9 (VP7) on a DNA level (section 3.3.1) and not with VP7 on a protein level. The contamination of pFBqVP2/6 must have occurred after the recombinant baculovirus expressing VP2/6 was constructed.

Some other bands that were visible on the blot were attributed to non-specific binding of the antibodies to baculovirus proteins, as these bands are also visible in the FB control. Furthermore, these non-specific bands are also present in lanes 5-6 (Figure 3.6). Although these bands correspond to the expected size of either VP2 or dVP2-8* fragments, the bands were not detected in any of the other western blot analyses.

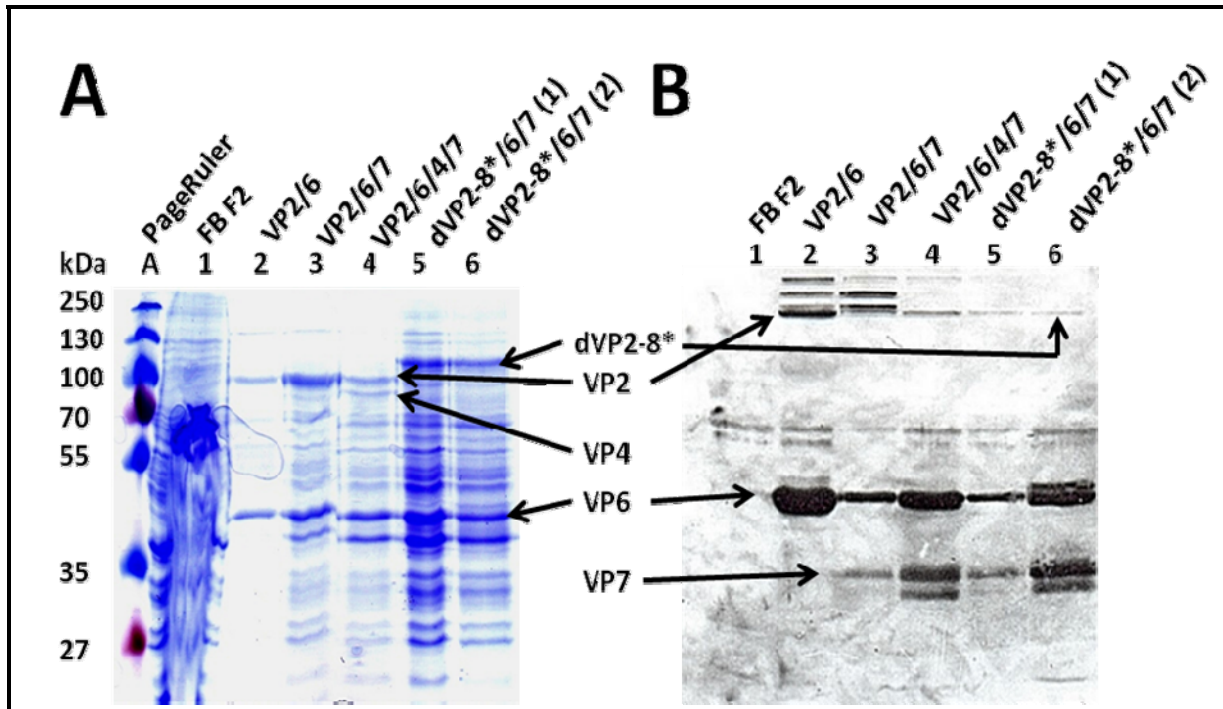


Figure 3.6 – Verification of the expression of rotavirus recombinant proteins VP2, VP6, VP7, VP4 and dVP2-8* by SDS-PAGE (A) and western blot (B) analysis: Lanes: A, 5 μ l of PageRuler; 1, 20 μ l of newly constructed FB control baculovirus; 2, 20 μ l of expressed recombinant baculovirus VP2/6; 3, 20 μ l of expressed recombinant baculovirus VP2/6/7; 4, 20 μ l of expressed recombinant baculovirus VP2/6/4/7; 5, 20 μ l of expressed recombinant baculovirus dVP2-8*/6/7 (resuspended in 20 mM Tris-HCl pH 7.5); 6, 20 μ l of expressed recombinant baculovirus dVP2-8*/6/7 (resuspended in 1 \times PBS).

Having determined that rotavirus recombinant VP2, VP4, VP6, VP7 and dVP2-8* were being expressed by the P2 viral stocks that were not plaque purified, the expression of the viral proteins by plaque purified baculovirus stocks needed confirmation. The expression of the plaque purified baculovirus expressing VP2/6 was previously verified by Dr. H.G. O'Neill (results not shown). Of the VP2/6 expressing baculoviruses, plaque number 3 showed the best expression. This baculovirus was chosen for further experimental analyses during this study. Individual plaques from the various recombinant baculoviruses (VP2/6/7, VP2/6/4/7 and VP2-8*/6/7) were picked, infected (section 2.2.5.6) and harvested (section 2.2.5.7) independently, to avoid cross-contamination. Expression of the rotavirus recombinant proteins were evaluated (section 2.2.5.8). The expression analysis results of VP2/6/7 are shown in Figure 3.7. FB was included as a negative control during the expression analysis. With regard to VP2, all four plaque purified baculoviruses (VP2/6/7) showed expression. Plaque 1 (PI.1) and PI.3 showed very high levels of expression of VP2. VP6 expression was detected in PI.2, PI.3 and PI.4, but

not in PI.1. No expression of VP7 was detected for any of the plaque purified baculoviruses (VP2/6/7). Therefore, VP7 expression was verified by western blotting (Figure 3.9 (D)).

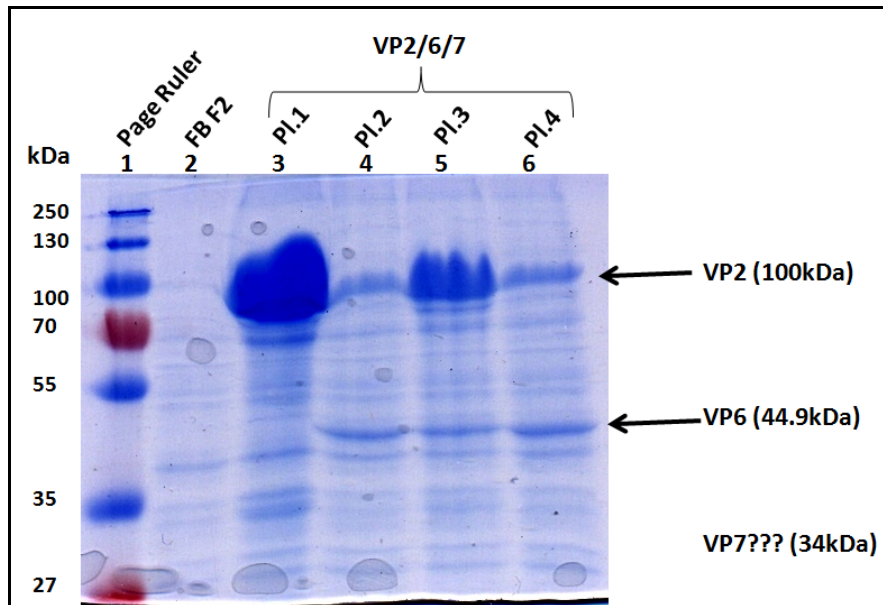


Figure 3.7- 10% Coomassie Blue stained SDS-PAGE analyses of the expression of plaque purified baculoviruses expressing VP2/6/7: Lanes: 1, 5 μ l of PageRuler (Fermentas); 2, 20 μ l of the newly constructed FB control; 3-6, 20 μ l of the respective, purified baculoviruses expressing VP2/6/7.

The expression analysis results of dVP2-8*/6/7 and VP2/6/4/7 are shown in Figure 3.8. FB was included as a negative control during the expression analysis. All the plaque purified baculoviruses showed expression for the rotavirus recombinant VP2, VP6, VP4, VP7 and dVP2-8*. However, VP7 expression could also not be confirmed and had to be verified with western blotting.

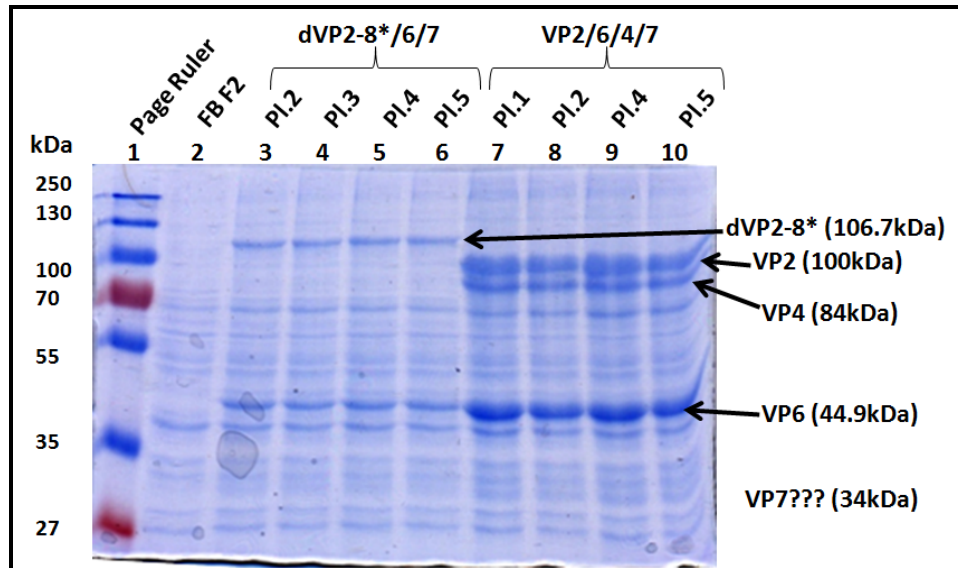


Figure 3.8 – 10% Coomassie Blue stained SDS-PAGE analyses of the expression of plaque purified dVP2-8/6/7 and VP2/6/4/7 baculoviruses: Lanes: 1, 5 μ l of PageRuler (Fermentas); 2, 20 μ l of newly constructed FB control; 3-6, 20 μ l of respective, purified baculoviruses expressing dVP2-8*/6/7; 7-10, 20 μ l of respective, purified baculoviruses expressing VP2/6/4/7.*

In order to verify the expression of VP7 by all the plaque purified baculoviruses, western blot analyses were performed (section 3.2.2). The expected size for the apparent molecular weight of VP7 was 34 kDa. The analysis results are shown in Figure 3.9 (B) and (D), respectively. The presence of VP7 was detected in all of the recombinant baculoviruses with western blot analysis (Figure 3.9 - B and D). Furthermore, the expression of VP6 was also verified with the western blot analysis, since a polyclonal antibody was used. As before (Figure 3.6) VP4 expression was not detected with the western blot assay, but was visible in the SDS-PAGE reference gel. Even though the western blot conditions do not differ from those used before (Figure 3.6), the expression of VP2 and dVP2-8* was not detected with the western blot assay. There was, however, expression of VP2 and dVP2-8* visible with the SDS-PAGE reference gels (Figure 3.9 - A and C).

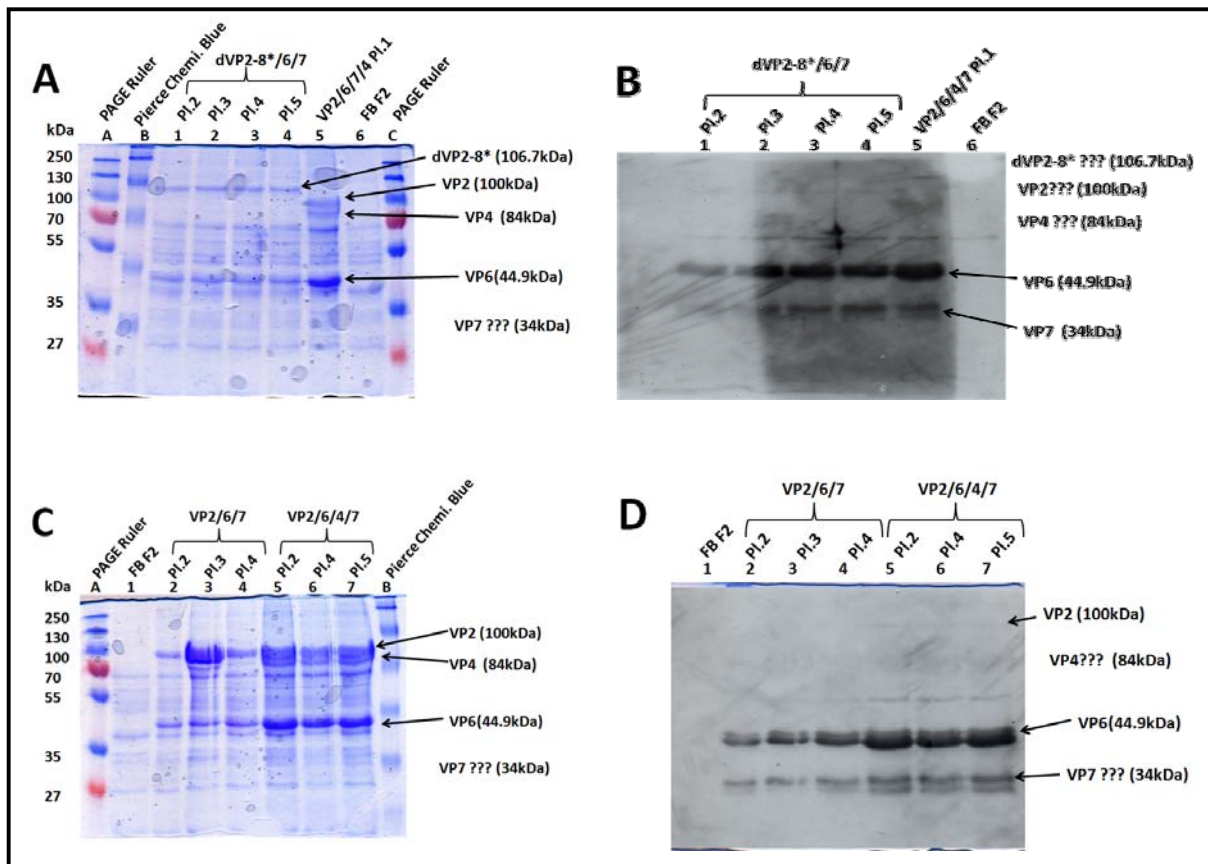


Figure 3.9 – SDS-PAGE (A and C) and western blot analyses (B and D) showing the expression of rotavirus recombinant proteins VP2, VP6, VP7, VP4 and dVP2-8*: A and B - Lanes: A, 5 μ l of PageRuler (Fermentas); B, 5 μ l of Pierce Chemiluminescent Blue Prestained Peroxidase-Labelled Protein Molecular Weight Marker (Pierce); 1-4, 20 μ l of respective, plaque purified baculoviruses expressing dVP2-8*/6/7; 5, 20 μ l of plaque purified baculovirus #1 expressing VP2/6/4/7; 6, 20 μ l of the newly constructed FB control; C, 5 μ l of PageRuler (Fermentas). C and D - Lanes: A, 5 μ l of PageRuler (Fermentas); 1, 20 μ l of the newly constructed FB control; 2-4, 20 μ l of the respective, plaque purified baculoviruses expressing dVP2-8*/6/7; 5-7, 20 μ l of the plaque purified baculovirus #1 expressing VP2/6/4/7; B, 5 μ l of Pierce Chemiluminescent Blue Prestained Peroxidase-Labelled Protein Molecular Weight Marker (Pierce).

Upon the verification of rotavirus recombinant VP2, VP6, VP7, VP4 and dVP2-8*, the plaque purified baculoviruses which showed the best expression were selected for further analysis. These purified baculoviruses were rBac VP2/6/7 Pl.4 (Figure 3.9 (C and D) – lane 4), rBac dVP2-8*/6/7 Pl. 2 (Figure 3.9 (A and B) – lane 1) and rBac VP2/6/4/7 pl.4 (Figure 3.9 (C and D) – lane 6). These baculoviruses were used during subsequent particle production experiments.

3.3.6. Evaluation of recombinant rotavirus protein expression VP2, VP6, VP7, VP4 and dVP2-8* in Sf9 Mimic cells

One of the speculations concerning the lower expression levels of VP7 is the probable inability of the Sf9 cells to completely support the process of glycosylation. Glycosylation plays a primary role in the formation of VP7, as it is a glycoprotein. Sf9 Mimic cells (Invitrogen) are derived from Sf9 cells and were engineered to express a variety of mammalian glycosyltransferases, which support the process of glycosylation. Sf9 insect cells exhibit the inability to express N-Glycans to the same extent as mammalian cells. This presents the drawback of influencing the structure, antigenicity, function and enzymatic activity of the produced proteins. The mammalian glycosyltransferases expressed by the Mimic cells exhibits the ability to produce biantennary, terminally sialyated N-glycans (Legardinier *et al.*, 2005).

A pilot study was constructed to compare the expression of VP7 in the Sf9- and Sf9 Mimic cells. The recombinant baculoviruses expressing the protein combinations of VP2/6/7, VP2/6/4/7, and dVP2-8*/6/7 were used to infect Sf9- and Sf9 Mimic cells (section 2.2.5.6). Suspension cultures of 25ml, containing 1×10^6 cells/ml, were used. The Sf9 cells were suspended in Excell Titre High medium (SAFC Biosciences) and the Sf9 Mimic cells were suspended in Grace's medium (Invitrogen). The cells were infected with an MOI of approximately 1.5. Cell viability was observed with the use of a haemocytometer (Nunc) in the presence of 0.4 % trypan blue solution. When CPE of approximately 95 % was achieved 96 hpi, the cells and P3 viral stock was harvested (section 2.2.5.7). The expression of the recombinant proteins for VP2/6/7 was evaluated with the use of SDS-PAGE (section 2.2.5.8) and is shown in Figure 3.10. A negative baculovirus control (FB) was included during the analysis. Expression of VP2 (100 kDa) and VP6 (44.9 kDa) was visible with the expression in Sf9 cells in lanes 3-5 (Figure 3.10). The expression in Sf9 cells of recombinant VP7 (34 kDa) could once again not be confirmed and western blot analysis would have to be performed. The expression in the Sf9 Mimic cells of rotavirus recombinant VP2, VP6 and VP7 could not be confirmed during the SDS-PAGE analysis. Bands of the same sizes as those thought to be VP2, VP6 and VP7 are also present in the FB negative control. However, this does not necessarily entail that VP2, VP6 and VP7 were not expressed at all. These proteins could simply have been expressed at a very low level and due to the limitations of Coomassie staining were disguised by proteins of Sf9 Mimic cell or baculoviral origin. This occurrence was found and described later in section 3.3.9, where VP7 expression could be verified with SDS-PAGE and western blot analysis, once the protein sample was purified by fractionation. Further optimisation would be required for the expression

of VP2, VP6 and VP7 in Sf9 Mimic cells. The rBac(VP2/6/7) used in this pilot study was originally transfected, amplified and purified in Sf9 cells. Thus, a possible approach for increasing the levels of expression of the recombinant proteins would consist of the reproduction (involving transfection, amplification and purification) of the rBacVP2/6/7.

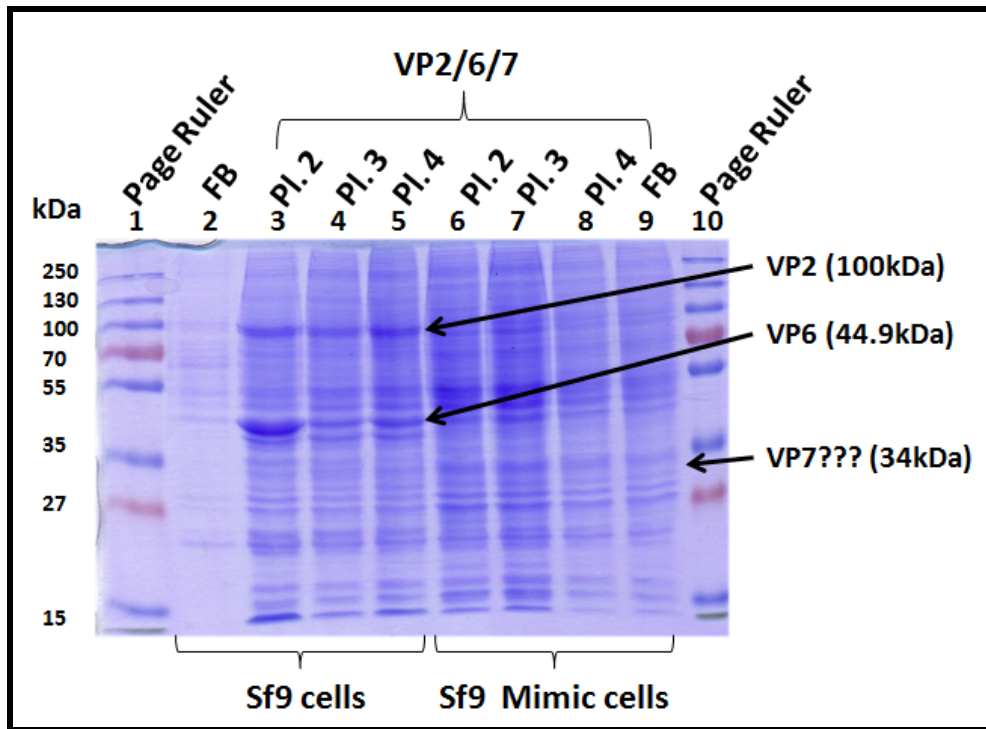


Figure 3.10 – 10% SDS-PAGE analysis of the plaque purified VP2/6/7 baculoviruses expressed in Sf9- and Sf9 Mimic cells, respectively: Lanes: 1 and 10, 5 μ l of PageRuler (Fermentas); 2 and 9, 20 μ l of newly constructed FB control; 3 - 8, 20 μ l of respective, purified baculoviruses expressing VP2/6/7. Lanes 1-4 and lanes 5-9 were expressed in Sf9 and Sf9 Mimic cells, respectively.

3.3.7. Rotavirus-like particle production, purification and visualisation

This section reports on the selected plaque purified recombinant baculoviruses (section 3.3.5), which express the various rotavirus protein combinations. The viruses were amplified and prepared for evaluation of particle formation. Various rotavirus-like particles (rVLPs) were produced, namely double-layered particles, DLPs (VP2/6), triple-layered particles, TLPs (VP2/6/7), TLPs containing VP8* (dVP2-8*/6/7) and virus-like particles, VLPs (VP2/6/4/7). The recombinant baculoviruses, expressing these proteins, were previously plaque purified by Mrs. R. van der Sluis. The baculovirus amplification, infection and isolation methodology was

described in sections 3.2.3 and 3.2.5. The titres of these respective baculoviruses were determined (Section 3.2.4) and are depicted in Table 3.3. The rotavirus-like particles were isolated and purified (Section 3.2.6). During purification the generated rotavirus-like particles were subjected to sucrose gradient centrifugation and fractionation. The results of the quantification of the protein content of the collected fractions (section 3.2.7), of the various recombinant protein combinations are displayed in Figures 3.11 (B) and 3.12 (B and F).

Table 3.3 - The titres determined for the respective recombinant baculoviruses

Recombinant baculovirus	Titre (pfu/ml)
rBac VP2/6	3.1×10^7
rBac VP2/6/7	2.1×10^7
rBac VP2/6/4/7	4×10^6
rBac dVP2-8*/6/7	4×10^7

Fractions containing the highest protein quantity from the BCA-assay were analysed with SDS-PAGE (section 2.2.5.8). The corresponding SDS-PAGE analyses of these quantified fractions are displayed in Figures 3.11 (C) and 3.12 (C and G). During the various BCA protein quantifications, the R^2 -values were documented and ranged between 0.992-0.998. These values are an estimate of the accuracy of the protein quantification results and should be in close proximity to the value of 1.

3.3.8. Analysis of the production of double-layered (VP2/6) rotavirus-like particles

The medium and the cell pellets of Sf9 cells infected with rBac VP2/6 were analysed separately for the presence of DLPs by means of sucrose gradients. The band of DLPs was clearly visible in the gradient (Figure 3.11 (A)). The fraction with the highest protein content of both the medium (281.8 µg) and cell pellet (130.8 µg) was fraction 15 (Figure 3.11 (B)). The medium fractions showed a gradual increase in protein content (fractions 12-18) and were analysed with SDS-PAGE (Figure 3.11 (C)). The analyses results indicate that fraction 15 contained the highest level of recombinant VP2/6 expression which corresponds with the results found of the BCA protein quantification assay (Figure 3.11 (B)).

TEM was used to analyse whether the rotavirus G9P[6] expressed proteins (VP2 and VP6) present in medium, assembled into double-layered rotavirus-like particles. The fraction

containing the most VP2/6 was analysed as described in section 3.2.8. Particles ranging between approximately 60-63 nm in size were assembled (Figure 3.11 (D)) with a similar morphology resembling that of DLPs as previously reported by Charpilienne and co-workers (2002) and Jiang and co-workers (1998). A large quantity of rota-DLPs was present, which seem to indicate good assembly of recombinant rotavirus VP2/6 into DLPs under the conditions used. During further quantification experiments, the particles obtained from lysed cells were excluded from analyses, as more than 90 % of the rotavirus-like DLPs were present in the medium. Although this might not be the case with the production of triple-layered particles, the long-term production strategy of rVLPs involves the isolation of the particles from the culturing medium. The other peaks found during the quantification analysis (fractions 1, 8, 12 and 17 - Figure 3.11 (B)) could either be attributed to the presence of single-layered particles (containing primarily VP2), unassembled or denatured proteins.

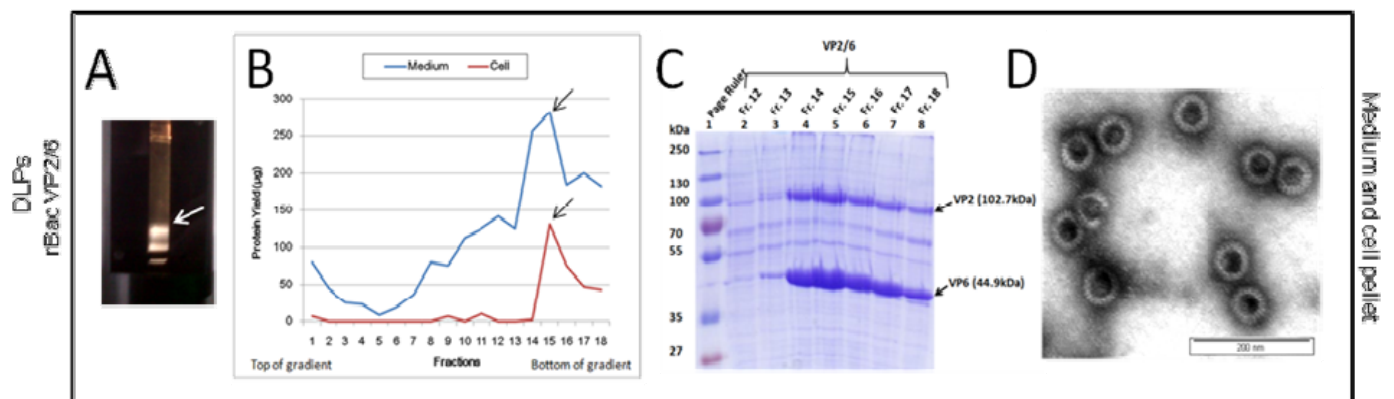


Figure 3.11 – The results of the purification and isolation process of rBac VP2/6 assembled DLPs: (A) Photograph of the sucrose gradient; (B) BCA protein quantification of sucrose gradient fractionation of rBac VP2/6 infected cells. Blue and red lines represent the medium and cell pellet protein quantification, respectively; (C) 10% SDS-PAGE analysis of the proteins in the medium fractions 12 to 18 of rBac VP2/6 infected Sf9 cells. Lanes: 1, 5 µl of PageRuler (Fermentas); 2 - 8, 20 µl of respective, sucrose gradient fractions (12 - 18) of the medium of rBac VP2/6 infected cells; (D) Electron micrograph showing the assembled DLPs of rotavirus G9P[6] VP2/6. The rota-DLPs were stained with 1% uranyl acetate. Magnification bar is 200nm.

3.3.9. Analysis of the production of triple-layered (VP2/6/7 and dVP2-8*/6/7) rotavirus-like particles

The band of rotavirus VP2/6/7- (Figure 3.12 (A)) and dVP2-8*/6/7 (Figure 3.12 (E)) TLPs was clearly visible in the respective sucrose gradients. The protein quantification results of VP2/6/7 are illustrated in Figure 3.12 (B). The figure clearly illustrates the highest protein concentration

of the medium in fraction 10 (43 µg). However, the virus-like particles found in fraction 10 might be a mixture of DLPs and TLPs as the sucrose used to compose the gradient does not necessarily separate the TLPs and DLPs from one another. Thus, the precise concentration of DLPs and TLPs cannot be determined independently. For a more specific separation of the TLPs and DLPs a cesium-chloride (CsCl) density ultracentrifugation gradient could be used. Cesium chloride gradients separate the VLPs according to molecular density. These particles migrate in the gradient, until they reach a state of neutral buoyancy. Furthermore, the protein concentrations in each fraction could be determined by exposing a small volume of each fraction to ethidium bromide and eliminating these samples at 302 nm. However, as the purpose of separation was only to purify the VLPs for the confirmation that particles were being assembled and not to quantify the ratio of the production between TLPs and DLPs. Thus, the use of the sucrose gradient for separation was sufficient. The high protein concentration, found in fraction 19 at the bottom of the gradient could probably be attributed to cellular debris, baculoviral proteins or proteins present within the culturing cell suspension medium. The other peak (Fr. 14) found during the quantification analysis could be attributed to the presence of single-layered particles, unassembled or denatured rotavirus proteins, but was not further investigated.

The fractions showing an increase in protein content (fractions 8-13) were analysed with SDS-PAGE and are shown in Figure 3.12 (C). The results showed the highest expression of all of the proteins of interest (VP2, VP6 and VP7) in fraction 10. Thus, it was assumed that the correctly assembled TLPs could most probably be located in this particular fraction. This corresponds with the BCA protein quantification results (Figure 3.12 (B)). In addition, when examining the SDS-PAGE gel, the expression of VP7 (at 34 kDa) was observed. This led to the conclusion that the other proteins present in earlier analysed non-purified samples might conceal the expression of this particular protein, but that it was expressed nonetheless.

The same methodology was applied to the production and purification of the triple-layered particle dVP2-8*/6/7. The quantification, of the protein content of the collected fractions (section 3.2.7), is displayed in Figure 3.12 (F). This Figure clearly illustrates the highest protein yield of the medium in fractions 1 (116 µg), 10 (37 µg), 12 (34 µg) and 19 (117 µg). The increased protein content in fraction 1 and 19 was attributed to unassembled rotavirus proteins. It was concluded that these infections should be harvested at a later stage, in order to provide some time for particle assembly and increase particle yield.

The medium fractions showing an increase in protein content (fractions 8-13) were analysed with SDS-PAGE (Figure 3.12 (G)). The results showed the highest expression of all of the proteins of interest (dVP2-8*, VP6 and VP7) in fraction 12. This does not correspond to the results found with BCA quantification assay of dVP2-8*/6/7 (Figure 3.12 (F)), which shows the highest protein content in fraction 10. When comparing the results from the SDS-PAGE analysis to that of the BCA assay, it was confirmed that DLPs were present in a larger quantity than TLPs, and further experiments to optimise the dVP2-8*/6/7 TLP production were necessary for the optimal assembly of rotavirus dVP2-8*/6/7 TLPs. Since the fraction with the highest protein content, was not the fraction with the highest dVP2-8*, VP6 and VP7 expression, the expression analysis results were used to judge the yield of TLPs.

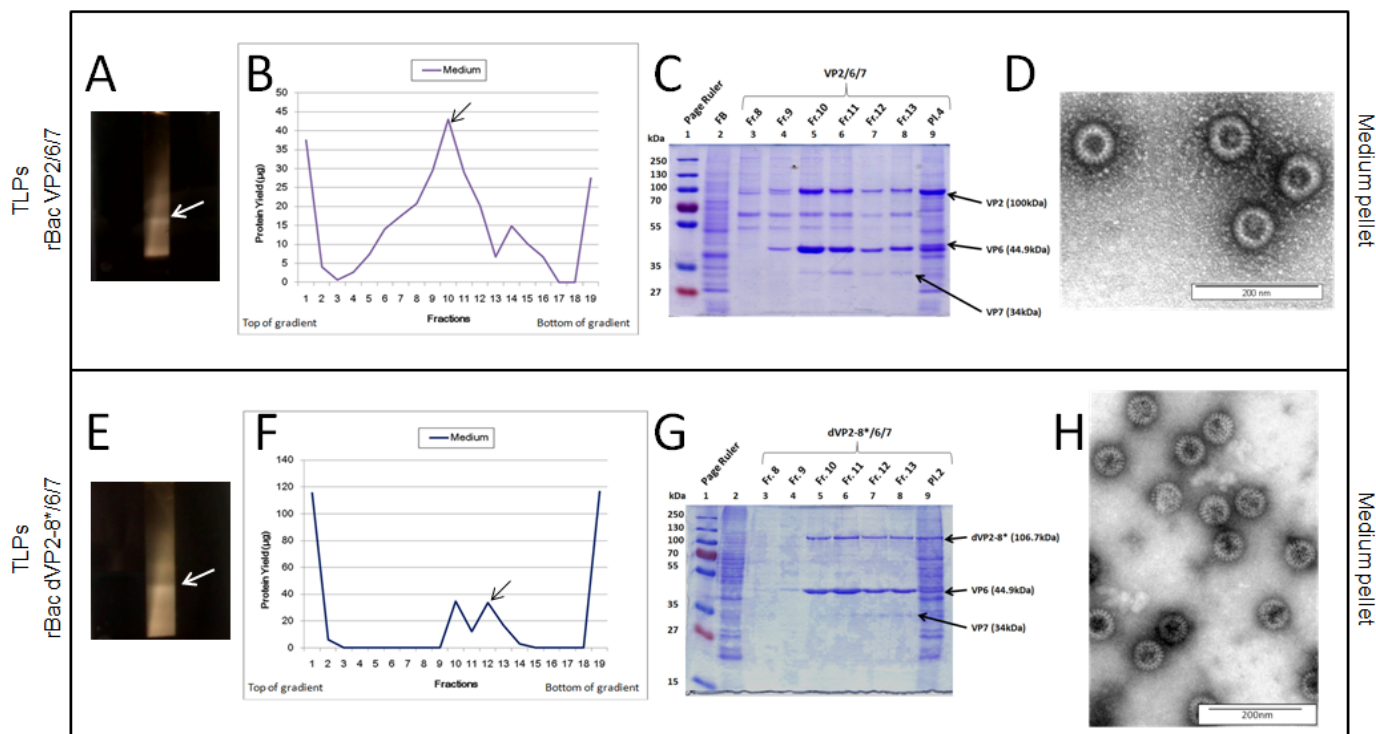


Figure 3.12 – The results of the purification and isolation process of rBac VP2/6/7 and rBac dVP2-8*/6/7 assembled TLPs: (A and E) Photograph of the sucrose gradient; (B and F) BCA protein quantification of sucrose gradient fractionation of rBac VP2/6/7 and rBac dVP2-8*/6/7 infected cells, respectively; (C and G) 10% SDS-PAGE analysis of the proteins in the fractions 8 to 13 of the medium of rBac VP2/6/7 and dVP2-8*/6/7 infected Sf9 cells, respectively; (D and H) Electron micrograph showing the assembled TLPs of rotavirus G9P[6] VP2/6/7 and dVP2-8*/6/7, respectively. The rota-TLPs were stained with 1% uranyl acetate. Magnification bar is 200nm.

Even though VP7 expression was visible in Figure 3.12 (C and G), western blot analysis (section 3.2.2) was performed to confirm the VP7 expression in rBacVP2/6/7 fraction 11 (Figure 3.12 (C) – lane 6) and rBacdVP2-8*/6/7 fraction 12 (Figure 3.12 (G) – lane 7). The western blot analysis results are illustrated in Figure 3.13. Both of these samples, respectively, expressed all of the proteins of interest: dVP2-8* (106.7 kDa), VP2 (100 kDa), VP6 (44.9 kDa) and VP7 (34 kDa). As before (Figure 3.9 –B and D), the detection of rotavirus VP2 and dVP2-8* was unsuccessful with the western blot analysis, even though the same conditions (section 3.2.2) were applied and the transfer of rotavirus VP2 and dVP2-8* onto the membrane was verified with Ponceau S solution (Fluka Biochemika). The expression of rotavirus VP2 and dVP2-8* was visible with SDS-PAGE (Figure 3.13 (A)) and this phenomenon was not further investigated.

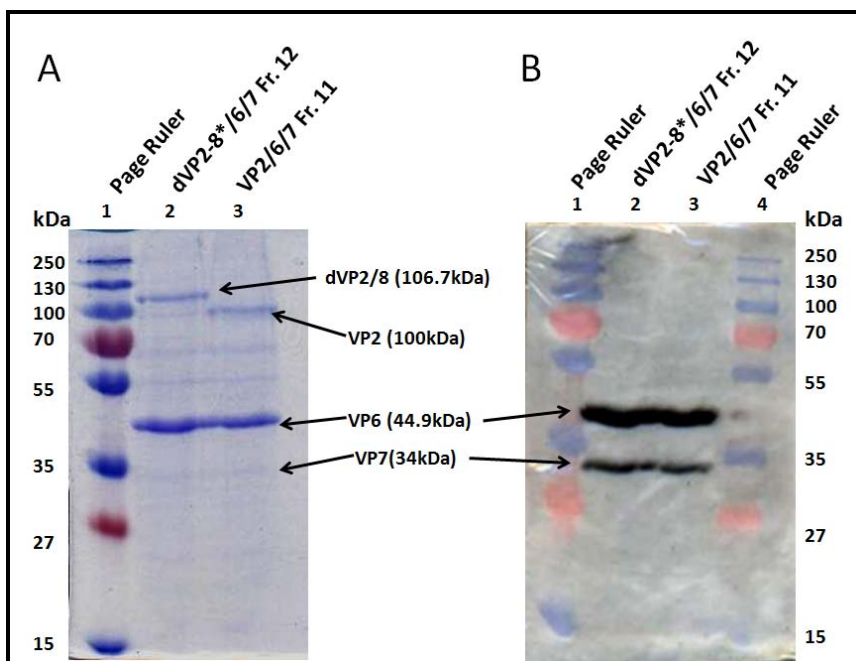


Figure 3.13 – 10% SDS-PAGE (A) and western blot (B) analyses of fractions 12 and 11 of dVP2-8*/6/7 and VP2/6/7 sucrose gradient: Lanes: 1 and 4, 5 μ l PageRuler (Fermentas); 2, 20 μ l of fraction 12 of dVP2-8*/6/7 sucrose gradient; 3, 20 μ l of fraction 11 of VP2/6/7 sucrose gradient.

TEM (section 3.2.8) was used to evaluate the assembly of the rotavirus G9P[6] expressed protein combinations (VP2/6/7 and dVP2-8*/6/7) into triple layered rotavirus-like particles (Figure 3.12 (D and H)). The particles contained wheel-like structures and were approximately 69-70 nm in size. Although some of the TEMs were not calibrated recently, particle analysis was mainly performed based on morphology. The particles were evaluated for smooth (TLP) vs.

rough (DLP) edges of the outer rims and thickness thereof. Although VP2/6/7 and dVP2-8*/6/7 was expressed, TEM primarily detected particles corresponding to the morphology of DLPs (Figure 3.11 - D and H) with rougher edges. However, this does not necessarily entail that VP7 did not associate with the particle whatsoever, but rather incomplete assembly of VP7 onto the intermediate layer (consisting of VP6). The incomplete assembly could be attributed to lower expression levels of VP7, in comparison with VP2 and VP6. It is suspected that the glycosylation pathway (of the Sf9 insect cells) might play a fundamental role in the low expression levels obtained from the glycoprotein. This hypothesis was discussed and tested in section 3.3.6. Another reason for incomplete TLP formation was that low calcium levels lead to the dissociation of VP7 from the TLP (Jayaram *et al.*, 2004). No calcium supplementation was used during the production process of the TLPs. Thus, VP7 could have been assembled onto the intermediate particle, but dissociated from it thereafter.

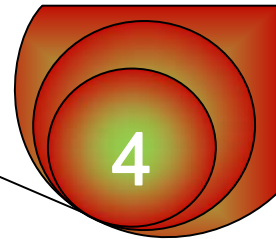
3.4. Summary

The expression of rotavirus recombinant VP7 was detected and verified in all of the recombinant baculovirus combinations expressing VP2/6/7, dVP2-8*/6/7 and VP2/6/4/7 with the use of western blot analysis (section 3.3.5). Furthermore, it was determined that VP7 was visible with Coomassie-stained SDS-PAGE when rotavirus TLPs were purified with sucrose gradient ultracentrifugation. This expression was confirmed with western blot analysis (Figure 3.13 (B)).

A pilot study was performed between Sf9 and Sf9 Mimic cells to compare the levels of VP2, VP6 and VP7 expression. Sf9 Mimic cells are derived from Sf9 cells and were engineered to express a variety of mammalian glycosyltransferases, which support the process of glycosylation. The glycosylation process is necessary for the production of VP7 as it is a glycoprotein. No expression in Sf9 Mimic cells of VP2, VP6 and VP7 could be confirmed with SDS-PAGE analysis, but that does not necessarily mean that these proteins were not expressed at all. Further expression optimisation could include the reproduction (transfection, amplification and purification) of the rBacVP2/6/7 in Sf9 Mimic cells.

The assembly of DLPs were efficient and particles corresponding to the morphology of rough edged wheel-like structures were detected (Figure 3.11 (D)). The assembly of TLPs were not as efficient since particles detected resembled similar morphology to that of DLPs. However, this does not necessarily entail that VP7 did not associate with the particle whatsoever, but

rather that it did not assemble completely. The inefficient assembly of VP7 onto the VP6 layer of the DLPs was attributed to the lower expression levels of rotavirus recombinant VP7 in comparison to that of VP2, VP6 and dVP2-8* (Figure 3.12 (C and G)).



CHAPTER 4: CONCLUDING REMARKS

Rotavirus causes gastroenteritis, especially severe gastroenteritis, globally with the highest mortality rates in developing countries such as those in sub-Saharan Africa. The currently licensed vaccines Rotarix and Rotateq vaccines contain live attenuated viruses, which are associated with a number of potential risks (Chapter 1 - section 1.9.1.3). Thus, non-live, subunit vaccines are being considered as an alternative, because of their various advantages (Chapter 1 – section 1.9.3.4). Furthermore, current vaccines only show a combined efficacy of 61.2% in Africa (Madhi *et al.*, 2010). This could be attributed to various factors, such as more frequent occurrences of breastfeeding and malnutrition, increased levels of transplacental antibodies and the simultaneous enteric infections (Patel *et al.*, 2012). This might also be attributed to the fact that the rotavirus serotypes, occurring within the vaccines, are not prevalent in these regions. The local strain used during the study contains the G9 and P6 serotypes, which have been found to be highly prevalent in sub-Saharan African regions. Thus, a vaccine based on these serotypes could potentially increase the protection efficiency against rotavirus infections occurring in sub-Saharan Africa.

The first experimental chapter (Chapter 2) of the study reported on the generation and expression of a recombinant rotavirus fused-protein dVP2-8* for the G9P[6] rotavirus strain. The generation of the fused-protein involved three main steps: Firstly, the coding regions encoding dVP2 and VP8* were amplified from the genome segments 2 and 4 encoding VP2 and VP4, respectively (section 2.3.2). Secondly, the two truncated coding regions of dVP2 and VP8* were digested with the use of BamHI, EcoRI and XbaI; along with the pFBq vector containing genome segments 6 and 9 encoding VP6 and VP7 (pFBqVP6/7), respectively (section 2.3.3). Thirdly, the two truncated coding regions encoding dVP2 and VP8* were ligated together with pFBqVP6/7 in order to produce pFBqdVP2-8*/6/7 (section 2.3.3). The pFBqdVP2-8*/6/7 construct was sequenced and analysed with the use of an *in silico* prepared sequence of pFBqdVP2-8*/6/7 (section 2.3.4). Despite the fact that a part of the sequence was not characterised (5944-6126 bp) subsequent experiments were continued. The genome segments encoding dVP2-8*, VP6 and VP7 were transposed into the baculovirus genome (contained within ACC DH10Bac *E.coli* cells) (section 2.3.5) through the process of homologous recombination (Figure 2.12). The baculovirus genome containing the genome segments encoding dVP2-8*, VP6 and VP7 were transfected into Sf9 insect cells (section 2.3.5). The

expression of dVP2-8* (106.7 kDa) and VP6 (44.9 kDa) was successful with the BEVS and visualised with the use of SDS-PAGE (Figure 2.15). The expression of VP7 was, however, an uncertainty since the protein band (thought to be VP7 at 37kDa) was also present in the baculovirus negative control (FB). Three possible explanations were formulated for this occurrence: one, these protein bands are from baculovirus origin and are not VP7; two, these protein bands are from Sf9 insect cell origin and are not VP7; or three, the negative control was possibly contaminated with VP7 prior to the expression analysis. Further investigations into the expression of VP7 were performed and described in Chapter 3.

The second experimental chapter (Chapter 3) of the study reported on the verification of recombinant rotavirus VP7 expression, along with the verification of the expression of VP2, dVP2-8*, VP6, VP7 and VP4 in their various combinations (by plaque purified rBacVP2/6, rBacVP2/6/7, rBacVP2/6/4/7 and rBacdVP2-8*/6/7) in Sf9 insect cells. Furthermore, these plaque purified recombinant baculoviruses (rBacVP2/6, rBacVP2/6/7, rBacVP2/6/4/7 and rBacdVP2-8*/6/7) were evaluated for rotavirus particle formation by TEM.

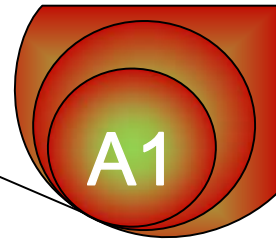
The confirmation of recombinant rotavirus VP7 expression involved three steps: Firstly, a new baculovirus negative control (FB) was constructed (section 3.3.1) due to suspicions of VP7 contamination within the previously used baculovirus negative control (FB) (Figure 2.15). SDS-PAGE analysis (Figure 3.3) showed the same protein band (thought to be VP7 (37 kDa)) in all of the newly constructed FB controls; concluding that this particular band was not VP7, but rather of baculoviral or insect cell origin. Secondly, the presence of the coding regions of genome segments 9 (VP7) and 6 (VP6); contained within the recombinant baculovirus genome used to transfect the Sf9 insect cells; was verified for rBacVP2/6, rBacVP2/6/7, rBacVP2/6/4/7 and rBacdVP2-8*/6/7 (section 3.3.4 - Figure 3.5 A and B). Furthermore, different combinations of the genome segment 9 (VP7) primers (Appendix 3) were used during the amplification, to yield amplicons of 1100 bp, 940 bp and 992 bp, respectively. Thirdly, the expression of VP7 by rBacVP2/6/7, rBacVP2/6/4/7 and rBacdVP2-8*/6/7 in Sf9 insect cells, was verified by western blot analysis (section 3.3.5 - Figure 3.6). Western blot analysis was performed with the use of a polyclonal goat antibody (Abcam). Therefore, rotavirus recombinant VP7 was expressed by BEVS, but could not be detected by Coomassie stained SDS-PAGE gel due to lower expression levels of VP7 in comparison to that of VP2, VP6, VP4 and dVP2-8*.

Expression of rotavirus recombinant VP2, VP6, VP4, VP7 and dVP2-8* was verified independently for purified rBacVP2/6 PI.3 (by Dr. H.G. O'Neill – results not shown); rBacVP2/6/7 PI.4 (Figure 3.9, C and D – lane 4); rBacVP2/6/4/7 PI.4 (Figure 3.9, C and D – lane 6) and rBacdVP2-8*/6/7 PI.2 (Figure 3.9, A and B – lane 1) with SDS-PAGE and western blot analysis (section 3.3.5).

The purified rBacVP2/6 PI.3, rBacVP2/6/7 PI.4, rBacVP2/6/4/7 PI.4 and rBacdVP2-8*/6/7 PI.2 were used to evaluate the formation of rotavirus particles by TEM (section 3.3.7). The rBacVP2/6 yielded efficient assembly of DLPs and particles corresponding to the morphology of rough edged wheel-like structures were detected (Figure 3.11 (D)). Based on the rough edges of the particles yielded from rBacVP2/6/7 and rBacdVP2-8*/6/7 these particles were classified as DLPs and not TLPs. This does not necessarily mean that VP7 did not associate with the particle whatsoever, but rather entails the incomplete assembly of VP7 onto the DLPs. Partial association of VP7 with the intermediate particle could be attributed to the following: Firstly, low calcium levels lead to the dissociation of VP7 from the TLP (Jayaram *et al.*, 2004). No calcium supplementation was used during the production process of the TLPs. Thus, VP7 could have been assembled onto the intermediate particle, but dissociated from it thereafter. Secondly, the insect cells used during the production process were not necessarily optimised for the production of VP7, as it requires glycosylation. Sf9 cells do not express the necessary mammalian glycosidases to support the glycosylation process. The Sf9 mimic cells (section 3.3.6) do however express these glycosidases and with optimisation, these cells might be able to improve the expression levels of VP7.

Once complete RV-VLPs of the G6P[6] rotavirus strain can be produced effectively, particle immunisation studies will be performed on mice, where these RV-VLPs will be utilised in combination with an effective adjuvant. When an immune response can be established in mice, immunisation trails can be considered in gnotobiotic pigs, followed by human trails. These RV-VLPs can be used in various ways to protect against rotavirus infection and disease. The first approach could be to use these RV-VLPs as a safer alternative to the live attenuated vaccines. The second approach is to use the RV-VLP based vaccine for vaccination in older children, as currently recommended by the WHO. Patel and co-workers (2012) assessed statistics on first dose rotavirus vaccination in older children. They concluded that deaths caused by vaccine associated intussusception in older children will be far less than the lives saved by the vaccination (Patel *et al.*, 2012). The third approach is to use the RV-VLPs as a prime boost

vaccination regiment together with currently licensed vaccines Rotarix and RotaTeq. The use of this approach might broaden the protection provided by vaccines as the booster regiment contains two of the most prevalent serotypes (G9 and P[6]) found in sub-Saharan Africa.



APPENDIX 1

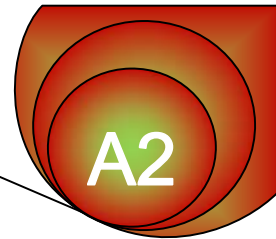
MATERIALS UTILISED IN STUDY

Item	Product number	Supplier
4 × Dual Color Protein Loading buffer	R1011	Fermentas
6 × Orange loading dye	R0631	Fermentas
Acetic acid (Glacial)	1.00063.2500	Merck
Acrylamide	1.00209.10	Merck
Agar	BX.10.500	Merck
Agarose	H111206	Hispanagar
Agarose Type VII (used for plaquing purposes)	A9045.25g	Sigma
Ammonium persulfate	A3678	Sigma
Amphotericin B (Fungizone)	A2942	Sigma
Ampicillin	A0166	Sigma
BamHI buffer	B57	Fermentas
BamHI enzyme	ER0051	Fermentas
Bicinchoninic acid solution	B9643	Sigma
Bovine serum albumin	23209	Thermo Scientific
Coomassie Brilliant Blue R250	B8647	Sigma
Copper sulfate solution	C2284	Sigma
dNTP mix	BG3001A	Takara
Donkey-anti-goat IgG	ab97120	Abcam
EcoRI buffer	B12	Fermentas
EcoRI enzyme	ER0271	Fermentas
EDTA	03685	Fluka analytical

Ethanol	1.00983.2500	Merck
Etidium Bromide	160539	Sigma
Excell Titre High medium	I5408	SAFC Biosciences
Ex-Taq buffer	RR01AM	Takara
Ex-Taq enzyme	RR001	Takara
Fugene 6 Reagent	11815091001	Roche
GeneRuler Express DNA Ladder	SM1553	Fermentas
Gentamycin	G4793	Sigma Aldrich
Glycerol	49780	Fluka
Glycine	1.04169.1000	Merck
Grace's medium (TNM-FH)	04-649F	BioWhittaker
Hydrochloric acid	SAAR3063040LP	Merck
Ilford Phenisol Developing solution	175 7635	Ilford
Ilford Phenisol Fixer	198 4565	Ilford
IPTG	R0391	Fermentas
Isopropanol	1.09634.2500	Merck
Kanamycin	11815-032	Gibco
Lactogen	8302113	Nestle
Machery Nagel Nucleospin II PCR cleanup and gel extraction kit	740 609.50	Machery Nagel
Magnesium chloride	8.14733.0500	Merck
Magnesium chloride (PCR purposes)	F510MG	Finnzymes
Methanol	1.06009.2500	Merck
N,N' Bisacrylamide	130672	Sigma

Nonidet P 40 substitute	74385	Fluka Biochemika
Nuclease free water	P119C	Promega
O'Gene Ruler DNA Ladder Mix	SM1173	Fermentas
PageRuler Prestained Protein Ladder	26619	Fermentas
Penicillin-Streptomycin Solution	15140122	Gibco
Phosphate buffered Saline	P4417	Sigma
Pluronic F68 solution (10%)	P5556	Sigma
Polyclonal goat primary antibody	ab69560	Abcam
Ponceau S solution	81462	Fluka Biochemika
Potassium acetate	204.8222	Fluka Biochemika
Potassium chloride	AB004936.500	Merck
Potassium hydroxide	1.05033.0500	Merck
Promega PureYield plasmid midiprep kit	C#A1220	Promega
RNase A (solution or powder)	R6,513	Sigma
Sodium Chloride	S3014	Sigma
Sodium dodecyl sulfate	L-4390	Sigma
Sodium hydroxide	S5881	Sigma
Sucrose	S0389	Sigma
T4 DNA ligase buffer	B3705	Fermentas
T4 DNA ligase enzyme	EL 0011	Fermentas
Tango Buffer	BY5	Fermentas
TC100 medium	T3160	Sigma
TEMED	1.10732-026	Merck

Tetracycline	T7660	Sigma Aldrich
Thiazolyl Blue Tetrazolium bromide	M2128	Sigma
Tris base	11814273001	Roche
Triton X-100	1.08603.1000	Merck
Tryphan blue	T6146	Sigma
Tryptose broth	1.10676.0500	Merck
Tween 20	7SEC30D	Schering Cis Bio International
Xbal enzyme	ER0681	Fermentas
X-Gal	GX1-500	SBS genetech
Yeast extract powder	HG000BX6.500	Merck
Gene Pulser Electroporation Cuvette	165-2089	BioRad



APPENDIX 2

PREPARATION OF BUFFERS UTILISED IN STUDY

1. 1 × Tris-acetate and EDTA (TAE) buffer

The TAE buffer contained 40mM Tris-acetate and 1mM EDTA (Sambrook and Russell, 2001). All agarose electrophoresis gels were prepared with 1 × TAE buffer.

2. 1 × Phosphate Buffered Saline (PBS) buffer

1× PBS was prepared with use of PBS pellets from Sigma. When dissolving 1 tablet in 200ml 18.2 Ω distilled water, the concentration is 1 × PBS.

3. 1 × Tris, Glycine and SDS (TGS) buffer

TGS buffer consists of 25 mM Tris, 2 M Glycine and 0.1% SDS, resuspended in 18.2 Ω distilled water.

4. LB medium

LB medium consists of 10 mg/ml Tryptone, 1.5 mg/ml Yeast extract and 10 mg/ml NaCl (Sodium-chloride).

5. Agar plates with various antibiotics

The agar plates were prepared with the use of LB medium, containing 10 mg/ml Tryptone, 1.5 mg/ml Yeast extract and 10 mg/ml NaCl (Sodium-chloride). The agar (Merck) was subsequently added to the medium and sterilized. The antibiotics of interest were added before pouring the agar onto the plates and allowed to set. The antibiotics that were used are 0.01mg/ml Ampicilin, 0.05mg/ml Kanamycin, 0.02mg/ml Tetracycline, 0.007mg/ml Gentamycin, 0.2mg/ml X-gal and 0.04mg/ml IPTG. Plates containing ampicilin were used during the transfection and ligation procedures and plates containing the remainder of the antibiotics were used during the transformation procedure.

6. Agarose overlay utilized during viral plaque assay

For a 1 h incubation period, place Grace's complete medium in 40 °C waterbath. Add 1% Agarose powder to 18.2 Ω distilled water very slowly, whilst stirring continuously. Dissolve agarose in microwave & leave to cool down until it can be touched. Add to Grace's medium in waterbath and leave until needed. (50% Grace's: 50% 1% agarose)

7. Blocking buffer utilised during western blot analysis

Blocking buffer containing 5% skim milk, 0.1% Tween-20, 0.2 M NaCl and 0.05 M Tris-HCl (pH7.4) resuspended in 1 × PBS.

8. Excell Titre High medium

0.005% penicillin/streptomycin (Gibco) and 5 ml 0.0125 µg/ml Amphotericin B/Fungizone (Gibco) was added to Excell Titre High medium prior to insect cell treatment. This was a FBS free medium.

9. Glucose Tris-chloride EDTA (GTE) buffer

The GTE buffer consisted of 50 mM glucose, 10 mM EDTA, 25 mM Tris/HCl pH 8, 0.1 mg/ml Rnase.

10. SDS-PAGE staining and destaining buffers

1.10.1. Coomassie staining buffer

The Coomassie staining buffer consisted of 45% (v/v) methanol, 10% (v/v) acetic acid, 0.4% (w/v) Coomasie brilliant blue R250.

1.10.2. Destaining buffer

The destaining buffer consisted of 45% (v/v) methanol and 10% (v/v) acetic acid, diluted in 18.2 Ω distilled water.

11. Restriction Enzyme-STOP (RESTOP) buffer

The RESTOP consisted of 8 parts 6 × Loading buffer and 1 part 0.5M ethylene diamine-tetra-acetic acid (EDTA).

12. Sucrose, TritonX-100, EDTA and Tris (STET) buffer

The STET buffer consisted of 8% sucrose, 5% TritonX-100, 50 mM EDTA, 50 mM Tris and 1 mg/ml Lysozyme, which was resuspended in 18.2 Ω distilled water.

13. Super optimal broth, with catabolite repression (SOC) medium

When preparing SOC medium dissolve 2 g/ml Tryptone, 0.05 g/ml Yeast extract, 0.5 g/ml NaCl in 250 mM KCl. Autoclave to sterilize and add filter-sterilized volumes of 20 ml 1 M Glucose and 5 ml 2 M MgCl₂ to complete the buffer.

14. TC100 insect cell medium

0.5% FBS (Sigma), 0.005% penicillin/streptomycin (Gibco) and 5 ml 0.0125 µg/ml Amphotericin B/Fungizone (Gibco) was added to TC100 medium prior to insect cell treatment.

15. Thiazolyl Blue Tetrazolium Bromide (MTT)

Dissolve 0.1% solution in 1 x PBS and subsequently filter sterilize.

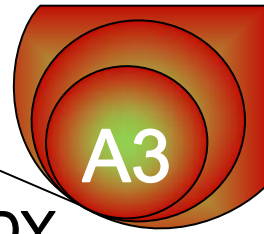
16. Transfer buffer utilised during western blot analysis:

The transfer buffer consisted of 0.025 M Tris, 0.2 M Glycine and 20% methanol (pH 8.4) resuspended in 1 × PBS.

17. Tryphan blue solution

Dissolve 0.4% (w/v) tryphan blue solution in 1 x PBS.

APPENDIX 3



OLIGONUCLEOTIDES UTILISED IN THE STUDY

Table 1 - Oligonucleotides utilised in the study

Primer name	Sequence (5' - 3')	Purpose	Reference
VP8FOR	CC GAATTC ATGGCTTCCCTGATCTACCG	Cloning	This study
VP8REV	GGATCCTCTAGA GGAACGGGAGGACAGAG	Cloning	This study
DELTAVP2FOR	GA TCTAGAGGATCC AAGACCATCCCCACCTTCG	Cloning	This study
VP2REV	CGAGC GAATTC TTATTACAGCTCG	Cloning	This study
VP2intR1	CGTACAGGTTCCAGGAAGTACTCG	Nucleotide sequencing	Dr. Trudi O'Neill
VP2intF1	CATCTGCGACGCTATCTTCC	Nucleotide sequencing	Dr. Trudi O'Neill
VP2intF2	GCATGCAGCGTATGCACTACC	Nucleotide sequencing	Dr. Trudi O'Neill
Primer R2	GGACCTTTAATTCAACCCAACAC	Nucleotide sequencing	Dr. Trudi O'Neill
F4	GCTATAGTTCTAGTGGTTGGC	Nucleotide sequencing	Dr. Trudi O'Neill
M13FOR	GTTTTCCAGTCACGAC	PCR analysis of Bacmid	Bac-to-Bac® (Invitrogen)
M13REV	CAGGAAACAGCTATGAC	PCR analysis of Bacmid	Bac-to-Bac® (Invitrogen)
VP7FOR	CCTATAAATATCGGATCCA	PCR analysis of rBacs	Dr. Trudi O'Neill
VP7REV	ACTACATCAACCAGATCGTGC	PCR analysis of rBacs	Dr. Trudi O'Neill
VP7FOR2	GACTTCATCATCTACCGTTTCCTCCTCC	PCR analysis of rBacs	Dr. Trudi O'Neill
VP7REV2	AGTACTAGAGGATCATAATCAG	PCR analysis of rBacs	Dr. Trudi O'Neill
VP6FOR	GA ACTCCACCTCCACGTTGTT	PCR analysis of rBacs	Dr. Trudi O'Neill
VP6REV	GTGTTGGGTTGAATTAAGGT	PCR analysis of rBacs	Dr. Trudi O'Neill

*All of the restriction enzyme recognition sites of the oligonucleotides used for cloning purposes are formatted in bold and indicated with different colors: EcoRI (red), BamHI (blue) and XbaI (green). The linker is underlined and formatted in bold.

APPENDIX 4

LIST OF FIGURES

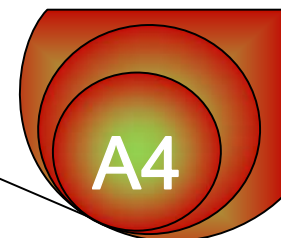
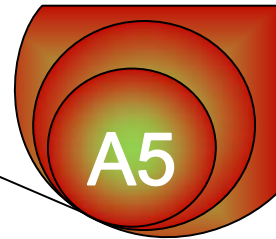


Figure 1.1. The structural organization of rotavirus.....	5
Figure 1.2. - The structural organization of VP4.....	9
Figure 1.3. – The estimated rotavirus diarrhoea mortality of children younger than 5 across the world	11
Figure 1.4. – The life cycle of rotavirus.....	13
Figure 1.5. Composition of the existing live, oral, attenuated vaccine RotaTeq.....	17
Figure 1.6. Composition of the existing oral, live, attenuated vaccine Rotarix.....	18
Figure 1.7. - The Bac-to-Bac system.....	20
Figure 1.8. - A schematic representation of the multifaceted rotavirus-like particle production process.....	22
Figure 2.1 - The plasmid map of pFastBACquad (pFBq).....	30
Figure 2.2 – A schematic representation of the construction of pFBqdVP2-8*/6/7.....	40
Figure 2.3 – Multiple alignment of the partial VP2 amino acid sequences of selected type A rotaviruses to that of G9P[6]*	41
Figure 2.4 – Partial DNA sequence of genome segment 2 (VP2), showing the annealing position of the primer designed for the amplification of the truncated region of genome segment 2 encoding dVP2).....	42
Figure 2.5 – The DNA sequence of G9P[6] genome segment 4 (VP4), showing the annealing positions of primers designed for the amplification of the region of genome segment 4 encoding VP8*.....	45
Figure 2.6 – 1% Agarose gel analysis of amplification of the regions encoding VP8* (of genome segment 4) and dVP2 (of genome segment 2).....	46
Figure 2.7 – In silico BamHI digestion of pFBqdVP2-8*/6/7.....	48
Figure 2.8 – 1% Agarose gel analyses of BamHI digestion of possible pFBqdVP2-8*/6/7 plasmid.....	49
Figure 2.9 - In silico XbaI digestion of pFBqdVP2-8*/6/7.....	50
Figure 2.10 – 1% Agarose gel analyses of EcoRI and XbaI digestion of possible pFBqdVP2-8*/6/7 plasmid.....	51

Figure 2.11 - The multiple alignment of the partial in silico sequence (pFBqdVP2-8*/6/7) and the sequenced data of the region encoding dVP2-8*.....	55
Figure 2.12 – Strategy to analyse recombinant bacmids.....	56
Figure 2.13 – 1% Agarose gel analyses of the recombinant bacmids.....	58
Figure 2.14 - 1% Agarose gel analyses of the recombinant bacmids prepared for transfection.....	59
Figure 2.15 – 10% SDS-PAGE analyses of the expression of dVP2-8*/6/7.....	60
Figure 2.16 – 10% SDS-PAGE analyses of the expression of dVP2-8*/6/7 resuspended in three separate buffers.....	62
Figure 3.1 – 1% Agarose gel analysis of the amplification of new pFBq plasmid DNA using segment 9 (VP7) primers.....	71
Figure 3.2– 1% Agarose gel analyses of recombinant FB bacmids.....	72
Figure 3.3 – 10% SDS-PAGE analyses of the expression of recombinant baculovirus negative control (FB).....	74
Figure 3.4 – 10% Coomassie blue stained SDS-PAGE analyses of the baculovirus expression of recombinant rotavirus VP2, VP4, VP6, VP7 and dVP2-8*.....	76
Figure 3.5 – 1% Agarose gel analyses showing the verification of the presence of coding regions of genome segments 9(VP7) and 6(VP6) in DNA isolated from baculoviruses expressing combinations of VP2/6, VP2/6/7, VP2/6/4/7 and dVP2-8*/6/7, respectively.....	77
Figure 3.6 – Verification of the expression of rotavirus recombinant proteins VP2, VP6, VP7, VP4 and dVP2-8* by SDS-PAGE (A) and western blot (B) analysis.....	80
Figure 3.7- 10% Coomassie Blue stained SDS-PAGE analyses of the expression of plaque purified baculoviruses expressing VP2/6/7.....	81
Figure 3.8 – 10% Coomassie Blue stained SDS-PAGE analyses of the expression of plaque purified dVP2-8*/6/7 and VP2/6/4/7 baculoviruses.....	82
Figure 3.9 – SDS-PAGE (A and C) and western blot analyses (B and D) showing the expression of rotavirus recombinant proteins VP2, VP6, VP7, VP4 and dVP2-8*.....	83
Figure 3.10 – 10% SDS-PAGE analysis of the plaque purified VP2/6/7 baculoviruses expressed in Sf9- and Sf9 Mimic cells, respectively.....	85
Figure 3.11 – The results of the purification and isolation process of rBac VP2/6 assembled DLPs.....	87
Figure 3.12 – The results of the purification and isolation process of rBac VP2/6/7 and rBac dVP2-8*/6/7 assembled TLPs.....	89

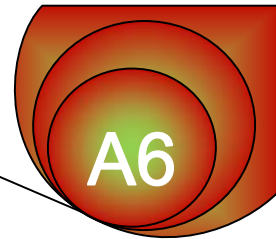
Figure 3.13 – 10% SDS-PAGE (A) and western blot (B) analyses of fractions 12 and 11 of dVP2-8*/6/7 and VP2/6/7 sucrose gradient.....90



APPENDIX 5

LIST OF TABLES

Table 1.1 - Characteristics of the VP4 trypsin cleavage products.....	8
Table 1.2 – The accumulation sites of various rotavirus-like particles.....	23
Table 2.1 – DNA concentrations of recombinant bacmids.....	57
Table 2.2 - The isolated recombinant bacmid DNA prepared for transfection.....	59
Table 3.1 – TEM models used for the visualisation of rVLPs.....	69
Table 3.2 – Concentrations of the isolated recombinant bacmid DNA of FB negative control.....	73
Table 3.3 - The titres determined for the respective recombinant baculoviruses.....	86



APPENDIX 6

LIST OF ABBREVIATIONS

Chapter 1:

CD4⁺ T-cells: T-helper cells
CD8⁺ T-cells: Cytotoxic T cells
ER: Endoplasmic reticulum
G-type: Glycosylated structure
HRR: Host-range restriction
IFN: Interferon
IgA: Immunoglobulin A
MAbs: Monoclonal antibodies
mRNA: Messenger ribonucleic acid
NSP: Non-structural protein
ORFs: Open reading frames
P-type: Protease sensitivity
RNA: Ribonucleic acid
rota-VLP: Rotavirus-like particle
SA: Sialic-acid
SLPs: Single-layered particles
USA: United States of America

Chapter 2:

µg: Microgram
µl: Microliter
3D: Three dimensional
APS: Ammoniumperoxodisulphate
BSL-2: Biosafety level 2
cDNA: Complementary deoxyribonucleic acid
CPE: Cytopathic effect
DNA: Deoxyribonucleic acid
dNTP: Deoxynucleotide Triphosphate
DOC: Organic carbon
DPRU: Diarrhoeal Pathogens Research Unit

dsRNA: Double stranded deoxyribonucleic acid
EDTA: Ethylenediaminetetraacetic Acid
EM: Electron microscopy
FBS: Fetal bovine serum
GTE: Glucose Tris-chloride EDTA
IPTG: Isopropyl- β -D-thio-galactoside
MCS: Multiple cloning site
min: Minutes
ml: Millilitre
mM: Millimolar
ng: Nanogram
nm: Nano metre
NP40: Nonyl phenoxy-polyethoxyl-ethanol
Ori: Origin of replication
PBS: Phosphate buffered saline
PCR: Polymerase chain reaction
RE: Restriction enzymes
RESTOP: Restriction enzyme stop
RNase A: Ribonucleic acid enzyme A
rpm: Rotation per minute
RV: Rotavirus
SDS: sodium-dodecyl-sulphate
SOC: Super optimal culture
ssRNA: Single stranded ribonucleic acid
STET: Sucrose, TritonX-100, EDTA, Tris
SV40 polyA: SV40 polyadenylation signal
TAE: Tris acetate EDTA (Ethylenediaminetetraacetic Acid)
TE: Tris EDTA
TEMED: Tetramethylethylenediamine
TGS: Tris, Glycine, SDS
Tris: Tris(hydroxymethyl)aminomethane
Tris-Cl: Tris Chloride
UV: Ultraviolet
v/v: volume/volume

V: Volt

VLPs: Virus-like particles

w/v: weight/volume

X-gal: X-galactosidase

μF: Microfarad

Chapter 3:

× g: G-force

Bac-gDNA: Baculovirus genomic DNA

BCA: Bicinchoninic

BSA: Bovine serum albumin

cm³: cubic centimetres

CsCl: Cesium-chloride

ddH₂O: Double distilled water

ECL: Enhanced chemiluminescent

gDNA: Genomic deoxyribonucleic acid

hpi: Hours post-infection

IgG: Immunoglobulin G

kV: Kilovolt

MOI: Multiplicity of infection

MTT: Tetrazolium Bromide

MWapp: Apparent molecular weight

NaCl: Sodium chloride

NCDV: Nebraska calf diarrhoea virus

P1/2/3/4: Passage 1/2/3/4

Pfu: Plaque forming units

rBac: Recombinant baculovirus

rVLP: Rotavirus-like particles

SIS: Soft Image Systems

ZR: Zymo research

Chapter 4:

Bp: Basepairs

BVES: Baculovirus expression system

DLPs: Double-layered particles

dVP: Delta viral protein

E.coli: *Escherichia coli*

FB: FastBac

kDa: Kilo Dalton

pFBq: pFASTBACquad

pFBqdVP: pFASTBACquad delta viral protein

PI.1/2/3/4: Plaque

rBacdVP: Recombinant baculovirus delta viral protein

RV-VLP: Rotavirus virus-like particle

SDS-PAGE: Sodium-dodecyl-sulphate polyacrylamide gel electrophoresis

Sf9: *Spodoptera Frugiperda* 9

TEM: Transmission electron microscopy

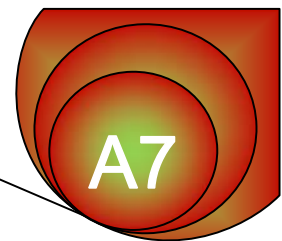
TLPs: Triple-layered particles

VP: Viral protein

WHO: World Health Organisation

APPENDIX 7

REFERENCES



1. Agnello, D., Herve, C. A., Lavaux, A., Darniot, M., Guillon, P., Charpillienne, A., & Pothier, P. (2006). Intrarectal immunization with rotavirus 2 / 6 virus-like particles induces an antirotavirus immune response localized in the intestinal mucosa and protects against rotavirus infection in mice. *Journal of Virology*. 80(8): p3823–3832.
2. Angel, J., Franco, M. a, & Greenberg, H. B. (2007). Rotavirus vaccines: recent developments and future considerations. *Nature reviews. Microbiology*. 5(7): p529–539.
3. Aoki, S. T., Settembre, E., Trask, S. D., Greenberg, H. B., Stephen, C., & Dormitzer, P. R. (2009). Structure of rotavirus outer-layer protein VP7 bound with a neutralizing Fab. *Science*. 324(5933): p1444–1447.
4. Bac-to-Bac® Baculovirus Expression System manual: an efficient site-specific transposition system to generate baculovirus for high-level expression of recombinant proteins. Catalog no. 10359-016 (Life Technologies, Grand Island, NY).
5. Beisner, B., Kool, D., Marich, A, & Holmes, I. H. (1998). Characterisation of G serotype dependent non-antibody inhibitors of rotavirus in normal mouse serum. *Archives of Virology*. 143(7): p1277–1294.
6. Benavides, J., Mena, J. A., Cisneros, M., Ramírez, O. T., Palomares, L. A., Rito-Palomares, M. (2006). Rotavirus-like particles primary recovery from insect cells in aqueous two-phase systems. *Journal of Chromatography*. 842(1): p48–57.
7. Bernstein, D. I., Sack, D. a, Rothstein, E., Reisinger, K., Smith, V. E., O'Sullivan, D., Spriggs, D. R., Ward, R.I. (1999). Efficacy of live, attenuated, human rotavirus vaccine 89-12 in infants: a randomised placebo-controlled trial. *Lancet*. 354(9175): p287–290.
8. Bucardo, F., Rippering, C. M., Svensson, L., Patton, J. T. (2012). Vaccine-derived NSP2 segment in rotaviruses from vaccinated children with gastroenteritis in Nicaragua. *Infection, Genetics and Evolution*. 12(6): p1282-1294.
9. Butz, A. M., Fosarelli, P., Dick, J., Cusack, T., Yolken, R. (1993). Prevalence of rotavirus on high-risk fomites in day-care facilities. *Pediatrics*. 92: p202–205.
10. Castro-Acosta, R. M., Revilla, A. L., Ramirez, O.T., Palomares, L.A. (2010). Separation and quantification of double and triple-layered rotavirus-like particles by CZE. *Electrophoresis*. 31(8): p1376-1381.
11. Chan, W. K., Penarande, M. E., Crawford, S. E, Estes, M. K. (1986). Two glycoproteins are produced form the rotavirus neutralization gene. *Virology*. 151(2): p243-252.

12. Charpillienne, A., Nejmeddine, M., Berois, M., Parez, N., Neumann, E., Hewat, E., Trugnan, G., Cohen J. (2001). Individual rotavirus-like particles containing 120 molecules of fluorescent protein are visible in living cells. *The Journal of Biological Chemistry*. 276(31): p29361–29367.
13. Chen, D., Luongo, C. L., Nibert, M. L., & Patton, J. T. (1999). Rotavirus open cores catalyze 5'-capping and methylation of exogenous RNA: evidence that VP3 is a methyltransferase. *Virology*. 265(1): p120–130.
14. Chibo, S., Yokoyama, T., Nakata, S., Morita, Y., Urasawa, T., Taniguchi, K. Urasawa, S. & Nakao, T. (1986). Protective effect of naturally acquired homotypic and heterotypic rotavirus antibodies. *Lancet*. 2: p417-421.
15. Ciarlet, M., Crawford, S. E., Barone, C., Bertolotti-Ciarlet, A., Ramig, R. F., Estes, M. K., & Conner, M. E. (1998). Subunit rotavirus vaccine administered parenterally to rabbits induces active protective immunity. *Journal of Virology*. 72(11): p9233–9246.
16. Cohen, J., Laporte, J., Charpillienne, A., & Scherrer, R. (1979). Activation of rotavirus RNA polymerase by calcium chelation. *Archives of Virology*. 60: p177-86.
17. Conner, M. E., Crawford, S. U. E. E., Barone, C., & Estes, M. K. (1993). Rotavirus vaccine administered parenterally induces protective immunity. *Journal of Virology*. 67(11): p6633–6641.
18. Corthesy, B., Benureau, Y., Perrier, C., Fourgeux, C., Parez, N., Greenberg, H., & Schwartz-Cornil, I. (2006). Rotavirus anti-VP6 secretory immunoglobulin A contributes to protection via intracellular neutralization but not via immune exclusion. *Journal of Virology*. 80: p10692-10699.
19. Coste, A, Sirard, J. C., Johansen, K., Cohen, J., & Kraehenbuhl, J. P. (2000). Nasal immunization of mice with virus-like particles protects offspring against rotavirus diarrhea. *Journal of Virology*. 74(19): p8966–8971.
20. Coulson, B.S., Londrigan, S.L., & Lee, D.J., (1997). Rotavirus contains integrin ligand sequences and a disintegrin-like domain that are implicated in virus entry into cells. *Proceedings of the National Academy of Science U.S.A*. 94: p5389–5394.
21. Crawford, S. E., Labbé, M., Cohen, J., Burroughs, M. H., Zhou, Y. J., & Estes, M. K. (1994). Characterization of virus-like particles produced by the expression of rotavirus capsid proteins in insect cells. *Journal of Virology*. 68(9): p5945–5952.
22. Crawford, S. U. E. E., Estes, M. K., Ciarlet, M. A. X., Barone, C., Neal, C. M. O., Cohen, J., & Conner, M. E. (1999). Heterotypic protection and induction of a broad heterotypic

- neutralization response by rotavirus-like particles. *Journal of Virology*. 73(6): p4813–4822.
23. Desselberger, U., Iturriza-Gomara, M., & Gray, J. J. Rotavirus epidemiology and surveillance. (2001). In: Chadwick D, Goode JA, editors. *Gastroenteritis Viruses*. Chichester: Wiley. p125-152.
 24. Desselberger, U., Manktelow, E., Li, W., Cheung, W., Iturriza-Gomara, M., & Gray, J. (2009). Rotaviruses and rotavirus vaccines. *British Medical Bulletin*. 90(1): p1–15.
 25. Dormitzer, P. R., Greenberg, H. B., & Harrison, S. C. (2000). Purified recombinant rotavirus VP7 forms soluble, calcium-dependent trimers. *Virology*. 277(2): p420–428.
 26. Dowling, W., Denisova, E., Monica, R. L. A., & Mackow, E. R. (2000). Selective membrane permeabilization by the rotavirus VP5 * protein is abrogated by mutations in an internal hydrophobic domain. *Journal of Virology*. 74(14): p6368–6376.
 27. Estes, M.K. and Kapikian, A.Z. (2007). Rotaviruses. In Fields' Virology, Knipe, D.M., Howley, P.M. (eds) 5th edition. Philadelphia: Lippincott, Williams & Wilkins. p1918–1974.
 28. Feng, N., Kim, B., Fenaux, M., Nguyen, H., Vo, P., Omary, M. B., & Greenberg, H. B. (2008). Role of interferon in homologous and heterologous rotavirus infection in the intestines and extraintestinal organs of suckling mice. *Journal of Virology*. 82(15): p7578–7590.
 29. Fiore, L., H. B. Greenberg, & E. R. Mackow. (1991). The VP8 fragment of VP4 is the rhesus rotavirus hemagglutinin. *Virology*. 181: p553–563.
 30. Fischer, T. K., Bresee, J. S., & Glass, R. I. (2004). Rotavirus vaccines and the prevention of hospital-acquired diarrhea in children. *Vaccine*. 22: S49–S54.
 31. Franco, M. A., Greenberg, H. B. (1999). Immunity to rotavirus infection in mice. *Journal of Infectious Diseases*. 179 Suppl 3: S466-469.
 32. Fromantin, C., Jamot, B., Cohen, J., Piroth, L., Pothier, P., & Kohli, E. (2001). Rotavirus 2/6 virus-like particles administered intranasally in mice, with or without the mucosal adjuvants cholera toxin and Escherichia coli heat-labile toxin, induce a Th1/Th2-like immune response. *Journal of Virology*. 75: p11010–11016.
 33. Glass, R. I., & Parashar, U. D. (2006). The promise of new rotavirus vaccines. *The New England Journal of Medicine*. 354(1): p75–77.
 34. Gonzalez, A. M., Nguyen, T. V., Azevedo, M. S. P., Jeong, K., Agarib, F., Losef, C., Chang, K., Lovgren-Bengtsson, K., Morein, B., & Saif, L. J. (2004). Antibody responses to human rotavirus (HRV) in gnotobiotic pigs following a new prime/boost vaccine

- strategy using oral attenuated HRV priming and intranasal VP2/6 rotavirus-like particle (VLP) boosting with ISCOM. *Clinical and Experimental Immunology*. 135(3): p361–372.
35. Gouvea, V., and Brantly, M. (1995). Is rotavirus a population of reassortants? *Trends in Microbiology*. 159: p159–162.
 36. Graff, J. W., Mitzel, D. N., Weisend, C. M., Flenniken, M. L., Hardy, M. E. (2002). Interferon regulatory factor 3 is a cellular partner of rotavirus NSP1. *Journal of Virology*. 76: p9545-9550.
 37. Greenberg, H. B., & Estes, M. K. (2009). Rotaviruses: From Pathogenesis to Vaccination. *Gastroenterology*. 136(6): p1939–1951.
 38. Guerrero, C. A., Méndez, E., Zárate, S., Isa, P., López, S., & Arias, C. F. (2000). Integrin alpha(v)beta(3) mediates rotavirus cell entry. *Proceedings of the National Academy of Science U.S.A.* 97: p14644–14649.
 39. Heaton, P. M., Goveia, M. G., Miller, J. M., Offit, P., & Clark, H. F. (2005). Development of a pentavalent rotavirus vaccine against prevalent serotypes of rotavirus gastroenteritis. *The Journal of Infectious Diseases*. 192 Suppl 1: S17–21.
 40. Hewish, M., Takada, Y., & Coulson, B. (2000). Integrins $\alpha 2\beta 1$ and $\alpha 4\beta 1$ can mediate SA11 rotavirus attachment and entry into cells. *Journal of Virology*. 74: p228-236.
 41. Hjelt, K., Graubelle, P. C., Paerregaard, A., Nielsen, O. H., & Krasilnikoff, P. A. (1987). Protective effect of pre-existing rotavirus-specific immunoglobulin A against naturally acquired rotavirus infection in children. *Journal of Medical Virology*. 21: p39-47
 42. Hoshino, Y., Gorziglia, M., Valdesuso, J., Askia, J., Glass, R.I. & Kapikian, A.Z. (1987). An equine rotavirus (FI-14 strain) which bears both subgroup 1 and subgroup II specificities on its VP6. *Virology*. 157: p488-496.
 43. Istrate, C., Hinkula, J., Charpilienne, A., Poncet, D., Cohen, J., Svensson, L., & Kari, J. (2008). Rotavirus virus-like particles (RF 8-2/6/7) administered parenterally in a one-dose regimen induce protective immunity in mice. *Vaccine*. 26(35): p4594–4601.
 44. Ito, H., Minamoto, N., Goto, H., Rong, L. T., Sugiyama, M., & Kinjo, T. (1996). Expression of the major inner capsid protein, VP6, of avian rotavirus in mammalian cells. *Veterinary Microbiology*. 49(3-4): p257–265.
 45. Jayaram, H., Estes, M. K., & Prasad, B. V. V. (2004). Emerging themes in rotavirus cell entry, genome organization, transcription and replication. *Virus Research*. 101(1): p67–81.

46. Jere, K. C., Sawyerr, T., Seheri, L. M., Peenze, I., Page, N. A., Geyer, A., & Steele, A. D. (2011). A first report on the characterization of rotavirus strains in sSierra Leone. *Journal of Medical Virology*. 83: p540–550.
47. Jiang, B., Barniak, V., Smith, R. P., Sharma, R., Corsaro, B., Hu, B., & Madore, H. P. (1998). Synthesis of rotavirus-like particles in insect cells: comparative and quantitative analysis. *Biotechnology and bioengineering*. 60(3): p369–74.
48. Jiang, X., Jayaram, H., Kumar, M., Ludtke, S. J., Estes, M. K., & Prasad, B. V. V. (2006). Cryo-electron microscopy structures of rotavirus NSP2-NSP5 and NSP2-RNA complexes : implications for genome replication. *Journal of Virology*. 80(21): p10829–10835.
49. Kaba, S.A., Nene, V., Musoke, A.J., Vlak, J.M., & van Oers, M.M. (2002). Fusion to green fluorescence protein improves expression levels of Theileria parva sporozoite surface antigen p67 in insect cells. *Parasitology*. 125: p497–505.
50. Kabcenell, a K., & Atkinson, P. H. (1985). Processing of the rough endoplasmic reticulum membrane glycoproteins of rotavirus SA11. *The Journal of Cell Biology*. 101(4): p1270–1280.
51. Kaljot, K. T., Shaw, R. D., Rubin, D. H., & Greenberg, H. B. (1988). Infectious rotavirus enters cells by direct cell membrane penetration, not by endocytosis. *Journal of Virology*. 62(4): p1136–44.
52. Kapikian, A. Z., Hoshino, Y., Chanock, R. M., & Pérez-Schael, I. (1996). Efficacy of a quadrivalent rhesus rotavirus-based human rotavirus vaccine aimed at preventing severe rotavirus diarrhea in infants and young children. *The Journal of Infectious Diseases*. 174 Suppl 1: S65–72.
53. Keljo, D.J., Kuhn, M., & Smith, A. (1988). Acidification of endosomes is not important for the entry of rotavirus into the cell. *Journal of Pediatric Gastroenterology and Nutrition*. 7: p257–263.
54. Labbé, M., Baudoux, P., Charpilienne, a, Poncet, D., & Cohen, J. (1994). Identification of the nucleic acid binding domain of the rotavirus VP2 protein. *The Journal of General Virology*. 75 (Pt 12): p3423–3430.
55. Labbé, M., Charpilienne, a, Crawford, S. E., Estes, M. K., & Cohen, J. (1991). Expression of rotavirus VP2 produces empty corelike particles. *Journal of Virology*. 65(6): p2946–2952.
56. Laemmli, U. K. (1970). Cleavage of structural protein during the assembly of the head of bacteriophage T4. *Nature*. 227: p680-685.

57. Larralde, G., Li, B. G., Kapikian, A. Z., & Gorziglia, M. (1991). Serotype-specific epitope(s) present on the VP8 subunit of rotavirus VP4 protein. *Journal of Virology*. 65(6): p3213–3218.
58. Lawton, J. A., Zeng, C. Q., Mukherjee, S. K., Cohen, J., Estes, M. K., & Prasad, B. V. (1997). Three-dimensional structural analysis of recombinant rotavirus-like particles with intact and amino-terminal-deleted VP2: implications for the architecture of the VP2 capsid layer. *Journal of Virology*. 71(10): p7353–7360.
59. Lawton, J.A., Estes, M.K., & Prasad, B.V. (2000). Mechanism of genome transcription in segmented dsRNA viruses. *Advances in Virus Research*. 55: p185–229.
60. Lecce, J.G., Cummins, J. M., Richards, A.B. (1990). Treatment of rotavirus infection in neonate and weanling pigs using natural human interferon alpha. *Molecular Biotherapy*. 2(4): p211–216.
61. Legardinier, S., Klett, D., Poirier, J., Combarous, Y., Cahoreau, C. (2005). Mammalian-like nonsialyl complex-type N-glycosylation of equine gonadotropins in Mimic insect cells. *Glycobiology*. 15(8): p776-790.
62. Li, Z., Baker, M. L., Jiang, W., Estes, M. K., & Prasad, B. V. V. (2009). Rotavirus architecture at subnanometer resolution. *Journal of Virology*. 83(4): p1754–1766.
63. Liu, K., Yang, X., Wu, Y., & Li, J. (2009). Rotavirus strategies to evade host antiviral innate immunity. *Immunology Letters*. 127(1): p13–18.
64. Lodish, H., Baltimore, D., & Darnell, J., (1986). *Molecular Cell Biology*. Scientific American Books, Inc., New York, USA.
65. Lopez, S., Arias, C. F., Bell, R., Strauss, J. H., & Espejo, R. T. (1985). Primary structure of the cleavage site associated with trypsin enhancement of rotavirus SA11 infectivity. *Virology*. 144: 11-19.
66. Lopez, S., Espinosa, R., Greenberg, H. B., & Arias, C. F. (1994). Mapping the subgroup epitopes of rotavirus protein VP6. *Virology*. 204: p153-162
67. Ludert, J. E., Ruiz, M. C., Hidalgo, C., & Liprandi, F. (2002). Antibodies to rotavirus outer capsid glycoprotein VP7 neutralize infectivity by inhibiting virion decapsulation. *Journal of Virology*. 76(13): p6643–6651.
68. Mackow, E. R., Barnett, J. W., Chan, H., & Greenberg, H. B. (1989). The rhesus rotavirus outer capsid protein VP4 functions as a hemagglutinin and is antigenically conserved when expressed by a baculovirus recombinant. *Journal of virology*. 63(4): p1661–1668.

69. Madhi, S. A., Cuncliffe, N. A., Steele, D., Witte, D., Kirsten, M., Louw, C., Ngwira, B., Victor, J. C., Gilliard, P. H., Chevart, B. B., Han, H. H., & Neuzil, K. M. (2010). Effect of human rotavirus vaccine on severe diarrhea in African infants. *New England Journal of Medicine*. 362(4): p289–298.
70. Maranga, L., Cruz, P. E., Aunins, J. G., & Carrondo, M. J. T. (2002). Production of core and virus-like particles with baculovirus infected insect cells. *Advances in Biochemical Engineering and Biotechnology*. 74: p183–206.
71. Marshall, J., Botes, J., Gorrie, G., Boardman, C., Gregory, J., Griffith, J., Hogg, G., Dimitriadis, a., Catton, M., & Bishop, R. (2003). Rotavirus detection and characterisation in outbreaks of gastroenteritis in aged-care facilities. *Journal of Clinical Virology*. 28: p331–340.
72. Martella, V., Banyai, K., Matthijnssens, J., Buonavoglia, C., Ciarlet, M. (2010). Zoonotic aspects of rotaviruses. *Veterinary Microbiology*. 140: p246–255.
73. Matsui, S. M., Mackow, E. R. & Greenberg, H. B. (1989). Molecular determinant of rotavirus neutralization and protection. *Advances in Virus Research*. 36: p181-214.
74. Matthijnssens, J., Mino, S., Papp, H., Potgieter, C., Novo, L., Heylen, E., Zeller, M., Garaiceochea, L., Lengyel, G., Kisfal, P., Cullinane, A., Collins, P. J., Ciarlet, M., O'Shea, H., Parreno, V., Banyai, K., Barandeguy, M., & Van Ranst, M. (2012). Complete molecular genome analysis of equine rotavirus A strains from different continents reveal several novel genotypes and a largely conserved genotype constellation. *Journal of General Virology*. 93(Pt 4): p866-875.
75. Mcneal, M. M., Rae, M. N., Conner, M. E., & Ward, R. L. (1998). Stimulation of local immunity and protection in mice by intramuscular immunization with triple- or double-layered rotavirus particles and QS-21. *Virology*. 243: p158–166.
76. Mellado, M. C. M., Franco, C., Coelho, A., Alves, P. M., & Simplicio, A. L. (2008). Sodium dodecyl sulfate-capillary gel electrophoresis analysis of rotavirus-like particles. *Journal of Chromatography*. 1192(1): p166–172.
77. Mena, J. A., Ramirez, O. T., & Palomares, L. A. Quantification of rotavirus-like particles by gel permeation chromatography. (2005). *Journal of Chromatography B Analytical Technology and Biomedical Life Science*. 824(1/2): p267–276.
78. Méndez, E., Arias, C. F., & López, S. (1996). Interactions between the two surface proteins of rotavirus may alter the receptor-binding specificity of the virus. *Journal of Virology*. 70(2): p1218–1222.

79. Moon, H. W. (1994). Pathophysiology of viral diarrhea. In: Kapikian AZ (ed) *Viral infections of the gastrointestinal tract*. Marcel Dekker, New York. p27–52.
80. Murata, K., Lechmann, M., Qiao, M., Gunji, T., Alter, H. J., & Liang, T. J. (2003). Immunization with hepatitis C virus-like particles protects mice from recombinant hepatitis C virus-vaccinia infection. *Proceedings of the National Academy of Science*. 100(11): p6753–6758.
81. Murphy, T.V., Gargiullo, P.M., Massoudi, M. S., Nelson, D. B., Jumaan, A. O., Okoro, C. A., Zanardi, L. R., Setia, S., Fari, E., LeBarron, C. W., Wharton, M., & Livengoo, J. R.; Rotavirus Intussusception Investigation Team. (2001). Intussusception among infants given an oral rotavirus vaccine. *New England Journal of Medicine*. 344(8): p564–572.
82. Nene, V., Inumaru, S., McKeever, D., Morzaria, S., Shaw, M., Musoke, A. (1995). Characterization of an insect cell-derived *Theileria parva* sporozoite vaccine antigen and immunogenicity in cattle. *Infection and Immunity*. 63: p503–508.
83. Noad, R., & Roy, P. (2003). Virus-like particles as immunogens. *Trends in Microbiology*. 11(9): p438–444.
84. O’Neil, C. M., Crawford, S. E., Estes, M. K., & Conner, M. E. (1997). Rotavirus virus-like particles administered mucosally induce protective immunity. *Journal of Virology*. 71(11): p8707-8717.
85. Padilla-Noriega, L., Dunn, S. J., Lopez, S., Greenberg, H. B., & Arias, C. F. (1995). Identification of two independent neutralization domains on the VP4 trypsin cleavage products VP5* and VP8* of human rotavirus ST3. *Virology*. 154: p148–154.
86. Paliard, X., Liu, Y., Wagner, R., Wolf, H., Baenziger, J., & Walker, C. M. (2000). Priming of strong, broad, and long-lived HIV type 1 p55gag-specific CD8+ cytotoxic T cells after administration of a virus-like particle vaccine in rhesus macaques. *AIDS Research of Human Retroviruses*. 16: p273–282.
87. Palomares, L. A., Lopez, S., Ramirez, O. T. (2002). Strategies for manipulating the relative concentration of recombinant rotavirus structural proteins during simultaneous production by insect cells. *Biotechnology and Bioengineering*. 78(6): p635–644.
88. Perez, N. (2008). Rotavirus gastroenteritis: why to back up the development of new vaccines? *Comparative Immunology, Microbiology and Infectious Diseases*. 31(2-3): p253–269.
89. Perez, N., Fourgeux, C., Mohamed, A., Dubugouy, C., Pillot, M., Dehee, A., Charpilienne, A., Poncet, D., Schwartz-Cornil, I., & Garnarg-Chenon, A. (2006). Rectal immunization with rotavirus virus-like particles induces systemic and mucosal humoral

- immune responses and protects mice against rotavirus infection. *Journal of Virology*. 80(4): p1752–1761.
90. Parez, N., Garbarg-Chenon, A., Fourgeux, C., Le Deist, F., Servant-Delmas, A., Charpilienne, A., Cohen, J., & Schwartz-Cornil, I. (2004). The VP6 protein of rotavirus interacts with a large fraction of human naive b cells via surface immunoglobulins. *Journal of Virology*. 78(22): p12489–12496.
 91. Patel, M. M., Clark, A.D., Sanderson, C. F. B., Tate J., Parashar, U. D. (2012). Removing the age restrictions for rotavirus vaccination: A benefit-risk Modeling Analysis. *PLOS Medicine*. 9(10): p1-13.
 92. Parra, G.I., Bok, K., Martínez, M., & Gomez, J.A. (2004). Evidence of rotavirus intragenic recombination between two sublineages of the same genotype. *Journal of General Virology*. 85: p1713–1716.
 93. Patton, J.T. (2008). Segmented Double-stranded RNA viruses: structure and molecular biology. Laboratory of Infectious Diseases, NIAID, NIH, Bethesda, MD 20892-8026, US.
 94. Payne, D. C., Edwards, K. M., Bowen, M. D., Keckley, E., Peters, J., Esona, M. D., Teel, E. N., Kent, D., Parashar, U. D., & Gentsch, J. R. (2010). Sibling transmission of vaccine-derived rotavirus (RotaTeq) associated with rotavirus gastroenteritis. *Pediatrics*. 125(2): e438–e441.
 95. Pérez-Schael, I., Guntinas, M. J., Pérez, M., Pagone, V., Rojas, A. M., González, R., Cunto, W., Hoshino, Y., & Kapikian, A. Z. (1997). Efficacy of the rhesus rotavirus–based quadrivalent vaccine in infants and young children in Venezuela. *The New England Journal of Medicine*. 337(17): p1181–1187.
 96. Pesavento, J. B., Crawford, S. E., Estes, M., & Prasad, B. V. (2006). Rotavirus proteins: structure and assembly. *Currunt Topics in Microbiology and Immunology*. 309: p189-219.
 97. Phan, T.G., Okitsu, S., Maneekarn, N., & Ushijima, H. (2007). Evidence of intragenic recombination in G1 rotavirus VP7 genes. *Journal of Virology*. 81: p10188–10194.
 98. Pickering, L. K., Evans, D.G., DuPont, H. L., Vollet, J. J., & Evans, D. J. (1981). Diarrhea caused by shigella, rotavirus, and giardia in day-care centers: prospective study. *Journal of Pediatrics*. 99: p51–56.
 99. Possee, R.D., Thomas, C.J., & King, L.A. (1999). The use of baculovirus vectors for the production of membrane proteins in insect cells. *Biochemical Society Transactions*. 27: p928–932.

100. Potgieter, A.C., Page, N.A., Liebenberg, J., Wright, I.M., Landt, O., & van Dijk, A.A. (2009). Improved strategies for sequence-independent amplification and sequencing of viral double-stranded RNA genomes. *Journal of General Virology*. 90: p1423–1432.
101. Prasad, B. V. V., J. W. Burns, E. Marietta, M. K. Estes, & W. Chiu. 1990. Localization of VP4 neutralization sites in rotavirus by three-dimensional cryo-electron microscopy. *Nature*. 343: p476–479.
102. Prasad, B.V., Rothnagel, R., Zeng, C.Q., Jakana, J., Lawton, J.A., Chiu, W., & Estes, M.K. (1996). Visualization of ordered genomic RNA and localization of transcriptional complexes in rotavirus. *Nature*. 382: p471–473.
103. Prasad, B.V., Wang, G.J., Clerx, J.P., & Chiu, W. (1988). Three-dimensional structure of rotavirus. *Journal of Molecular Biology*. 199: p269–275.
104. Prasad, B.V.V. & Estes, M.K. (1997). Molecular basis of rotavirus replication: structure and function correlations in structural biology of viruses (Chiu, W., Burnett, R., and Garcia, R., (eds). *Oxford University Press, New York and Oxford*. p239-268.
105. Roldão, A., Vieira, H. L. a, Charpilienne, A., Poncet, D., Roy, P., Carrondo, M. J. T., Alves, P. M., & Oliveira, R. (2007). Modeling rotavirus-like particles production in a baculovirus expression vector system: Infection kinetics, baculovirus DNA replication, mRNA synthesis and protein production. *Journal of Biotechnology*. 128(4): p875–894.
106. Roldão, A., Vieira, H. L. a., Alves, P. M., Oliveira, R., & Carrondo, M. J. T. (2006). Intracellular dynamics in rotavirus-like particles production: Evaluation of multigene and monocistronic infection strategies. *Process Biochemistry*. 41(10): p2188–2199.
107. Rueda, P., Forminaya, J., Langeveld, J. P., Brusckke, C., Vela, C., & Casal, J. I. (2000). Effect of different baculovirus inactivation procedures on the integrity and immunogenicity of porcine parvovirus- like particles. *Vaccine*. 19: p726–734.
108. Ruggeri, F. M., & Greenberg, H. B. (1991). Antibodies to the trypsin cleavage peptide VP8 neutralize rotavirus by inhibiting binding of virions to target cells in culture. *Journal of Virology*. 65(5): p2211–2219.
109. Ruiz, M. C., Abad, M. J., Charpilienne, A, Cohen, J., & Michelangeli, F. (1997). Cell lines susceptible to infection are permeabilized by cleaved and solubilized outer layer proteins of rotavirus. *The Journal of General Virology*. 78 (Pt 11): p2883–2893.
110. Ruiz-Palacios, G. M., Pérez-Schael, I., Velaquez. F. R., Abate, H., Breuer, T., Clemens, S. C., Chevart, B., Espinoza, F., Gillard, P., innis, B. L., Vervantes, Y., Linhares, A. C., Lopez, P., Macias-Parra, M., Ortega_barria, E., Richarson, V., Rivera-Medina, D. M., Rivera, L., Salinas, B., Pavia-Ruz, N., Salmeron, J., Ruttimann, R., Tinoco, J. C., Rubio,

- P., Nunez, E., Guerrero, M. L., Yarzabal, J. P., Damaso, S., Tornieporth, N., Saez-Llorens, X., Vergara, R. F., Vesikari, T., Bouchenooghe, A., Clemens, R., De Vos, B., & O'Brian, M.; Human Rotavirus Study Group. (2006). Safety and efficacy of an attenuated vaccine against severe rotavirus gastroenteritis. *New England Journal of Medicine*. 354: p11-22.
111. Sabara, M., A. Barrington, & L. A. Babiuk. (1985). Immunogenicity of a bovine rotavirus glycoprotein fragment. *Journal of Virology*. 56: p1037-1040.
 112. Sabara, M., Parker, M., Aha, P., Cosco, C., Gibbons, E., Parsons, S., & Babiuk, L. A. (1991). Assembly of double-shelled rotavirus-like particles by simultaneous expression of recombinant VP6 and VP7 proteins. *Journal of Virology*. 65(12): p6994–6997.
 113. Sambrook, J. and Russell, D. W. (2001). Molecular cloning – A laboratory manual. *Cold Spring Harbour Laboratory Press*. Third edition. p1.119, 1.44, 5.41 – 5.46, A 1.26.
 114. Schirmbeck, R., Böhm, W., & Reimann, J. (1996). Virus-like particles induce MHC class I-restricted T-cell responses. Lessons learned from the hepatitis B small surface antigen. *Intervirology*. 39: p111–119.
 115. Schwers, A., Van den Broecke, C., Maenhoudt, M., Beduin, J. M., Werenne, J., Pastoret, P. P. (1985). Experimental rotavirus diarrhoea in colostrum-deprived newborn calves: assay of treatment by administration of bacterially produced human interferon (Hu-IFN alpha 2). *Annales de Recherches Veterinaires*. 16: p213–218.
 116. Settembre, E. C., Chen, J. Z., Dormitzer, P. R., Grigorieff, N., & Harrison, S. C. (2010). Atomic model of an infectious rotavirus particle. *The European Molecular Biology Organisation Journal*. 30(2): p408–416.
 117. Shaw, A.L., Rothnagel, R., Chen, D., Ramig, R.F., Chiu, W. & Prasad, B.V.V. (1993). Three-dimensional visualization of the rotavirus hemagglutinin structure. *Cell*. 74: p693-701.
 118. Shaw, A.L., Samal, S.K., Subramanian, K., & Prasad, B.V. (1996). The structure of aquareovirus shows how the different geometries of the two layers of the capsid are reconciled to provide symmetrical interactions and stabilization. *Structure*. 4: p957–967.
 119. Shuttleworth, G., Eckery, D. C., & Awram, P. (2005). Oral and intraperitoneal immunization with rotavirus 2/6 virus-like particles stimulates a systemic and mucosal immune response in mice. *Archives of Virology*. 150(2): p341–349.
 120. Staat, M. A., Azimi, P. H., Berke, T., Roberts, N., Bernstein, D. I., Ward, R. L., Pickering, L. K., & Matson, D. O. (2002). Clinical presentations of rotavirus infection among hospitalized children. *Pediatric Infectious Disease Journal*. 21: p221–227.

121. Stirzaker, S. C., Whitfeld, P. L., Christie, D. L., Bellamy, a R., & Both, G. W. (1987). Processing of rotavirus glycoprotein VP7: implications for the retention of the protein in the endoplasmic reticulum. *The Journal of Cell Biology*. 105(6 Pt 2): p2897–2903.
122. Suzuki, Y., Gojobori, T., & Nakagomi, O. (1998). Intragenic recombinations in rotaviruses. *Federation of European Biochemical Societies Letters*. 427: p183–187.
123. Taniguchi, K., Hoshino, Y., Nishikawa, K., Green, K. Y., & Morita, W. L. M. (1988). Cross-reactive and serotype-specific neutralization epitopes on vp7 of human rotavirus : nucleotide sequence analysis of antigenic mutants selected with monoclonal antibodies. *Journal of Virology*. 62(6): p1870–1874.
124. Tate, J. E., Burton, A. H., Boschi-Pinto, C., Steele, a D., Duque, J., & Parashar, U. D. (2012). 2008 Estimate of worldwide rotavirus-associated mortality in children younger than 5 years before the introduction of universal rotavirus vaccination programmes: a systematic review and meta-analysis. *The Lancet Infectious Diseases*. 12(2): p136–141.
125. Tihova, M., Dryden, K. A., Bellamy, A. R., Greenberg, H. B., & Yeager, M. (2001). Localization of membrane permeabilization and receptor binding sites on the VP4 hemagglutinin of rotavirus : Implications for Cell Entry. *Journal of Molecular Biology*. 4: p985–992.
126. Trask, S. D., McDonald, S. M., & Patton, J. T. (2012). Structural insights into the coupling of virion assembly and rotavirus replication. *Nature reviews. Microbiology*. 10(3): p165–177.
127. Valenzuela, S., Pizarro, J., Sandino, A. M., Vasquez, M., Fernandez, J., Hernandez, O., Patton, J., & Spencer, E. (1991). Photoaffinity labeling of rotavirus VP1 with 8-azido-ATP: identification of the viral RNA polymerase. *Journal of Virology*. 65: p3964–3967.
128. Velazquez, F. R., Matson, D. O., Guerrero, M. L., Shults, J., Calva, J. J., Morrow, A. L., Glass, R. I., Pickering, L. K., & Ruiz-Palacios, G. M. (2000). Serum antibody as a marker of protection against natural rotavirus infection and disease. *Journal of Infectious Diseases*. 182(6): p1602-1609.
129. Vesikari, T., Isolauri, E., & D'Hondt, E. (1984). Protection of infants against rotavirus diarrhea by RIT 4237 attenuated bovine rotavirus strain vaccine. *Lancet*. 1: p977–981.
130. Vesikari, T., Matson, D. O., Dennehy, P., Van Damme, P., Santosham, M., Rodriguez, Z., Dallas, M. J., Heyse, J. F., Gouveia, M. G., Black, S. B., Shinefield, H. R., Christie, C.D.C., Ylitalo, S., Itzler., R. F., Coia, M. L., Onorato, M. T., Adeyi, B. A., Marshall, G. S., Gothefors, L., Campens, D., Karvonen, A., Watt., J. P., O'Brien, K. L., DiNubile, M. J., Clark, H. F., Boslego, J. W., Offit, P. A., & Heaton, P. M. (2006). Safety and efficacy of a

- pentavalent human-bovine (WC3) reassortant rotavirus vaccine. *The New England Journal of Medicine*. 354(1): p23–33.
131. Vieira, H. L. a, Estêvão, C., Roldão, A., Peixoto, C. C., Sousa, M. F. Q., Cruz, P. E., Carrondo, M. J. T., & Alves., P. M. (2005). Triple layered rotavirus VLP production: kinetics of vector replication, mRNA stability and recombinant protein production. *Journal of Biotechnology*. 120(1): p72–82.
 132. Vollet, J. J., Ericsson, C. D., Gibson, G., Pickering, L. K., DuPont, H. L., Kohl, S., Conklin, R. H. (1979). Human rotavirus in an adult population with travelers' diarrhea and its relationship to the location of food consumption. *Journal of Medical Virology*. 4: p81–87.
 133. Wang, Y., Dennehy, P. H., Keyserling, H. L., Tang, K., Gentsch, J. R., Glass, R. I., & Jiang, B. (2007). Rotavirus Infection Alters Peripheral T-Cell Homeostasis in Children with Acute Diarrhea. *Journal of Virology*. 81(8): p3904–3912.
 134. Ward, R. L. (2008). Rotavirus vaccines: how they work or don't work. *Expert Reviews in Molecular Medicine*. 10(February): e5.
 135. Yeager, M., Dryden, K.A., Olson, N.H., Greenberg, H.B. & Baker, T.S. (1990). Three-dimensional structure of rhesus rotavirus by cryo-electron microscopy and image reconstruction. *Journal of Cellular Biology*. 110: p2133-2144.
 136. Zarate, S., Espinosa, R., Romero, P., Guerrero, C.A., Arias, C.F., & Lopez, S. (2000). Integrin alpha2beta1 mediates the cell attachment of the rotavirus neuraminidase-resistant variant nar3. *Virology*. 278; p50– 54.
 137. Zeng, C. Q., Estes, M. K., Charpilienne, A., & Cohen, J. (1998). The N terminus of rotavirus VP2 is necessary for encapsidation of VP1 and VP3. *Journal of Virology*. 72(1): p201–208.
 138. Zeng, C.Q., Labbe, M., Cohen, J., Prasad, B.V.V., Chen, D., Ramig, R.F., & Estes, M.K. (1994). Characterization of rotavirus VP2 particles. *Virology*. 201: p55–65.